

**OPTIMAL CONFIGURATION AND PLACEMENT
OF ENERGY STORAGE SYSTEMS TO
ENHANCE THE RESILIENCY OF RENEWABLE
ENERGY INTEGRATED ELECTRICAL
DISTRIBUTION GRID**

A Thesis submitted to the
University of Petroleum and Energy Studies

*For the Award of
Doctor of Philosophy
in
Electrical Engineering*

By
Balaji Venkateswaran V

November 2020

Supervisor(s):

**Dr. Madhu Sharma
Dr. Devender K. Saini**



**Department of Electrical and Electronics
Engineering,
School of Engineering
University of Petroleum & Energy Studies,
Dehradun Uttarakhand, India - 248007**

**OPTIMAL CONFIGURATION AND PLACEMENT
OF ENERGY STORAGE SYSTEMS TO
ENHANCE THE RESILIENCY OF RENEWABLE
ENERGY INTEGRATED ELECTRICAL
DISTRIBUTION GRID**

A Thesis submitted to the
University of Petroleum and Energy Studies

*For the Award of
Doctor of Philosophy
in
Electrical Engineering*

By
Balaji Venkateswaran V

January 2021

Supervisor:

Dr. Madhu Sharma,
Sr. Associate Professor,
School of Engineering, UPES.

Co-Supervisor:


Dr. Devender K. Saini,
Assistant Professor (S.G),
School of Engineering, UPES.



**Department of Electrical and Electronics
Engineering,
School of Engineering
University of Petroleum & Energy Studies,
Dehradun Uttarakhand, India - 248007**

Declaration

I declare that the thesis entitled "Optimal Configuration & Placement of Energy Storage Systems to enhance the Resiliency of Renewable Energy Integrated Electrical Distribution Grid" has been prepared by me under the guidance of Dr. Madhu Sharma, Sr. Associate Professor, School of Engineering and Dr. Devender K Saini, Assistant Professor SG, School of Engineering. No part of this thesis has formed the basis for the award of any degree or fellowship previously.


Balaji Venkateswaran V
Department of Electrical and Electronics Engineering,
University of Petroleum and Energy Studies,
Dehradun, Uttarakhand, India - 248007

Date:

Certificate

We certify that Balaji Venkateswaran V has prepared his thesis entitled "*Optimal Configuration and Placement of Energy Storage Systems to enhance the Resiliency of Renewable Energy Integrated Electrical Distribution Grid*", for the award of PhD degree of the University of Petroleum and Energy Studies, under our guidance. He has carried out the work at the Department of Electrical and Electronics Engineering, School of Engineering, University of Petroleum and Energy Studies.

Internal Supervisor:


Dr. Madhu Sharma

Sr. Associate Professor,
School of Engineering,

University of Petroleum and Energy Studies, Dehradun.

Internal Co-Supervisor:


Dr. Devender K. Saini

Assistant Professor (S.G),
School of Engineering,

University of Petroleum and Energy Studies, Dehradun.

Abstract

In recent days, the integration of renewable-based distributed generators (DGs) is increasing, mainly to decarbonize the grid, thereby achieving a sustainable power grid. On the other hand, from the archives of National Disaster Management Authority (NDMA), India, it is evident that the country has faced several major disasters in the recent decade and this trend is increasing. Comprising these factors into consideration, it is essential to develop a sustainable distribution grid in the future, which integrates energy storage devices to cater to both normal and extreme conditions.

This thesis proposes novel strategies/techniques to improve the system resiliency along with system flexibility of a renewable integrated distribution system via optimal planning of energy storage units (ESUs). The first part of the thesis focuses on reviewing various resiliency improvement strategies mainly using ESUs, and methods applied to analyze the system performance during emergency conditions. Henceforth, this thesis proposes a generalized ESU planning methodology, which enhances both the system flexibility and resiliency. Besides, this thesis proposes a unique method to quantify the performance of the system against short-term and long-term resiliency.

The second part of the thesis focuses on the optimal configuration of ESUs to formulate hybrid ESUs (HESUs) and its placement across the distribution system to improve the system flexibility by considering the environmental and other practical constraints as the key variables. The problem formulated to achieve the optimal configuration of HESU mainly depends on the minimization of the overall environmental impact and satisfying the required demand. Later, the formulated mixed-integer nonlinear problem (MINLP), constrained with practical parameters such as renewable purchase obligation (RPO), the land space required to install HESU, and its associated cost and arbitrage cost (to generate revenue from HESU) on top of grid performance parameters identifies the optimal size and location of HESUs across the distribution system.

In recent days, the prospect of availability of either small-scale domestic ESUs, also known as battery inverter set (BIS) or electric vehicles (EVs) or standalone solar photovoltaic rooftops (SPVRs) or its combination at home is high. Therefore, all these resources of power generation and storage are considered as components of home battery inverters

(HBIs). The third part of the thesis focuses on proposing resiliency enhancement plans by combining both grid-side resiliency (which includes large-scale ESUs) and demand-side resiliency (which includes BIS, EVs and SPVRs). Initially, a generalized proactive framework for optimal planning of ESUs against natural disasters is proposed, which combines the grid-side (by using optimal ESU) and the demand-side (by using BIS installed across the distribution system) by assuming the availability of communication infrastructure to get the state of charge (SOC) level of BIS. Later, a three-dimensional hardening methodology is proposed, which includes underground cables (UCs), large-scale ESUs, and communication infrastructure for HBIs. Since hardening involves significant capital investment, it is essential to optimize the overall expenditure considering the technical constraints and practical scenarios.

For better planning against natural disasters, it is essential to typically identify the vulnerable substations and distribution lines of the network. This is achieved by depicting the natural disaster and performing vulnerability assessment, thereby the probability of failure of key components are evaluated. With the results of vulnerability assessment as input, the MINLP is solved by implementing the hybrid algorithm based on meta-heuristic approach to achieve optimal hardening of the system. In this thesis, earthquakes are considered as a major natural disaster. Therefore, the real-world distribution system of Dehradun district, Uttarakhand, India, which comes under seismic zone IV is considered for this comprehensive study. From the case studies, it is proved that the proposed approaches considerably improve the system performance under both normal and extreme conditions.

As the significant outcomes, it is economical for the utilities to plan large-scale ESUs by considering other small-scale energy storage devices connected to the system like HBIs on top of grid-tied renewable energy sources (RESs) to improve the overall system performance both during normal and extreme conditions. Furthermore, it is evident from the results that the optimally configured HESUs can appreciably reduce the damage cost on the environment. To achieve the most appropriate planning solution, extensive surveys have been conducted across Dehradun district to identify the distribution of HBIs across the grid. Therefore, the result of the optimal planning of ESUs is to be performed by considering the vulnerability of the electrical infrastructure for improved system performance during the emergency conditions. Besides, including the capacity of HBIs in the distribution system can considerably increase the energy served during the emergency conditions, thereby improving the system performance.

Acknowledgement

This thesis would not be possible without the support and encouragement of many people. First and foremost, I would like to express my sincerest gratitude to Dr. Madhu Sharma to complete my doctoral studies under her guidance. Her constant motivation and encouragement helped me at various stages of research and thesis writing. I thank her for taking me under her wings and providing numerous inputs in the work.

My sincere gratitude to Dr. Devender K. Saini for his deep insights and suggestions. I always felt that I had a mentor with whom I could discuss topics on a common level and from whom I could learn a lot. His efforts to read this thesis and sharing valuable comments and suggestions helped me to work at faster pace to complete and submit the thesis.

I am grateful to Dr. Kamal Bansal for his constant and continuous encouragement to carry out the surveys conducted related to the thesis.

I am thankful to DigSILENT PowerFactory, Germany for sponsoring me the PowerFactory software tool under PF4T license to carry out this research.

Above all, my most important and greatest debt of appreciation goes to my parents, without whom I would never have been able to achieve so much. I extend gratitude and thank my wife Mrs. Meenakshi for being a constant source of strength and inspiration. I can truly say that it was her constant reassurance that made it possible for me to see this work through to the end. I also thank my brother, Hari Haran for his support at the final stage of the thesis. Lastly, my daughter, Vaishnavi, who missed my attention, is very kind and supportive during this journey.

I am grateful and thankful to each and everyone in the department who helped me directly or indirectly during this work.

Contents

Nomenclature	vi
List of Figures	xiv
List of Tables	xvi
1 Introduction	1
1.1 Overview and Motivation	1
1.2 Contributions	4
1.3 Thesis Outline	5
2 Literature Survey	7
2.1 Background Study	7
2.1.1 Formulation of Optimization Problem	9
2.1.2 Methodologies designed for Optimal Planning of ESUs	17
2.1.3 Performance of the methodologies proposed in the literature	23
2.2 Closing Remarks	31
3 Power System Resiliency	32
3.1 Introduction	32
3.2 Definitions for Resilience	33
3.3 Comparison of Risk and Resilience Framework	34
3.4 Resiliency Enhancement Strategies	36
3.5 Metrics to Quantify Resiliency	37
3.6 Novel Approach to Quantify Resiliency	39
3.7 Proposed Methodology	40
3.8 Closing remarks	43
4 Distribution System Modeling	44
4.1 Introduction	44
4.2 Uncertainty Modeling	45
4.2.1 Uncertainty of Solar PV Generation	46
4.2.2 Uncertainty of Load	46
4.3 Vulnerability Assessment against Earthquakes	47
4.3.1 Modeling seismic activity	48
4.3.2 Fragility Model	49
4.3.3 Damage Probability of Electrical Infrastructure	49

4.4	Monte-Carlo based Probabilistic Earthquake hazard Model	51
4.5	DigSILENT PowerFactory Model of Distribution Grid – A Case Study	52
4.6	Closing Remarks	53
5	Practically Constrained Optimal Planning of Energy Storage Units	57
5.1	Introduction	57
5.2	System Modeling	58
5.2.1	Clustering of Distribution Network	58
5.2.2	Selection of ESU Technology	60
5.3	Problem Formulation	61
5.3.1	REPs and Load Modelling	61
5.3.2	Optimization Problem	61
5.4	Methodology	65
5.5	Case Study Results	67
5.6	Closing Remarks	73
6	Resiliency Enhancement Strategies via Optimal ESU Planning	76
6.1	Introduction	76
6.2	Framework to enhance System Resiliency against Earthquakes	77
6.2.1	Proposed Framework	77
6.2.2	Proposed Methodology	80
6.2.3	Case Study Results	85
6.3	Three-Dimensional Optimal Hardening Strategy for Distribution Grid against Natural Disaster	93
6.3.1	Concept of HBI	94
6.3.2	Optimization Problem for Three Dimensional Hardening	94
6.3.3	Proposed Methodology	96
6.3.4	Results of Case Study	101
6.4	Closing Remarks	104
7	Closure of Thesis	108
7.1	Summary	108
7.2	Conclusions	109
7.3	Future Directions	110
	Bibliography	112
	Curriculum Vitae	133

Nomenclature

Abbreviations

<i>APSO</i>	Adaptive Particle Swarm Optimization
<i>BDA</i>	Bender Decomposition Algorithm
<i>BIS</i>	Battery Inverter Set
<i>BPSO</i>	Binary Particle Swarm Optimization
<i>DGs</i>	Distributed Generators
<i>DI</i>	Direct Impact
<i>DOD</i>	Depth of Discharge
<i>EDSO</i>	European Distribution System Operator
<i>EED</i>	Expected Energy Demand
<i>EENS</i>	Expected Energy NOT Satisfied
<i>ELO</i>	Line Outages during the event
<i>ERT</i>	Emergency Response Time
<i>ESUs</i>	Energy Storage Units
<i>FEMA</i>	Federal Emergency Management Agency
<i>GA</i>	Genetic Algorithm
<i>HBI_s</i>	Home Battery Inverters
<i>HESUs</i>	Hybrid Energy Storage Units
<i>IDI</i>	Indirect Impact
<i>LCI</i>	Land Cost Index
<i>LOLP</i>	Load Loss Probability
<i>LP</i>	Linear Programming
<i>MINLP</i>	Mixed-Integer Nonlinear Problem

<i>MNRE</i>	Ministry of New and Renewable Energy
<i>MSL</i>	Mean Sea Level
<i>NDMA</i>	National Disaster Management Authority
<i>NIAC</i>	National Infrastructure Advisory Council
<i>PDF</i>	Probability Density Function
<i>PGA</i>	Peak Ground Acceleration
<i>PGV</i>	Peak Ground Velocity
<i>POPF</i>	Probabilistic Optimal Power Flow
<i>PV</i>	Photovoltaic
<i>REPs</i>	Renewable Energy Plants
<i>RPO</i>	Renewable Purchase Obligation
<i>SERC</i>	State Electricity Regulatory Commission
<i>SOC</i>	State of Charge
<i>TOD</i>	Time of the Day
<i>UCs</i>	Underground Cables
<i>UPCL</i>	Uttarakhand Power Corporation Limited

Parameters

$\alpha \& \beta$	Shape parameters of probability density function
\mathbb{k}_{env}	Cost of environmental damage due to CO_2 emission per $kgCO_{2-eq}$
\mathbb{k}_{LL}	Cost of line loading in \$/p.u
\mathbb{k}_{Loss}	Cost of apparent power loss in \$/kVA
\mathbb{k}_{VD}	Cost of voltage deviation in \$/p.u
β_{ds}	Standard deviation of the lognormal of spectral displacement for a damage state
Δt	Sampling period
$\eta_{chi,i}$	Charging efficiency of ESU located at i_{th} bus
$\eta_{dis,i}$	Discharging efficiency of ESU located at i_{th} bus
$\gamma_{emi}^{ESU,i}$	The emission rate of i_{th} ESU in $kgCO_{2-eq}/kWh$

$\kappa^{ESU,i}$	Energy to Power ratio of ESU located at i_{th} bus
$\overline{S_{d,d_s}}$	Median value of spectral displacement
b_{BIS}	Binary index of BIS
b_{EV}	Binary index of EV
b_{PV}	Binary index of PV
$Budget_{max}$	Maximum budget allocated for $HESU$ planning
c_0, c_1, c_2 & c_3	Regression coefficients of seismic model
C_h	charging hours of electric vehicle
C_{ci}^{BIS}	Cost of Communication Infrastructure for BIS
C_{ci}^{EV}	Cost of Communication Infrastructure for EV
C_{ci}^{PV}	Cost of Communication Infrastructure for PV
C_{eff}	Charging efficiency of ESU
$C_{EI}^{ESU,i}$	Cost related to energy rating of i_{th} ESU
$C_{FI}^{ESU,i}$	Fixed installation cost of i_{th} ESU
C_{FI}^{HBI}	Fixed Investment cost for HBI communication infrastructure
C_{FOM}^{ESU}	Fixed Operation and Maintenance cost of ESU
C_{ipk}^{UC}	Cost of i_{th} UC per kilometer in \$
$C_{PI}^{ESU,i}$	Cost related to power rating of i_{th} ESU
D	distance between epicentre and the hypocentre
D_{eff}	Discharging efficiency of ESU
$E_{dem,b}$	Total energy demand installed at bus b
$E_{min}^{ESU,i}, E_{max}^{ESU,i}$	Minimum and maximum energy from ESU installed at i_{th} bus
EV_{DI}	Electric vehicle distribution index
EV_{s_h}	hourly scaling factor of electric vehicle load
f_n	future number of year
It_{max}	Maximum number of iterations
L_{s_h}	hourly scaling factor of general load

$L_{UC,i}$	Length of i_{th} UC in m
LCI^{N_b}	Land Cost Index at bus N_b
LL_{max}^l	Maximum permissible line loading of line l
LL_{max}^{UC}	Maximum permissible line loading of UC
M_w	Moment magnitude of earthquake
P_i	real power demand at i_{th} bus
P_{BIS}	Power output from BIS
$P_{D,t}^{do,k}$	Power demand of domestic load in k_{th} cluster at time t
$P_{ESU,i}$	Real power from ESU located at i_{th} bus
P_{EV}	Total electric vehicle demand in a particular region/cluster
$P_{min}^{ESU,i}, P_{max}^{ESU,i}$	minimum and maximum power from ESU installed at i_{th} bus
P_{pre}^D	Present value of real power demand
P_{pre}^P	Present value of power generated from solar power plant
$P_{pre}^{EV}(i_{N_c})$	Present value of electric vehicle power demand at i_{N_c} location of cluster N_c
P_{Purt}	Power purchased from grid at time t
P_{rated}^{ESU}	Total installed capacity of ESU
P_{Sellt}	Power sold to the grid by $HESU$ at time t
PV_{sh}	hourly scaling factor of solar PV
$Q_{ESU,i}$	Reactive power from ESU located at i_{th} bus
$SOC_{min}^{ESU,i}, SOC_{max}^{ESU,i}$	Minimum and maximum state of charge of ESU located at i_{th} bus
$SOC_{min}^{HESU}, SOC_{max}^{HESU}$	Minimum and maximum state of charge of $HESU$
$T_{Pur,t}$	Tariff of purchased energy at time t
$T_{Sell,t}$	Tariff of sold energy at time t
V_{min}, V_{max}	Minimum and Maximum bus voltage
V_{Rated}	Rated voltage of the bus in the system

w_1 & w_2	Importance factor of <i>SI</i> & <i>DBI</i>
Indices and sets	
co	Damage state : complete
ex	Damage state : extensive
ex	extreme event
i	Indices for bus or location
k	Cluster indices
Loc	Indices corresponding to the location affected by earthquake
mi	Damage state : minor
mo	Damage state : moderate
N_b	Indices for Total number of buses in the system
N_l	Indices for Total number of lines in the system
N_t	Total time period considered for this study
N_{ESU}	Indices for number of <i>ESUs</i> to form <i>HESU</i>
N_{es}	Set of locations for <i>ESU</i> installation
N_{HBI}	Total number of <i>HBI</i> in the system
N_{UC}	Total number of <i>UCs</i> to be installed in the system
no	Damage state : none
S_{ex}	Set of extreme event
Variables	
$A^{ESU,i}$	Physical size of <i>ESU</i> installed at bus i
BI	Binary Index
C_I^{ESU}	Investment cost of <i>ESU</i>
C_I^{HBI}	Investment related to Communication infrastructure of <i>HBI</i>
C_I^{HESU}	Investment cost of <i>HESU</i>
C_I^{UC}	Investment cost of <i>UCs</i>
C_{OM}^{UC}	Operation and Maintenance cost of <i>UCs</i>

C_P^G	Power grid performance cost due to <i>HESU</i>
C_{env}^{ESU}	Cost of environmental damage due to CO_2 emission
C_{env}^{HESU}	Environmental damage cost due to <i>HESU</i>
C_{land}^{HESU}	Cost of land to install <i>HESU</i>
C_{LL}^{Nl}	Total line loading cost in the system
C_{obj}	Cost of Objective Function: Three-Dimensional Hardening
C_{OM}^{HESU}	Operation and Maintenance cost of <i>HESU</i>
C_{SP}^{Nl}	Total cost of apparent power loss in the system
C_{VD}^{Nb}	Total voltage deviation cost in the system
C_{ex_i}	Load curtailed during the extreme event
CBI	Combined Binary Index
CQI	Cluster Quality Index
d_s	Damage state
DBI	Davies Bouldin Index
DSI	Damage State Index
$E_t^{ESU,i}$	Energy from <i>ESU</i> located at i_{th} bus at time t
FV	Future value
GF	Growth factor
h	hour of the day
LL_t^l	Line loading of line l at time t
LL_t^{UC}	Line loading of <i>UC</i> at time t
Obj	Cost of objective function
$P^{ESU,i}$	Installed capacity of <i>ESU</i> at i_{th} bus
P_D^{i,h,f_n}	Real power demand of the general load located at i_{th} bus at hour h of the day in the f_n^{th} year
$P_t^{ESU,i}$	Power from <i>ESU</i> located at i_{th} bus at time t
P_t^{SPP}	Power generated from Solar Power Plant at time t
$P_{ch,t}^{HESU}$	Charging power of <i>HESU</i> at time t

$P_{dis,t}$	Discharging power of <i>ESU</i> at time t
$P_{dis,t}^{HESU}$	Discharging power of <i>HESU</i> at time t
P_{EV}^{i,h,f_n}	Power demand of electric vehicle at i_{th} bus at hour h of the day in the f_n^{th} year
$P_{EV}^{iN_c,h,f_n}$	Real power demand of the electric vehicle load located at i_{th} bus of cluster N_c at hour h of the day in the f_n^{th} year
$P_{flow}^{i,t}$	Real power flow between bus i and j at time t
$P_{grid}^{i,t}$	Real power injected from the grid at i_{th} bus during time t
$P_{HESU}^{i,t}$	Real power absorbed or injected from <i>HESU</i> located at i_{th} bus at time t
$P_{loss,l}$	Real power loss in line l
P_{loss}^t	Real power loss at time t
P_{Obj}	Cost of Primary Objective function
P_{PV}^{i,h,f_n}	Real power generated from solar power plant located at i_{th} bus at hour h of the day in the f_n^{th} year
P_{ex_i}	Probability of power grid facing an extreme event
PDF_D	Probability density function corresponding to Power demand
PDF_{EV}	Probability density function corresponding to Power demand of Electric Vehicle
PDF_{Loc}	Probability density function of <i>Loc</i>
PDF_{M_w}	Probability density function of M_w
PDF_{PV}	Probability density function corresponding to Power output from Solar PV power plant
PDF_R	Probability density function of R
Q_D^{i,h,f_n}	Reactive power demand of the general load located at i_{th} bus at hour h of the day in the f_n^{th} year
$Q_{EV}^{iN_c,h,f_n}$	Reactive power demand of the electric vehicle load located at i_{th} bus of cluster N_c at hour h of the day in the f_n^{th} year

$Q_{flow}^{i,t}$	Reactive power flow between bus i and j at time t
$Q_{grid}^{i,t}$	Reactive power injected from the grid at i_{th} bus during time t
$Q_{HESU}^{i,t}$	Reactive power absorbed or injected from $HESU$ located at i_{th} bus at time t
$Q_{loss,l}$	Reactive power loss in line l
Q_{loss}^t	Reactive power loss at time t
Q_{PV}^{i,h,f_n}	Reactive power generated from solar power plant located at i_{th} bus at hour h of the day in the f_n^{th} year
RI	Resiliency Index
S_d	Spectral displacement
S_{Obj}	Cost of Secondary Objective function
SI	Silhouette Index
$SOC_t^{ESU,i}$	State of charge of ESU located at i_{th} bus at time t
SOC_t^{HESU}	State of charge of $HESU$ at time t
TI	Tourism Index
$V^{i,t}$	Voltage of i_{th} bus at time t
$V^{j,t}$	Voltage of j_{th} bus at time t
V_b^{HESU}	Bus voltage after installing the $HESU$ in the system
$v_{initial}$	Randomly generated initial velocity in PSO algorithm
v_{new}	Updated velocity for PSO particle
$w(t+1)$	Conditional inertia weights of PSO
X	peak ground acceleration or spectral displacement
x_{pre}	present value of x
LL^{HESU}	Percentage line loading after installing $HESU$ in the system
V_t^b	Bus voltage at time t

List of Figures

1.1	(a).Conventional Power Distribution System. (b). Future Power Distribution System	2
2.1	Solar PV penetration level of Indian states	8
3.1	Comparison of main features between Reliability and Resilience	34
3.2	Conceptual PAR risk framework	35
3.3	Comparison of Risk Analysis Framework and Resilience Framework	35
3.4	Microgrid Formation to enhance system resilience	37
3.5	Resilience Triangle	38
3.6	Ideal and Practical Resilience Trapezoid	38
3.7	System State curve for short- and long-term resiliency	40
3.8	Flowchart of Generalized Methodology to enhance system flexibility and resiliency	41
4.1	Procedure to perform Vulnerability Assessment against Earthquakes	48
4.2	The Fragility curves of (a) Electrical substation (b) Distribution line	50
4.3	Scaling factor of General Load during Summer and Winter	53
4.4	Scaling factor of Solar Power Plant	53
4.5	Procedure to Introduce load variations in PowerFactory model	54
4.6	Procedure to introduce uncertainty in PowerFactory model	55
4.7	DigSILENT PowerFactory Model of Dehradun Distribution Grid	56
5.1	Flowchart of the clustering method for mixed terrain network	59
5.2	Flowchart of Proposed Methodology	67
5.3	Optimal Charging and Discharging Characteristics of HESU during Summer (a) Li-ion ESU (b) Na-S ESU	70
5.4	Optimal Charging and Discharging Characteristics of HESU during Winter (a) Li-ion ESU (b) Na-S ESU	72
5.5	Cluster Quality Index for different number of clusters	73
5.6	Convergence of Proposed Methodology	73
5.7	Map of Dehradun district with Optimal number of clusters	74

5.8	Comparison of bus voltage profile with and without HESU in percentage	75
5.9	Comparison of CO2 Emission with only Li-ion and HESU	75
6.1	Framework to Improve Grid Flexibility and Resiliency	79
6.2	System Performance against natural disaster: without ESUs, with only ESUs, with ESUs and BIS	80
6.3	Flowchart of Algorithm I: Selection of Nodes for ESU Placement against worst and frequent Seismic hazard	81
6.4	Normalized Occurrence frequency of earthquakes in the region of study	87
6.5	Bus Voltage Profile Comparison - with and without ESU in percentage	90
6.6	Resiliency Index for various SOC levels of BIS	90
6.7	Accessible substations and distribution lines derived from Algorithm – I for Case A	92
6.8	Communication Infrastructure for HBIs	94
6.9	Flowchart of the clustering method for optimal vulnerable zones	98
6.10	Flowchart of the clustering method for optimal vulnerable zones	99
6.11	Flowchart of Algorithm III: Selection of Set of Buses and Lines	100
6.12	Cluster Quality Index of Substation for different number of clusters	102
6.13	Cluster Quality Index of Distribution Lines for different number of clusters	102
6.14	Bus Voltage Profile Comparison - with and without ESU in percentage	103
6.15	Set of Substations and Distribution Lines derived from Algorithm – III	107

List of Tables

1.1	Essential Parameters of Various ESU Technologies	3
2.1	Decision Variables and its corresponding constraints for ESU Planning	11
2.2	Methodologies designed in Literature for Optimal Planning of ESU	18
2.3	Optimal Solutions for Location and allocation of ESU & their effect on system resiliency	25
5.1	Input Parameters for Optimal Planning	68
5.2	Damage Cost Comparison	69
5.3	Distribution of EVs on Optimal Clusters based on EV Distribution Index	69
5.4	Size and Location of Optimal ESUs in Dehradun Distribution Grid	71
6.1	Predicted Peak Values of Critical/Priority-Based Loads . . .	86
6.2	Median and β_{d_s} Values Of Electrical Infrastructures For Different Damage States	87
6.3	Accessible Distribution Lines Followed by Worst Case Seismic Fault	88
6.4	Accessible Substations Followed by Worst Case Seismic Fault	88
6.5	Optimal Results of Distribution System Hardening	89
6.6	Total Size of ESU, BIS and Critical/Priority-Based Load In Optimal Clusters	91
6.7	Comparison of RI for various Resiliency Enhancement Strategies	93
6.8	Cost Comparison with Only ESUs and with BIS	93
6.9	Optimal Clusters and its Risk Possibility of Substations and Distribution Lines	103
6.10	Optimal Size and Location of ESUs	104
6.11	Optimal Locations of UCs	105
6.12	Comparison of Resiliency Index for Case A	105
6.13	Comparison of Resiliency Index for Case B	106

Chapter 1

Introduction

1.1 Overview and Motivation

Distribution system includes many components like substations, transformers, feeders, branches, nodes, circuit breakers, disconnectors, switches, protection devices, and other mechanisms to keep grid power flow to consumers. Conventionally, as shown in Figure 1.1(a), power flows from the utility to consumers through a distribution network. In the late 20th century, many researchers have proposed electric power generation within the distribution network via distribution generators (DGs), considering various technical and environmental reasons. In recent days, renewable-based DG integration is increasing to de-carbonize the grid and to create a sustainable power grid, thereby keeping a low depletion rate of fossil fuel.

Installation of wind and solar photovoltaic (PV) plants has increased in India to increase the capacity of renewable energy capacity. The world's largest renewable energy expansion program of India is aiming at introducing 175 MW of energy from RES till 2022 [1]. The introduction of renewables into the distribution grid has increased flexibility; however, it introduces various issues on the distribution grid, like stability, voltage deviation, line congestion, reactive power requirements, and other power quality issues. To address such problems and to create an interactive distribution grid, European Distribution System Operator (EDSO) proposed a future distribution grid as shown in Figure 1.1(b) [2]. Here, despite the wind and PV integration in the distribution grid, energy storage units (ESUs) play a vital role in energy management. The most viable solution considered is to place ESU in the system, which can typically store excess/surplus energy generated from the wind and can reduce the power flow congestion in the lines, voltage deviations, and spillage of wind power [3, 4]. However, the direct integration of ESUs into the distribution grid provides many distinct advantages like peak load shaving, strengthening the grid stability, increasing the probability of survivability of critical loads in case of grid failure, and balancing the forecasting deviations in renewable energy plants (REPs). For example, in

India, TATA Power has established an ESU at Rohini substation with a capacity of 10MW to manage the major challenges like peak management, effective management of renewables, and power quality [5]. Therefore, it is evident that placing ESUs in the distribution grid can improve the overall performance of the grid.

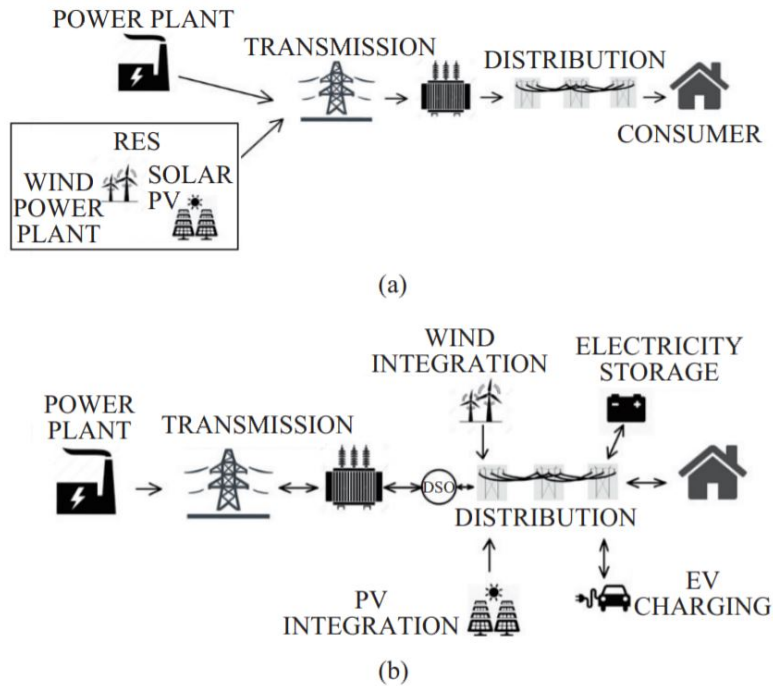


Figure 1.1: (a).Conventional Power Distribution System. (b). Future Power Distribution System

Considering the capital investment involved with the ESUs, it is economical to place the optimal sized ESUs at optimal locations in the distribution system [6]. The ESU technology preferred in most of the cases is Lithium-ion considering its high-power density. In [7], the environmental impact created by conventional sources and large-scale ESU (Lithium-ion based) is analyzed by satisfying an energy demand of 1 MWh; where the results are compared based on six ecological parameters like climate change ($\text{kg } CO_{2-eq}$), Photochemical Ozone formation ($\text{kg } NO_{x-eq}$), Freshwater Eutrophication (kg P-eq), matter formation ($\text{kg } PM_{2.5-eq}$). From the results, it is apparent that the impact created by the implementation of large-scale ESU is significant for the two parameters. However, characterization of ESUs is essential to mitigate the hazards caused during the failure of cells [8]. Therefore, given the circumstances, ESUs can carry out a significant role in improving grid performance with a considerable impact on the environment. In general, the choice of ESU technology considered is based on the electrical requirement, excluding the environmental impact created by it while planning ESU [9]. Therefore, it is essential to consider the climatic impact parameter for ESU planning

along with other parameters mentioned in Table 1.1 [10, 11].

Table 1.1: Essential Parameters of Various ESU Technologies

ESU Technology	Round trip Efficiency (in %)	Range of E/P ratio	DOD (in %)	Climate Impact(kg CO2-eq/kWh)
Na-S	75	6 — 8	80	30
Na-NiCl	86	3 — 5	85	116
Vanadium Redox	72	4 — 5	100	183
Pb-A	90	3 — 6	75	51.6
Li-ion	90	1 — 3	85	270.99

Further on, the frequency of occurrence of natural disasters has undoubtedly increased significantly compared to the past. From the official database of the National Disaster Management Authority (NDMA), India, it is evident that the country has faced seven major natural disasters between 1972 to 2000. However, this number has increased to nine between 2001 to 2010 and nineteen between 2011 to 2019 [12]. This increasing trend mandates the power system planners to improve the system resiliency at least by increasing the survivability of critical/priority-based loads. There are two major classifications of resiliency enhancement such as (i) hardening the system to improve the withstanding capacity against the disaster and (ii) operational enhancement to increase the survivability of at least critical/priority-based loads [13]. In general, measures like installation of renewable-based DGs, installation of ESUs, mobilization of repair crew, etc., strengthen the system, thereby improving the system resiliency via hardening; and measures like microgrid formation, topology reconfiguration, demand-side management, etc., improves the operational resiliency of the system. [14–27]. However, in these methodologies, there are possibilities of REPs, and ESUs failing to supply the expected energy demand (EED) during the event (natural disaster), because of the following: (i) failure of connected substations (ii) failure of distribution lines connecting critical demand, and (iii) failure of REPs and/or ESUs. Therefore, it is essential to design and place the REPs and ESUs by considering the effect of natural disasters (location specified) on top of grid parameters [28]. In [29], the proposed ESU planning strategy improves the system resiliency, however the problem restricts to satisfy partial critical loads.

In summary, the primary focus of improving resiliency is by channelizing the available distributed generation sources and storage units via partial hardening. In other words, the modified distribution system against the natural disaster serves only partial critical loads via limited feeders. Besides, there is less importance indicated for real-world constraints and

environmental aspects while planning ESUs for the distribution system.

This thesis focuses on the consideration of factors such as real-world constraints, environmental impact created by large-scale ESUs, vulnerability of electrical infrastructures, and the importance of considering the home battery inverters (HBIs) while planning ESUs for the distribution system. The first objective of this thesis is to develop the optimal configuration of ESUs to frame hybrid energy storage units (HESUs) by considering the real-world constraints on top of grid performance parameters for the renewable integrated distribution system. The second objective is to develop an optimal ESU planning methodology to enhance the short-term system resiliency under the consideration of REPs and HBIs in the system. The last objective of this thesis is to develop an optimized clustering model of the renewable integrated distribution system to enhance the long-term system resiliency by considering ESUs and HBIs spread across the system. In this thesis, earthquakes are considered as a major natural disaster; therefore, all the case studies are performed on a real-world distribution system of Dehradun district, Uttarakhand, India which comes under seismic zone IV.

From the above-mentioned primary objectives, the succeeding research questions have derived and addressed in the scope of this thesis:

- The optimal planning of ESU relies on real-world scenarios and constraints. In this context, it is essential to determine the most influencing practical parameters for ESU planning and to formulate the same in the objective function. Besides, it is essential to determine what is the impact of ESU on the environment.
- Furthermore, to utilize the large-scale ESU to its maximum potential during emergency conditions (on the occurrence of a natural disaster), it is necessary to develop a framework for optimal planning of large-scale ESUs by considering the vulnerability of electrical infrastructure against natural disasters. In this context, it is crucial to identify how the optimally placed ESUs satisfy the energy demand during emergency conditions. Moreover, it is essential to investigate the merits of considering small-scale ESUs, i.e., HBIs for resiliency studies. In other words, it is essential to investigate how to improve demand-side resiliency.
- Conclusively, it is essential to explore whether the optimally placed ESUs and the available HBIs can serve the maximum load of the system under both normal and emergency conditions.

1.2 Contributions

- **Unique methodology to quantify resiliency:** A unique methodology is developed which quantifies the performance of the

system against short and long-term resiliency.

- **A generalized framework for ESU planning** is developed to enhance both grid flexibility and resiliency. In this framework, uncertainty parameters corresponding to REPs and load (both general and storage loads), outage data, and weather data are integrated to solve the formulated optimization problem using either analytical or conventional or meta-heuristic approaches to derive the optimal planning of ESU.
- **Optimal planning of HESU:** HESUs are optimally configured by giving priority to the environment impact on top electrical constraints. The configured model is then adapted to the formulated optimal planning problem by which the grid flexibility has enhanced. This problem is formulated with real-world parameters such as (i) growth rate of renewable purchase obligation (RPO), (ii) growth rate of demand and grid-tied RES, (iii) placing the electric vehicle demand based on the survey conducted, (iv) availability of land and its associated cost to install the ESU and (v) environmental impact of ESU to obtain a realistic solution. The optimization problem is solved by applying a hybrid algorithm developed based on adaptive particle swarm optimization (APSO), binary particle swarm optimization (BPSO), and linear programming (LP).
- **Resiliency enhancement strategies:** Combining both the grid-side and demand-side strategies, two resiliency enhancement schemes are proposed in this thesis. The first scheme proposes a vulnerability constrained optimal planning of ESUs against earthquakes. In this, the optimization problem formulated combines the grid-side and demand-side strategies to formulate a mixed-integer nonlinear problem (MINLP) and derives an optimal plan for overall resiliency enhancement. In the second scheme, a three-dimensional hardening methodology against earthquakes is developed by utilizing underground cables (UCs), large-scale ESUs, and communication infrastructure for HBIs. In this, the formulated MINLP problem identifies the optimal hardening among grid-side and demand-side to improve the energy served during emergency conditions. Here, the effect of earthquakes on the electrical infrastructure is analysed using the developed Monte Carlo based probabilistic disaster hazard model.

1.3 Thesis Outline

Further, the thesis is divided into following chapters:

Chapter 2 elaborates various methodologies proposed in the literature which attempt to enhance both the grid flexibility and resiliency. In particular, methodologies concerned with ESU planning are compared to

derive the possibilities for improvement.

Chapter 3 introduces the theory behind power system resiliency and the methods to quantify resiliency. Besides, a unique methodology derived to quantify the system performance against short-and long-term resiliency is discussed.

Chapter 4 introduces the necessity of modelling the uncertainties associated with various parameters to derive the distribution system model. Furthermore, the vulnerability of distribution system components derived from the Monte Carlo based probabilistic disaster hazard model is discussed. Finally, through a case study, the procedure to implement the above-derived variables into the DigSILENT PowerFactory model is discussed.

Chapter 5 presents how the optimization problem is formulated with practical parameters & constraints for optimal planning of HESU to enhance the grid flexibility. Furthermore, the optimal operation of ESUs obtained by formulating an objective function based on arbitrage cost is discussed.

Chapter 6 presents the optimal ESU planning methodology which enhances both grid flexibility and resiliency. Here, two schemes were formulated by considering the grid-side and demand-side strategies. In both schemes, the optimization problem is formulated by considering the vulnerability of electrical infrastructure. Moreover, the benefits of improving demand-side resilience from the techno-economic viewpoint by considering HBIs are discussed.

Chapter 7 concludes the thesis and provides future directions.

Chapter 2

Literature Survey

This chapter typically focuses on the exhaustive survey carried on different methodologies for optimal planning of large-scale ESUs integrated into the distribution system. As an introduction, the integration of renewables into the grid, its benefits, and challenges are discussed. Later, various methodologies proposed in the literature towards optimal planning of ESUs were discussed, and its performance is compared with respect to the results presented in the literature.

2.1 Background Study

In recent years, considering the benefits, integration of REPs into the distribution grid is in increasing trend. In India, the integration of solar PV has increased by 370% in the last three years from around 2.6 GW to more than 12.2 GW by the implementation of plug and play model [1]. The Indian government has set the target as 175 MW for its power generation from renewable energy sources until 2022. This target was planned to achieve by installing various grid-tied solar PV plants (both rooftop and surface mount), solar thermal plants, wind energy conversion systems, etc. One of the ways implemented in India to achieve the target of solar PV is through RPO. Concerning the guidelines from the ministry of new and renewable energy (MNRE), the state electricity regulatory commission (SERC) of Indian states has directed primarily the open access customers having consumed a percentage of its total demand from renewable. For example, in Tamilnadu, India, the RPO has been raised from 9.5% to 14% within two years (from 2016 to 2018) which include the RPO from solar PV of 0.5% in the year 2016 which is increased to 5% in the year 2018 [30]. The number of solar PV installation, both rooftop standalone and grid-tied has grown tremendously in the recent years and the amount of PV injection into the power grid has become one of the major sources of power generation.

The PV market is fragmented into two major divisions. The first one includes large-scale grid-tied PV systems for utility applications which are mounted on ground. The second one includes distributed PV system

for industrial, commercial, and domestic applications which can be either off-grid or grid-tied. In India, the power rating of commercial PV systems generally varies from 5kW to 75kW and for industrial it is above 75kW. For domestic PV system, the power rating is up to 5kW. These power ratings can vary between Indian states. Therefore, it is evident that the power injection from renewable is going to be increased drastically in the coming years. While offering many benefits, renewable injection also introduces a few challenges into the distribution grid like voltage deviation, line congestion, reactive power requirement, etc. Studies in the literature have proved that grid stability is affected by the level of PV penetration into the distribution network [31]. Also, in the literature, authors have suggested penetration level for the problem considered [32–34]. Indian state renewable energy authorities have provided guidelines for penetration level of solar PV. The penetration level of various states is shown in Figure 2.1, in some states, this limit is not specified. The penetration levels of a few Indian states (which are above 30%), may lead the distribution network to a marginally stable state. For this reason, in the case of solar PV, the stability of the grid is improved by placing ESUs [35–38]. In the case of wind electrical systems, the power generated is less compared to the wind potential. The distribution system stability is affected by wind power penetration essentially due to reactive power consumption, change in X/R ratio, short-circuit capacity, energy fluctuations, and power quality [39–45]. In [46], the concept of wind rooftop is investigated to serve local demand.

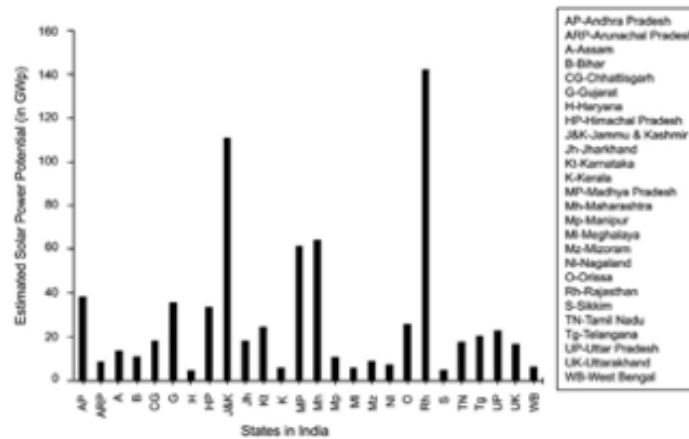


Figure 2.1: Solar PV penetration level of Indian states

In earlier days, the level of penetration of renewables (wind energy) into the power grid was limited and the utility claims the right to curtail wind energy to avoid any violations of the system constraints. Instead of spilling the surplus power generated, ESUs were deployed to store the same. The size of the ESU is calculated based on the maximum power spilled out during a specific hour [47]. Considering the capital cost of ESU, a business model with high penetration of wind energy is developed

which utilizes probabilistic optimal power flow (POPF) for minimizing the hourly society cost from the electricity market and to maximize the wind power utilization for scheduled time using the genetic algorithm (GA) [48]. Later, realizing the transformation of the distribution grid as shown in Figure 1.1, grid-tied ESUs are introduced. Considering the concept of reduced outages and the capital investment required, ESUs are optimally placed across the distribution system. For better utilization of ESU, the charging and discharging cycle length is optimized for each day using the formulated MINLP problem. Considering the energy to power ratio of various ESU technologies as shown in Table 1.1, it is evident that a single ESU technology might not satisfy the desired demand due to its limited operation. Therefore, hybrid ESU (two or more than two storage technologies integrated together) must be configured based on energy to power ratio. Since the planning of ESU can address a variety of purpose it is being formulated as an optimization problem with some constraints. Hence, it is essential to survey how the optimization problem is formulated and the methods used to solve it. By reviewing the articles in the literature, it is straightforward that the purpose of ESU planning can be categorized into the following:

- Improving Intermittency of REPs
- Network Loss Minimization
- Power Quality Improvement
- Reliability Improvement
- Increase in Arbitrage Cost
- Improving Hosting Capacity
- Resiliency Enhancement.

Hence, in further subsections, problem formulation and methodologies applied for ESU planning are discussed based on the above categorization.

2.1.1 Formulation of Optimization Problem

Optimal allocation, placement, and operation of ESUs in the distribution system are some of the most promising solutions to enhance system flexibility and resiliency. Hence, this problem is formulated as a constrained multi-objective optimization problem. In this section, an extensive study is carried out by reviewing various approaches followed in formulating this problem with reference to the objective function parameters, and its constraints.

In the literature, this problem is always formulated generally by recognizing the combined cost of ESUs as the objective function and the technical

parameters like bus voltage profile, short circuit limit, thermal limit of the feeder as constraints [6]. Later, together with the system complexity, the complexity of the objective function along with the constraints are increased to identify the optimal location, allocation and operation of ESUs under both normal and extreme conditions. A summary of decision variables and its constraints used in formulating the optimization problem is presented in Table 2.1 for the corresponding category.

In general, ESU with less energy to power ratio is mainly used for peak management whereas the one with high energy to power ratio is used to serve as a reserve power source in emergency conditions. Hence, only a single ESU technology may not provide a complete solution for the enhancement of grid flexibility and resiliency [49, 50]. From Table 2.1, it is evident that the placement of ESUs in the distribution system mainly aims to reduce the network loss, bus voltage deviation, line congestion, and for proper management of integrated REPs. To enhance the resiliency of the system using ESUs which are placed to improve the grid flexibility (without considering the effect of a natural disaster), the operation of ESUs is optimized i.e. the charging and discharging of ESUs are optimized to increase the survivability of critical loads. Besides, to enhance resiliency via hardening the ESUs were placed optimally in the distribution grids mainly by considering the cost of load shedding, estimated cost of power from the substation, and failure probability of distribution lines constrained to increase the survivability of only critical loads.

Table 2.1: Decision Variables and its corresponding constraints for ESU Planning

Classification	Objective Function Parameters	Constraints	References
Intermittency	Investment cost of ESU.	Power balance equation.	[4, 6, 47,
	The operational cost of ESU.	Capability curve limits of a conventional generator & ESU.	51-59]
	Constructional cost.	Power factor limits.	
	Maintenance cost.	Charging and discharging limits of ESU.	
	Residual of investment.	SOC limits of ESU, Budget for ESU.	
	Cost of environmental benefit from ESU.	The thermal capacity of the feeder.	
	Cost of network loss.	Short circuit limit of current.	
	Wheeling cost.	Voltage limits of the feeder.	
	Voltage deviation and its cost.	Reverse power.	
	Network loss and its cost.	Network loss with ESU is less than equal to 125% of Network loss without ESU.	
	Investment cost of RES.	The maximum number of RES and ESU.	
	Revenue generated from RES.	Customer satisfaction in kWh/year (amount of energy served per year is greater than 97%).	
	The annual cost of excess wind energy.	Real power output from RES.	
	Penalty factor.	Spinning and reserve capacity limits.	
	Real power from ESU.	Ramp-up and down of traditional generators limits.	
Cost of electricity from the external grid.	Current limits of the feeder.		
Cost of wind curtailment.	Depth of discharge of ESU.		
Cost of production and storage.	The minimum level of ESU penetration at the distribution bus.		

Classification	Objective Function Parameters	Constraints	References
Loss Minimization	<p>Real and Reactive power from ESU.</p> <p>Real power losses.</p> <p>Total energy loss in a day.</p>	<p>Real and Reactive power balance.</p> <p>Capability curve of ESU.</p> <p>Limits of power factor.</p> <p>Demand satisfaction.</p> <p>Line current limits from ESU.</p> <p>The energy of ESU should be within limits.</p> <p>The sum of energy absorbed and injected by ESU should be zero at the end of the day.</p> <p>Charging and discharging limits of ESU.</p> <p>Power balance equation.</p> <p>Voltage limits of the feeder.</p> <p>Real power from solar PV must be within limits.</p> <p>SOC of ESU must be within limits.</p>	[9, 60–63]
Power Quality Improvement	<p>Cost of the aggregate outage:</p> <ul style="list-style-type: none"> • The energy capacity of ESU. • The power rating of ESU. <p>Bus voltage quality.</p> <p>Power discharged from ESU.</p> <p>Charging power for ESU.</p> <p>Investment cost of ESU.</p> <p>O&M cost of ESU.</p> <p>Cost of loss due to solar PV and ESU</p>	<p>The total budget for ESU.</p> <p>Power balance equation.</p> <p>Maximum energy derived from individual ESU.</p> <p>Maximum energy stored in individual ESU.</p> <p>Power injected from solar PV must within limits.</p> <p>Capability curve limits of solar PV.</p> <p>SOC of ESU must be within limits.</p> <p>Power and energy rating must be within limits (Solar PV and ESU).</p> <p>The ratio of nominal power to energy must be within 0.1 to 8.</p>	[64–66]

Classification	Objective Function Parameters	Constraints	References
Reliability Improvement	<p>Bus voltage deviation and its cost.</p> <p>The minimum size of the battery.</p> <p>Distribution Network losses and its cost.</p> <p>Grid electricity cost.</p> <p>Location of ESU.</p> <p>Size of ESU.</p> <p>Expected cost for the interruption.</p> <p>Cost of storage device as a function of its capacity.</p> <p>Cost of generation from RES.</p> <p>Cost of power purchased.</p> <p>Investment cost of ESU.</p> <p>O&M cost of ESU.</p> <p>Residual cost.</p> <p>Cost of line congestion.</p> <p>Cost of DG, including its startup cost.</p> <p>Cost of load curtailment.</p> <p>Discharging and charging the cost of ESU.</p>	<p>Capability curve of ESU & DG.</p> <p>The maximum number of nodes in which ESUs can be installed.</p> <p>The total power rating of ESUs to be installed.</p> <p>The maximum power rating of individual ESU.</p> <p>Voltage limits of the feeder.</p> <p>Balanced Load flow.</p> <p>Power balance equation.</p> <p>Normalized impact factor for outages of generator and line must be within limits.</p> <p>Power generation limits.</p> <p>The increase and decrease of change in power are within its specified limits.</p> <p>Optimization is performed only for a specific number of hours h (time period for which deviation occurs).</p> <p>Current limits of the feeder.</p> <p>Power limits of a substation transformer.</p> <p>Operational limits of DG.</p> <p>Charging and discharging limits of ESU.</p> <p>State of Charge (SOC) limits of ESU.</p> <p>Load shedding limits.</p> <p>Annual benefits of peak shaving & load shifting.</p>	[67–75]

Classification	Objective Function Parameters	Constraints	References
Reliability Improvement	<p>Net Present Value (NPV) of energy losses, system upgrade, and arbitrage.</p> <p>Cost of undelivered energy:</p> <ul style="list-style-type: none"> • Average energy demand. • Failure rate. • Outage time. • Cost of penalty for undelivered energy. <p>The replacement cost of ESU.</p> <p>Expected cost for daily operation.</p> <p>Cost of reactive power:</p> <ul style="list-style-type: none"> • Reactive power loss. • Trade-in reactive power. <p>Cost of feeder loading.</p> <p>Investment cost of the feeder.</p> <p>Cost of interfacing device (need to interface ESU with grid).</p> <p>Load deviation.</p> <p>The capacity of ESU.</p>	<p>Energy stored in ESU per day is within limits.</p> <p>Conventional generator ramp limit.</p> <p>The budget of ESU and its location.</p> <p>Reverse power from ESU must be within limits.</p> <p>Wind power injected must be within limits.</p> <p>Solar power injected must be within limits.</p> <p>Reactive power support from the capacitor bank must be within limits.</p> <p>The transformer tap position must be within limits.</p> <p>Limits of the depth of discharge of ESU.</p> <p>The voltage unbalance factor must be within limits.</p> <p>The power and energy rating of ESU must be within limits.</p> <p>Real and reactive power limits of the feeder.</p> <p>The budget limit for network extension.</p> <p>Real Power balance equation.</p>	[49, 76–95]
Arbitrage Cost	<p>Generation cost.</p> <p>Start-up and shut-down cost of reserve units.</p> <p>Cost of operation of ESU.</p>	<p>Limits if reserve capacity.</p> <p>Limits of ESU capacity.</p> <p>Capability curve limits of both unit reserve and ESU.</p>	[96, 97]

Classification	Objective Function Parameters	Constraints	References
Arbitrage Cost		<p>SOC limits of ESU.</p> <p>Power balance equations.</p> <p>Voltage limits of the feeder.</p> <p>Power and Energy rating of ESU is within limits.</p> <p>Charging and discharging cycle efficiency of ESU is equal to the square root of overall round-trip efficiency.</p>	[96, 97]
Hosting Capacity	<p>Cost of ESU.</p> <p>Cost of network loss.</p> <p>Cost of voltage regulation.</p> <p>Cost of peak demand.</p> <p>Cost of power generation from ESU.</p> <p>Network loss function.</p>	<p>Voltage limits of the feeder.</p> <p>The voltage unbalance index is within limits.</p> <p>Power and Energy rating of ESU is within limits.</p> <p>Real and reactive power limits of ESU.</p> <p>Current limits of the feeder.</p> <p>SOC of ESU is within limits.</p> <p>The discharge rate of ESU is within limits.</p>	[98–100]
Resiliency	<p>Cost of interruption due to grid failure.</p> <p>Unreachability of the load center.</p> <p>The investment cost for enhancing resiliency.</p> <p>The operational cost of AC & DC – DGs.</p> <p>Start-up and shut-down cost of AC & DC – DGs.</p> <p>Arbitrage benefits.</p> <p>The penalty of load shedding.</p>	<p>Demand satisfy with PV+ESU.</p> <p>Limits for change of energy stored in ESU.</p> <p>Power generation limits of PV.</p> <p>Limits of the depth of discharge of ESU.</p> <p>Start-up and shut-down of the generator.</p> <p>Limits of feeder capacity.</p> <p>SOC of ESU must be within limits.</p> <p>Charging and discharging limits of ESU.</p> <p>Load curtailment is allowed.</p> <p>A maximum possible real power shift during a time period must be within limits.</p>	[14, 101]

Classification	Objective Function Parameters	Constraints	References
Resiliency	<p>Response during pre-event:</p> <ul style="list-style-type: none"> • Price of electricity generation. • Cost of load shedding. <p>Response during the event:</p> <ul style="list-style-type: none"> • Load shedding. <p>During post-event:</p> <ul style="list-style-type: none"> • Load shedding. <p>Estimated load shedding.</p> <p>Estimated buying power from the substation.</p> <p>The estimated cost of power from RES.</p> <p>Estimated cost for hardening power lines:</p> <ul style="list-style-type: none"> • Cost of overhead lines. • Probability of its failure. • Wind – load probability. <p>Cost of load loss.</p> <p>Cost of electricity price.</p> <p>Cost of electricity generation from DGs.</p>	<p>Operational limits of both DC and AC DGs.</p> <p>The power balance between buying and selling.</p> <p>Survivability of critical loads.</p> <p>Power balance equation.</p> <p>The ramp rate of generators.</p> <p>Power flow limits of a transmission line.</p> <p>Voltage & phase angle limits.</p> <p>Branch currents must be within limits.</p> <p>Load shedding must be less than the maximum demand.</p> <p>The system considered must be radial.</p> <p>Energy exchange between AC & DC DGs must be within limits.</p>	<p>[22, 24, 102–104]</p>

From the chosen decision variables and constraints in the literature, it is apparent that the optimization problem is mainly formulated concerning to electrical parameters and very less importance is given to practical constraints such land availability in the obtained optimal location, uncertainty in REPs and load, engagement of RPOs, and environmental impact created by ESUs.

2.1.2 Methodologies designed for Optimal Planning of ESUs

As mentioned, initially, the optimization of ESUs is performed to decrease the spilled energy from renewable [47], later this method is also applied to enhance system resiliency [14]. Hence, various methods employed to solve both kinds of problems are illustrated here. There are various procedures followed in the literature to solve this problem by using analytic, conventional optimization, meta-heuristic, and hybrid combinational optimization. Based on the formulation of the objective function and its constraints mentioned in Table 2.1; the applicability of various algorithms to solve problems such as siting, sizing, and operation of ESUs is listed in Table 2.2 according to the problem categories. The prime objective under normal conditions is to optimally place ESU by satisfying technical and economic parameters considering various constraints. However, the objective function under the disastrous condition is to enhance resiliency by maximizing critical demand satisfaction.

In most of the articles mentioned in Table 2.2, RES is considered during extreme conditions to increase the survivability of critical loads, but considering the most realistic situation during extreme weather conditions, authors of [23] have made RES out of service. In the ESU planning methodology, it is essential to consider the effect of natural disasters on the location where the ESU is to be placed. However, from Table 2.1 and Table 2.2, it is evident that most of the formulated problem did not address the location constraint against natural disaster. Therefore, this way of ESU planning might not satisfy the energy demand during extreme conditions.

Table 2.2: Methodologies designed in Literature for Optimal Planning of ESU

Category	Ref	Test System	Grid-Setup			Technique			Applied for		
			REPs	Capacity	Algorithms	Purpose	Si	St	Op		
<i>Intermittency</i>	[6]	17 node system radial system	WPP & Biomass	2 MW & 1 MW	GA & DP	For generating the initial population for both sizing and siting. To estimate the optimal profile of ESU	✓	✓	✓	×	
	[52]	IEEE node distribution system	34 ×	×	GA & AC-OPF	The initial solution for optimal location size of ESU. Evaluate the objective function	✓	✓	✓	×	
	[51]	LV distribution system in Yazd, Iran	Solar PV	×	GA & LP	Optimal number and location of ESU. Optimal charging and discharging of ESU	✓	✓	✓	✓	
<i>Loss minimization</i>	[105]	16 bus distribution system	Solar PV & WPP	2.5 MWp & 6 MW	PSO & OPF	Forecasting Wind, Solar PV and Load . Optimal location of ESU	×	✓	×	×	
	[106]	41 node radial distribution system	WPP	(3 × 10) MW	GA & OPF	Optimal charging and discharging hours of ESU. Evaluate the objective function.	×	×	×	✓	

Category	Ref	Test System	REPs	Grid-Setup		Technique			Applied for		
				Capacity	Algorithms	Purpose	Si	St	Op	Si	St
	[100]	Ontario distribution system	WPP	(5 × 1.98) MW	OPF (Sensitivity Analysis)	Optimal location & size of ESU	✓	✓	✓	✓	×
	[70]	IEEE 33 bus system	WPP & Solar PV	(2 × 1) MW, (3 × 400) kVA, (4 × 500) kVA	ABC	Optimal location of ESU	×	✓	✓	×	
	[63]	69 bus radial distribution system	Solar PV	3 MWp	IHSA	Optimal operation of PV integrated system	×	✓	✓	✓	
	[61]	CIGRE low voltage distribution grid	Solar PV	36 kWp	DP	Optimal operation of ESU via minimum loss	×	×	×	✓	
<i>Power Quality Improvement</i>	[54]	IEEE 8500 node system	Solar PV	×	GA & LP	The initial solution for sizing ESU. Evaluate the objective function for optimal siting.	✓	✓	✓	×	

Category	Ref	Test System	Grid-Setup			Technique			
			REPs	Capacity	Algorithms	Purpose	Applied for		
							Si	St	Op
	[98]	IEEE 33 bus system	WPP & Solar PV	(2 × 1) MW, (3 × 400) kVA, (4 × 500) kVA	IPA	Optimal charging/discharging and size of ESU	×	✓	✓
	[66]	69 node distribution system	Solar PV	(125 - 1250) kWp	OPF based SOCP	Optimal sizing and location of ESU	✓	✓	×
<i>Reliability Improvement</i>	[82]	Modified IEEE 33 bus system	WPP & Solar PV	400 kW, 420 kWp	Multi-subgroup hierarchical chaos hybrid algorithm	Optimal capacity of ESU	✓	✓	×
	[90]	IEEE 34 bus system	Micro-wind, & Solar PV	×	Clustering and Sensitivity analysis	Optimal sizing of ESU	×	✓	×
	[67]	IEEE 13 node system	Solar PV	(4 × 400) kWp	BD	Optimal location and size of ESU	✓	✓	×
	[107]	94 Portuguese radial distribution system	node ×	×	NSGA-II	Improved reliability parameters such as MAIFI and SAIDI by optimal siting and sizing of ESU	✓	✓	×

Category	Ref	Test System	Grid-Setup			Technique				
			REPs	Capacity	Algorithms	Purpose	Applied for			
			bus	WPP & Solar PV	PSO	Optimal capacity of ESU	Si	St	Op	
<i>Arbitrage Cost</i>	[72]	13 distribution system	bus	WPP & Solar PV	PSO	Optimal capacity of ESU	✓	×	×	
	[96]	IEEE 34 bus system	bus	WPP	(2 × 300) kW BBA	Optimal siting, sizing and operation	✓	✓	✓	
	[97]	IEEE 33 bus system	bus	WPP & Solar PV	(3 × 200) kW, (2 × 100) kW, 200 kWp,250 kWp,300 kWp,350 kWp	GA & OPF	To determine the optimal location and size of ESU (framed as outer optimization). To evaluate the inner objective function.	✓	✓	×
<i>Hosting Capacity</i>	[108]	IEEE 14 bus system	bus	WPP	×	OPF with quadratically constrained	Optimal location of ESU	×	✓	×
	[48]	IEEE 24 bus system	bus	WPP	1500 MW	GA	Optimal location of ESU	×	✓	×
	[109]	IEEE 33 bus system	bus	Solar PV	8 × (500 – 800) kWp	OPF Sensitivity Analysis	& Optimal size and location of ESU	✓	✓	×

Category	Ref	Test System	Grid-Setup			Technique			Applied for		
			REPs	Capacity	Algorithms	Purpose	Si	St	Op	Si	St
<i>Resiliency</i>	[14]	IEEE 33 bus system	WPP	5 MW	MINLP	Optimal Placement of WPP	×	✓	×	✓	✓
	[22]	Hybrid microgrid system	Solar PV	×	MILP	Optimal operation of microgrid	×	×	×	×	✓
	[102]	IEEE 33 bus system	WPP, Solar PV, Microturbine	(3×0.8) MW, 0.5 MWp, (2×3) MW, (2×2) MW	MIQCQP	Optimal operation of the power grid during natural disaster (wildfire)	×	×	×	×	✓
	[23]	IEEE 30 & 118 bus system	×	×	Markov Monte Carlo Simulation	Optimal operation of power grid during extreme condition	×	×	×	×	✓
	[24]	User-defined Microgrid	×	×	Two-step adaptive robust optimization	Optimal operation of the microgrid	×	×	×	×	✓

2.1.3 Performance of the methodologies proposed in the literature

The performance of the methodologies mentioned in the section 2.1.2 is reviewed based on the value of objective function parameters mentioned in Table 2.1. From the results obtained in the literature, these parameters are broadly clustered into technical and economic parameters. Major economic parameters are investment cost, cost of energy imported and exported, cost of outages, and cost of outages. Major technical parameters are the number of optimal locations to place ESU, total energy loss, voltage deviation, and loss reduction. To understand the problem towards system resiliency, two parameters are proposed in this thesis namely, direct impact (DI) and indirect impact (IDI). These parameter are used to identify the impact created by the optimization of ESU to enhance the system resiliency.

The parameter DI is defined as – “*distinct efforts towards improving the survivability of the load, and disaster data along with the restoration strategy applied is fed back for further analysis which can be utilized for future purpose*” and the parameter IDI is defined as – “*considering the generation and demand level, part of the load is curtailed to ensure the system stability and reliability. This is termed as IDI because, during the event (any outage), a part of the system load is satisfied*”. The results of the optimization problem from various research articles based on DI and IDI are listed in Table 2.3, along with the horizon (time of event/operation) considered.

Each optimization results of various methodologies proposed in the literature are categorized in terms of system resiliency using two impact parameters as defined above; from which it will be easier to identify the best suitable approach to enhance system resiliency. For easing the comparison, Table 2.3 is clustered into three categories, namely standard bus system, user-defined bus system, and real-time bus system. From the point of the optimal number of ESUs considering the standard bus system, with 13 to 15 nodes, the optimal number of ESUs is 5, which is obtained using BDA [67]. For 30 nodes, the optimal number of ESUs is six, which is obtained using combinatorial optimization with Bus Impact Severity analysis and GA [71]. The optimal number of ESUs for 33 nodes is 3, obtained by using the genetic algorithm and optimal power flow [97]. For large bus system, the optimal number of ESUs entirely depends on the circumstances considered. For instance, in [57], IEEE 906 bus system is considered; where the optimal number of ESUs obtained is two. This is mainly due because the system considered has high renewable energy penetration. In few articles, the maximum number of ESUs is fixed by the authors; for example, in [69], the maximum number of ESUs to be installed is set as 3. However, the optimal locations of three ESUs are found using genetic algorithm.

From sizing point of view, the optimal size of ESUs varies in the literature even for the same system; because of the different load being considered. Also, in few articles, authors have limited the size of ESU by assuming the maximum and minimum limits. For example, in [69], the authors have assumed that the total power of ESUs (sum of the power level of all ESUs) is equal to 600 kW, and its energy storage capacity is considered to be 3 MWh.

From Table 2.3 and the above discussion, for small system (with fewer nodes), benders decomposition algorithms prove to be promising in obtaining an optimal number of ESUs; whereas, for larger node system, genetic algorithm combined with optimal power flow algorithm and NSGA-II algorithm is more suitable in finding the optimal location of ESUs. This is evident from the literature that BD technique is applied to solve ESU planning problem for standard system with less complexity because this technique will get converged only if the subproblems are convex in nature. For larger system it is complicated to decompose the primary function into subproblems, which may be convex in nature. Also, it is apparent from the literature that NSGA II sorts the population into various non-dominated levels, which reduces the complexity of the problem. Hence it can be better suitable to solve larger systems. For optimal allocation of ESUs in a small network, genetic algorithm and mixed-integer programming are best suitable; whereas for a larger system, combinatorial algorithms (combining two algorithms) are more suitable. For optimal operation, conventional optimization algorithms are more appropriate.

Table 2.3: Optimal Solutions for Location and allocation of ESU & their effect on system resiliency

Ref	Test System	Opt ESUs	Obj fun value		Size of ESUs	Algorithm	SR		Horizon
			Without ESU	With ESU			DI	IDI	
[67]	IEEE 13 node system	5	×	Total voltage deviation with an amplitude of 13400 During winter: cost of energy – 84.2 p.u.\$/day and Energy loss is 3.1 MWh/day; During summer: cost of energy – 79 p.u.\$/day and Energy loss is 2.8 MWh/day	631 kVA; 290 kVA; 365 kVA; 250 kVA; 464 kVA	BD algorithm	×	✓	Not mentioned
[69]	IEEE 13 node system	3	×	During winter: cost of energy – 23.4 p.u.\$/day and Energy loss is 2.9 MWh/day; During summer: cost of energy – 15.6 p.u.\$/day and Energy loss is 2.1 MWh/day Cumulative arbitrage revenue under scenario II is 171.11 k\$; 342.15 k\$ and 342.15 k\$	66 kW, 200 kW, 334 kW	GA + AC-OPF	×	✓	24 hours with an interval of 2 hours
[48]	IEEE 24 bus system	1; 2; 3	×		1200 MWh, 1000 MWh	Probabilistic OPF + GA	×	✓	24 hours with an interval of one hour

Ref	Test System	Opt ESUs	Obj fun value		Size of ESUs	Algorithm	SR		Horizon
			Without ESU	With ESU			DI	IDI	
[71]	IEEE 30 bus system	6	×	Predefined Bus impact severity is 18 with NISF of 1.29577	0.1 MW, 0.025 MW, 0.025 MW, 0.075 MW, 0.05 MW, 0.05 MW	Bus impact severity analysis + GA	×	✓	Not mentioned
[97]	IEEE 33 bus system	3	×	Revenue from load shifting and loss reduction is 312.57 k\$ and 271.09 k\$ respectively For uniform ESU size of 0.724 MVA the % index of VD and LLT are 89.73 and 269.81 respectively	426 kWh, 379 kWh, 277 kWh, 522 kWh, 513 kWh, 435 kWh	GA + OPF	×	✓	24 hours with an interval of one hour
[70]	IEEE 33 bus system	8; 11		% index of VD and LLT are 89.73 and 269.81 respectively 75.753 and 241.128 respectively;	0.724 MVA; 0.335 0.378 0.383 0.823 0.1 0.128 0.1 2 1.442 0.725 0.781 (MVA)	ABC algorithm	×	✓	24 hours with an interval of one hour

Ref	Test System	Opt ESUs	Obj fun value		Size of ESUs	Algorithm	SR		Horizon
			Without ESU	With ESU			DI	IDI	
[103]	IEEE 33 bus system	2	×	For non-uniform ESU size, the % index of VD and LLT are 72.162 and 240.039 respectively. Restoration of disconnected loads is increased by 31.6% The emission level is reduced by 26.6 % for case 2 & 100kWh	400kWh	Greedy Search algorithm	✓	×	5 hours with one-hour interval
[4]	IEEE 33 bus system	5		Total system cost in \$/year is 9,625,602.547 (for case2) & 9,335,552.338 (for case3)	2424, 2731, 18312, 15196, 5739 (kWh) (case2); 2590, 2537, 7117, 2954 (kWh) (case3);	MILP	×	✓	24 hours with an interval of one hour

Ref	Test System	Opt ESUs	Obj fun value		Size of ESUs	Algorithm	SR		Horizon
			Without ESU	With ESU			DI	IDI	
[96]	IEEE 34 bus system	3	The reserve capacity is insufficient to trace the demand	The required reserve capacity is satisfied. Depending on demand the ESUs are placed at 2 to 5 buses to with the per-unit cost of load ranging between 663.6 \$/MWh to 1012.7 \$/MWh	3×0.6 MWh	BBA	\times	\checkmark	24 hours with an interval of one hour
[110]	Hybrid microgrid (user-defined)	1	\times	Total hybrid system cost varies between 6.15 – 7.69 M\$	Varies between 838.96 to 1101.6 kWh	ARMA+ Self-adapted evolutionary strategy (SAES)+FBA	\times	\checkmark	Not mentioned

Ref	Test System	Opt ESUs	Obj fun value		Size of ESUs	Algorithm	SR		Horizon
			Without ESU	With ESU			DI	IDI	
[22]	Hybrid microgrid (user-defined)	2	×	Load shedding is reduced 63.03% (assessing feasible islands) & 68.15% (assessing the survivability) An average increase of 17.4% in the budget to meet the operational uncertainty during the event	200 kW (DC-ESU); 100 kW (AC-ESU); & MILP	✓	×	2	5 hours with 15 minutes interval
[24]	Hybrid microgrid (user-defined)	2	×	17.4% in the budget to meet the operational uncertainty during the event	800kW, 980kW; 300kW, 350kW; 40kW, 50kW	Two-step Adaptive Robust Optimization	✓	×	5, 8, & 10 hours with a time interval of 2 hours
[35]	17 bus system	0;1;2;2	×	Daily losses in MWh are 1.417 (case1);1.394 (case2);1.287 (case3);1.297 (case4)	Case2: 1×250 kW; Case3: 3×500 kW, 1×500 kW; Case4: 3×500 kW, 500 kW, 250 kW;	GA + SQP-OPF	×	✓	24 hours with an interval of one hour

Ref	Test System	Opt ESUs	Obj fun value		Size of ESUs	Algorithm	SR		Horizon
			Without ESU	With ESU			DI	IDI	
[47]	41 node rural distribution system	5	5.11 million dollars	4.68 million dollars	19.48 MWh, 12.99 MWh, 8.44 MWh, 4.55 MWh, 6.49 MWh	ARMA + OPF	×	✓	24 hours with an interval of one hour
[106]	41 bus rural distribution system	3	×	Revenue generated - 1298\$/4-days; 1277\$/4-days; 918\$/4-days	1.948 MVA, 1.299 MVA, 0.455 MVA	Search algorithm + OPF	×	✓	24 hours with an interval of one hour
[73]	69 bus radial distribution system	1	The significant deviation is seen at bus 61	Voltage deviation is zero at bus 61	2 MW	BFA	×	✓	Not mentioned
[86]	Modified GE distribution system	7	Operation time of OLTC & SVR is close to 4000	Operation time of OLTC & SVR is between 1500 to 3500 depending upon the capacity of ESU	Varies between 0.5 p.u to 5 p.u	OPF	×	✓	5 hours with an interval of one hour

2.2 Closing Remarks

From the literature, it is clear that the decision variables and constraints are chosen for the optimization problem mainly focuses on the electrical parameters. For example, with the optimal planning methodology from the literature, the ESU may satisfy the demand as required. However, to achieve this, it is crucial to have adequate land space available for installing the ESUs as per the planning. Since the emission from ESU leads with significant damage to the environment, it is essential to consider the environmental impact created during planning. The ESU location is not constrained with the effect of the natural disaster. In other words, the ESU placement problem in the literature does not highlight the effect of natural disasters on the location in which the ESU is to be placed.

Therefore, to create an interactive grid which can withstand the impact of natural disasters and the changing load pattern of present and future scenario, it is crucial to redesign the planning methodology considering the real-world decision variables and constraints applied for the distribution grid.

Chapter 3

Power System Resiliency

This chapter introduces the concept of power system resiliency, various ways to recognize the system performance during emergency condition. A unique method proposed to quantify the system performance for short- and long-term resiliency is discussed. Besides, a proactive methodology is proposed to enhance the system resiliency using ESUs. This chapter is based on journal publication [28].

3.1 Introduction

The electric grid is a widely spread asset which has a great impact on the livelihood of the people. Therefore, it is essential that the power grid recovers as quickly as possible with minimal damage after any outage (including both intentional and unintentional). In recent years, the occurrence of natural calamities has increased compared to the past due to many reasons. From the database, it is evident that the power distribution system is more vulnerable against disasters. This situation mandates power system planners to improve the system resiliency which leads to serve at least the critical loads of the system during emergency condition. In this view, many researchers have attempted to enhance the resiliency considering various disasters such as windstorms, floods, wildfires, earthquakes, and icing. In some articles, the authors have enhanced the system resiliency by considering a generalized outage due to disaster [20, 22, 24, 104].

In [103], available microgrids across the distribution system have been utilized to improve the system resiliency via minimizing the loss of load during the hurricane. Here, the intensity of the hurricane and its uncertainty is modeled to identify the possible affected lines across the system. In [102], an operational strategy to enhance the resiliency of a distribution system against wildfires is proposed. Here, an optimal operation of the system during the event is achieved by minimizing the load shedding cost, generation of microturbines, the cost of grid power, and start-up and shut-down cost of microturbines by considering the uncertainty of wildfires. In [111], a system restoration scheme against

floods modeled using rainfall and wind speed data is proposed. Here, the uncertainty of the flood is introduced using Sequential Monte-Carlo simulation and thereby the component to be restored is identified. In most of the articles, the system resiliency enhancement strategy is proposed for a defined or targeted emergency response time (ERT). Typically, the system resiliency is enhanced based on parameters such as load loss probability (LOLP), expected energy not satisfied (EENS), line outages during the event (ELO) [112, 113]. To improve the understanding of power system resiliency, its definition and parameters to quantify resiliency are discussed further.

3.2 Definitions for Resilience

The term resilience originates from a Latin word “resilio” which refers to the ability of an object to recover or regain to its original state or situation after exposing to an event. The concept of resilience is defined in many fields like Infrastructure, economic, social, organizational systems. For instance, in economic systems the resilience is defined as “*the response to hazard that enables people and communities to avoid some economic losses at micro-macro market levels. It is the capacity for the enterprise to survive and adapt following market or environmental shocks*”.

In the context of power system, the definition for resiliency given by the IEEE task force is “*the ability to withstand and reduce the magnitude and/or duration of disruptive events, which includes the capability to anticipate, absorb, adapt to and/or rapidly recover from such an event*” [114]. Apart from this, UK Energy Research Center defines resilience as “*the capability of the power system to endure turbulence and continue to provide energy services by quickly recuperating from disturbance*” [115]. National Infrastructure Advisory Council (NIAC) defines a more generic definition of resilience applicable to any critical infrastructure which considers the lessons learnt from destabilizing events and adjust the system’s operation; and it also proposes a framework to restrain the effect of event in the future. Apart from this, NIAC proposes the main properties of resilient grid such as resistance, reliability, redundancy and recovery [116]. The Stockholm resilience center, Sweden defines resilience of a system is its ability to continually change and adapt yet stay within critical thresholds [117]. The United Nation-International Strategy for Disaster Reduction, Geneva, defines resilience as the system’s ability which is exposed to an event, to adapt through resistance or change to attain and retain a reasonable performance [118].

There are many definitions provided in the literature and are interminable; nevertheless, most of them focus on the system’s anticipatory capability, absorb the disturbance created by the event and recover from the shocks created by the event. Therefore, it is evident that a resilient power system

should anticipate the event resulting from severe weather conditions, absorb the event i.e. the ability of the system to minimize the damage brought by the event, recover from the event i.e. the ability to modify its damaged functions resulted from the event and also prepare itself for the upcoming event.

With reference to power system reliability, many attempts were made in literature to differentiate resilience from the reliability. Traditionally, the power system is mainly driven by reliability indices through normal conditions and expected emergencies. Figure 3.1 shows the important differences between reliability and resilience.

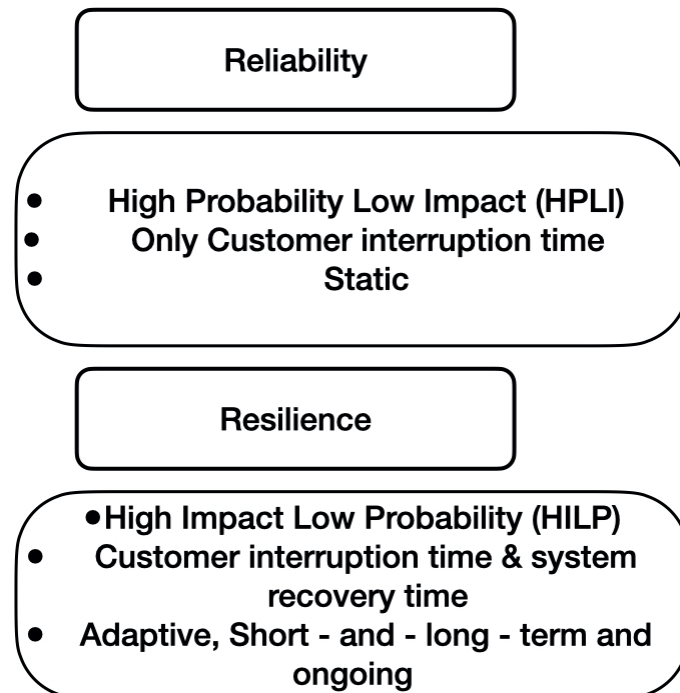


Figure 3.1: Comparison of main features between Reliability and Resilience

3.3 Comparison of Risk and Resilience Framework

Generally, in power system, based on the type of hazard and vulnerability of the system, risk assessment will be performed in the context of both system behavior and the physical characteristics as shown in Figure 3.2. This figure shows the conceptual PAR risk assessment framework proposed by Wisner [119]. Here, the disturbance caused by the event is categorized under four different parameters like probability of the disturbance, severity of the disturbance, system vulnerability and the system capacity which can absorb the disturbance. Therefore, understanding the nature of risk and

its consequence and the disturbances created to the system is a part of risk assessment procedure.

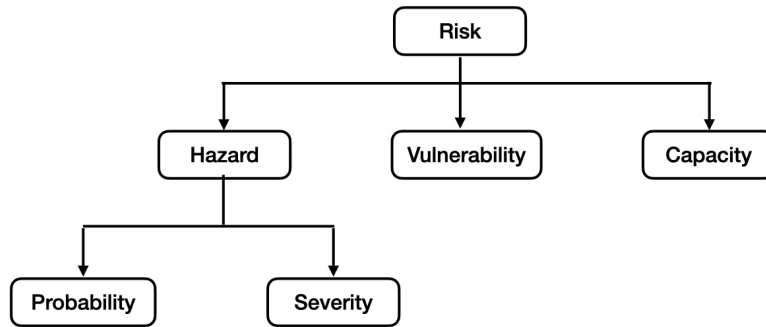


Figure 3.2: Conceptual PAR risk framework

In the context of power system resilience, in addition to the risk assessment, it is essential to frame the timely actions to be performed to protect the operational capability of the system against risk, perturbations and threats. Therefore, as mentioned in the previous section 3.2, the power system resilience must be more holistic, rigorous and dynamic than the risk assessment procedure. A comparison between resilience framework and risk assessment framework is shown in Figure 3.3 [120].

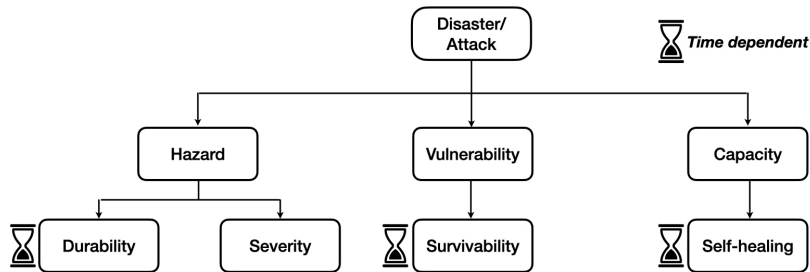


Figure 3.3: Comparison of Risk Analysis Framework and Resilience Framework

From Figure 3.3, it is evident that on top of the knowledge about the probability and severity of the hazard, it is essential to understand that how long the system will be exposed to the hazard. For example, longer the duration of disaster, the damage caused on the grid will be more. Therefore, the resilience of the system mainly depends on the reaction time followed by an event. In other words, a resilient power system must have the time-dependent characteristics like durability, survivability and self-healing. However, it is very difficult to predict the time duration for which the system will be exposed to an event. Therefore, in most of the resiliency enhancement strategies mentioned in the literature (as explained in the next section 3.4), the system performance is improved for the targeted exposure time.

3.4 Resiliency Enhancement Strategies

There are many preventive and restorative strategies/plans proposed in the literature to enhance the system resiliency. Most of the power system planner across the world realized the necessity of taking measures to enhance the system resilience against HILP events. The most popular strategies proposed in the literature are based on grid partitioning i.e., breaking the distribution system into many islands thereby by building AC and DC microgrids via adopting renewable based distribution system using intelligent control systems. These measures are broadly classified into two categories such as short-term and long-term. The measures taken towards improving short-term resilience are (i) proper weather forecast at the location and its severity aiming to minimize the generation in the most vulnerable areas, (ii) Implementing high number of recovery crews to act as quickly as possible, (iii) providing the backup for critical equipment for rapid replacement and (iv) other preventive actions. The measures taken towards improving the long-term resilience mainly focuses on grid hardening. In other words, increasing the strength of the system by implementing underground cables, building more transmission lines or relocation of transmission lines in the less-affected areas and demand side management by including the energy storage systems. These measures are largely focused on utilizing the available resources across the system.

In [121], the resilience of a microgrid which consist of REPs like solar PV, wind generators, microturbines, fuel cells and one main storage unit. Here, the resilience of the system is improved by coordinated operation between the EVs (utilized as the storage system) and the demand. In [26], the load restoration method based on microgrid formation is proposed to enhance the system resiliency. Here, the microgrid formation problem is formulated as MINLP problem by considering the power loss, voltage constraints, power balance and operational feasibility. In [27], a dynamic microgrid is formed based on MINLP problem which optimizes the various technologies like REPs, ESUs and other DGs within the microgrid. In [122], an optimal sizing and siting of ESUs and Solar PV is proposed to improve the system resilience by considering the investment and operation cost, electricity demand, and the power generated from non-black start generators. In [14], the system resilience is enhanced by optimal allocation of wind turbines and the reconfiguration of the system by considering the failure probabilities of system components due to natural disaster. Here, the optimization problem is formulated by considering the cost of load shedding, power generation and hardening cost of transmission lines constrained with power balance, power flow, current limits and system radiality. Therefore, it is evident that most of the enhancement strategies utilizes the available energy resources to form microgrids for coordinated demand response as shown in Figure 3.4 [120].

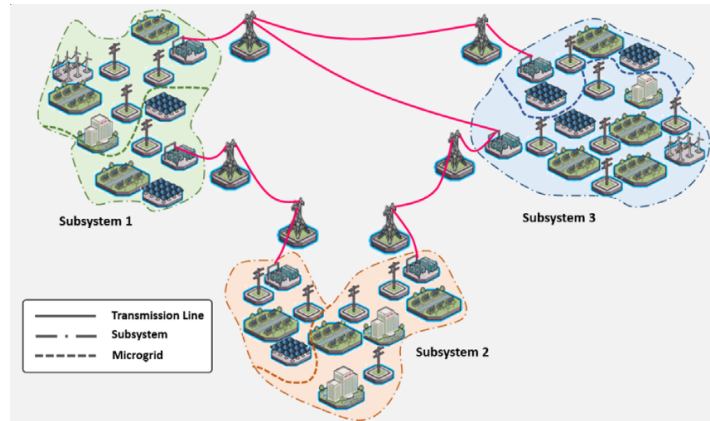


Figure 3.4: Microgrid Formation to enhance system resilience

3.5 Metrics to Quantify Resiliency

There are various ways in which the system resiliency can be enhanced; however, the performance of the enhancement strategy proposed is validated using the resiliency metrics. However, there is no clear methodology or set of metrics which quantifies the hardening and operational resiliency [123]. In the literature, many metrics to measure the system performance are proposed based on the resilience triangle and resilience trapezoid as shown in Figure 3.5 and 3.6, respectively [124–126]. In Figure 3.5, the triangle depicts the loss of the system functionality during the event. In other words, a fully functional system fails to serve the demand of the system from the time of event occurrence (t_{oe}) and continues to recover throughout the event and becomes fully functional at the end of the interruption (t_{ee}). The area of the triangle highlighted in Figure 3.5 indicates the energy demand is not satisfied during the event. Hence, a system having less triangular area is more resilient. In the resilience triangle approach, the slope of the hypotenuse defines how fast the system is being recovered by implementing the enhancement strategy. Although this approach can effectively apprehend the recovery of the system after an event, it fails to capture the critical dimension on how fast the system degrades once the disaster hits the infrastructure.

The traditional resilience triangle is extended to resilience trapezoid by introducing multiple phases to be faced by the power system during the event, such as disturbance progress, degraded system state, and restoration state [127]. The ideal expectation and practical system performance during the multiphase are shown in Figure 3.6. The shape of the triangle's hypotenuse and the lateral side of the trapezoid can vary depending on the effectiveness of the resiliency strategy (both operational and hardening). For instance, by implementing the effective hardening resiliency, system degradation level decreases and thereby the slope of the lateral side of the resilience trapezoid decreases. The main idea of a resilient grid is to serve the demand without much change in the

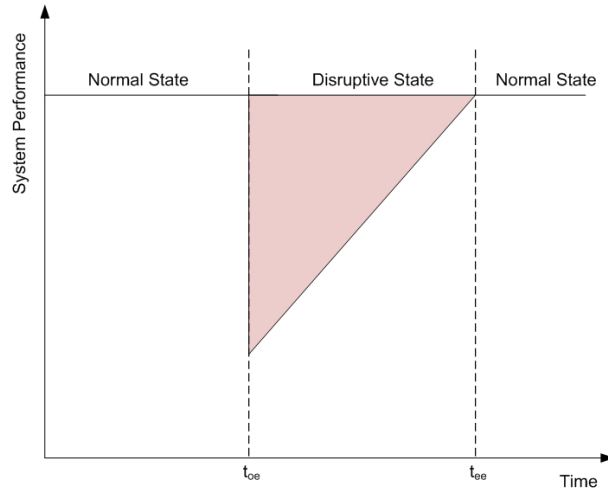


Figure 3.5: Resilience Triangle

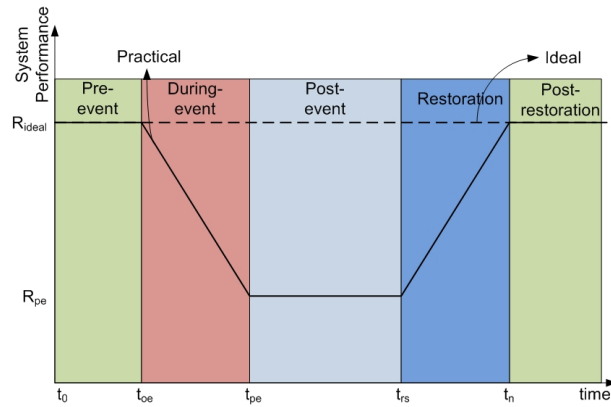


Figure 3.6: Ideal and Practical Resilience Trapezoid

system performance even during the event. Since the idea of enhancing power system resiliency is in its initial phase and there needs to be more awareness created and fund to be raised by the utility, the notion of a resilient power grid is restricted to serve at least critical loads such as hospitals, water pump houses, community centers (where the disaster affected people are accommodated) and priority loads.

As mentioned earlier, to quantify the resilience of the system, it is crucial to define a set of metrics to analyze the system performance during various phases of the resilience trapezoid. In [123], a four set of metrics is defined reflecting the resilience trapezoid called as FLEP, which defines ‘*how fast*’, and ‘*how low*’ the system performance drops and ‘*how extensive*’ and ‘*how promptly*’ the system performance improves. Here, with reference to operational resiliency, the metric ‘*how fast*’ and ‘*how promptly*’ represents the demand satisfaction aimed for a particular period (in hours), i.e., in MW/hr, the metric ‘*how low*’ represents the total system performance in MW and metric ‘*how extensive*’ represents the time for which the system faces the disaster in hours. With reference to hardening resiliency, the

metric ‘*how fast*’ represents the number of equipment going out-of-service for a particular time, the metric ‘*how promptly*’ represents the number of equipment restored for a particular time period, and the metric ‘*how low*’ represents the total number of equipment going out-of-service. Apart from these, different reliability indices such as LOLP, EDNS as given in equation 3.1 and 3.2 respectively have also been proposed to quantify the system resilience [112].

$$LOLP = \sum_{ex_i \in S_{ex}} P_{ex_i} \quad (3.1)$$

$$EDNS = \sum_{ex_i \in S_{ex}} P_{ex_i} C_{ex_i} \quad (3.2)$$

where ex_i represents the i_{th} extreme event, P_{ex_i} represents the probability of the power grid facing an extreme event ex_i , C_{ex_i} represents the load curtailed during the extreme event ex_i and S_{ex} represents the set of extreme events.

3.6 Novel Approach to Quantify Resiliency

In this thesis, a novel way to quantify the resiliency is conceptualized for short and long term resiliency in terms of system state curve as shown in Figure 3.7. This figure shows two curves; the red curve represents long-term and the green curve represents short-term resiliency. Here, the solid line (in both the curves) represent the impact on system without resiliency planning whereas the dotted one represents the impact on system with resiliency planning. The presented curve is based on three time zones viz. event time (time of event/disaster), dead time (time for which the system remains degraded after the event), restoration time (time taken to restore the system to normal condition). The line ‘*ab*’ to ‘*bc*’ represents the system behavior during event occurrence; the line ‘*cd*’ represents the dead time occurs post event; the line ‘*de*’ represents the system restoration time.

From Figure 3.7, it is evident that short-term and long-term resiliency can be enhanced by increasing the area of “*abcdefgh*” and “*ABCDEFGH*” respectively. To improve the area, three possibilities are in hands viz. decreasing the slope of the line ‘*bc*’ & ‘*BC*’, increasing the slope of line ‘*de*’ & ‘*DE*’ and by increasing the length of the line ‘*ab*’ & ‘*AB*’ whereas the length of line ‘*ef*’ & ‘*EF*’ depends on the slope of ‘*de*’ & ‘*DE*’ as the position of ‘*d*’ & ‘*f*’ are constant. The length of line ‘*ab*’ can be increased by improving the reliability and stability of power system components, whereas the length of ‘*AB*’ can be increased by improving flexibility, reliability, stability, and hardening of the network. The slope of line ‘*bc*’ can be made sluggish by satisfying the critical loads during event time (without any disturbances). The slope of ‘*BC*’ can be made sluggish by

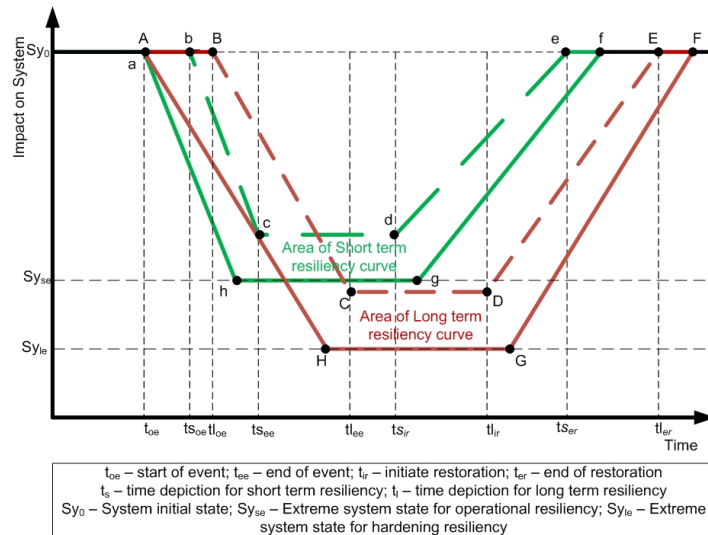


Figure 3.7: System State curve for short- and long-term resiliency

intelligent operation of optimally placed sectionalizers for survival of loads based on priority. Similarly, the slope of line ‘*de*’ & ‘*DE*’ can be improved by enhancing the developed strategies to be deployed for restoration of the system.

To implement the above points for resiliency enhancement of distribution grid, generalized procedure followed are (1) distribution grid modeling, (2) modeling of disaster (or event), (3) choice of design to handle the disaster, (4) identify the best scenario which can handle the disaster using optimization algorithms [128].

3.7 Proposed Methodology

As discussed earlier, resiliency enhancement can be achieved via developing operational and hardening strategies. From Chapter 2, it is clear that resiliency can be improved by planning ESUs for the distribution system. Since the planning methodologies mentioned in the literature refers mainly to enhance the survivability of critical loads during the extreme condition, the overall energy served remains low. Therefore, to reach the ideal state mentioned in Figure 3.6, it is essential to redesign the methodology. In other words, ESU planning must be done to improve the overall performance of the distribution grid during any situation (both normal and extreme conditions). This is essential because, in the literature, the resiliency enhancement using ESU placement can satisfy critical loads only for a particular horizon, after which ESUs may not be able to satisfy the demand. On the other hand, conventional ESU planning for improving the stability, loss minimization, arbitrage cost, etc., may not operate as desired during extreme conditions. Considering this, a generalized methodology is proposed which can be applied to solve both kinds of the problem (normal

& extreme condition) for a system; which is shown in Figure 3.8.

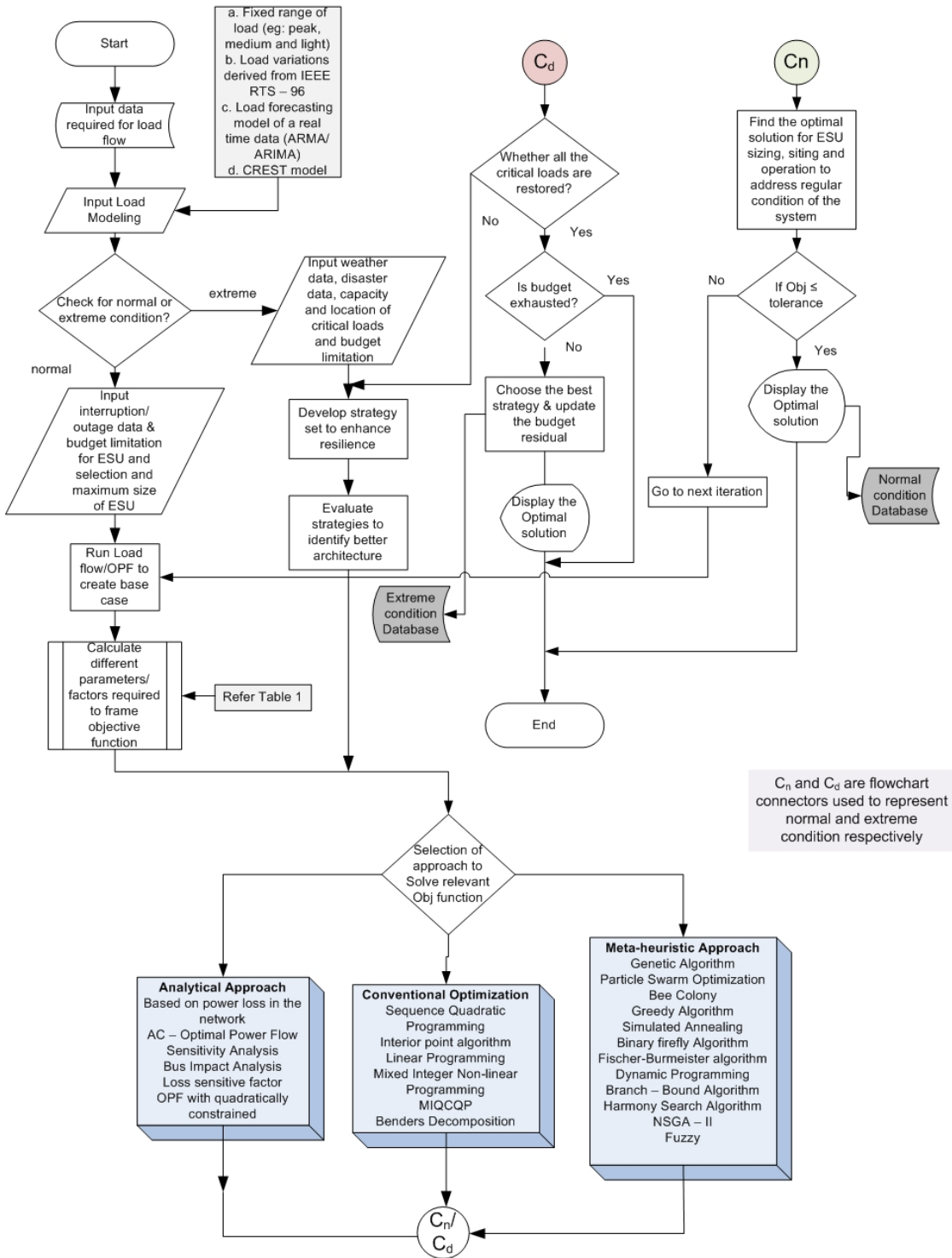


Figure 3.8: Flowchart of Generalized Methodology to enhance system flexibility and resiliency

The proposed conceptually designed steps to enhance flexibility and

resiliency are hereunder:

1. Collecting the distribution system data required for load flow, e.g. bus data, line data, capacity, and location of RES installed, if any, etc.
2. Modeling of the system load & load variations by using IEEE RTS-96 [129], CREST demand model [130], or by considering a fixed range of demand.
3. Designing the system for normal condition and extreme condition, if for normal condition goto *step 9* and for extreme condition designing (resilient system) go to *step 4*.
4. Collect weather data, disaster data (number of collapsed lines, poles, transformers, substation equipment, etc.), capacity and location of critical loads, and budget limits for the normal & resilient condition.
5. Develop system hardening strategies to enhance system resiliency by introducing switches (to create adaptive system architecture), parallel lines, enhanced communication, etc.
6. Evaluate the different strategies and identify a better suitable system architecture concerning the disaster.
7. Choose any approach (as mentioned in Figure 3.8) to solve the objective function of the optimization problem (under extreme condition) for identifying potential location and allocation of ESUs to maximize the survivability of critical loads constrained with electrical parameters and budget limitation.
8. Update the optimal results in the database concerning the disaster.
9. Collecting the interruption data (i.e., outage time of the distribution system's component), budget limitation of ESU.
10. Perform load flow/OPF studies to calculate different objective function parameters.
11. Choose any approach (as mentioned in Figure 3.8) to solve the objective function of the optimization problem (under normal condition) for identifying optimal location and allocation of ESUs to enhance the flexibility of the system constrained with electrical parameters.
12. Update the optimal results in the database.

The input data required for the proposed methodology are distribution system data, load model (as mentioned in *step 2* of the algorithm), bus at which critical loads are connected, weather data, system

withstanding capability for a particular disaster, budget limits, location of switches/sectionalizers. With the help of this data, firstly, load flow is performed to create a base case for the system's performance during normal conditions. Based on the objective function parameters and the constraints chosen (from Table 2.1), a suitable optimization algorithm (as mentioned in Figure 3.8) is used to minimize/maximize to obtain the optimal size, location, and operation of ESU to address normal conditions. The obtained result is stored in a normal condition database. Various sets of strategies are created to address various events, assuming this as the base case. Later, all these strategies are evaluated to minimize/maximize the objective function using a suitable optimization algorithm (as mentioned in *step 7* of the algorithm) to obtain the best possible strategy to face a particular event/disaster. The obtained results are stored in an extreme condition database. This way a robust database is created using the proposed methodology, which can improve the flexibility and resiliency of the distribution grid.

3.8 Closing remarks

In this chapter, a unique conceptual method to quantify the system performance against short and long-term resiliency is presented. With the minimized intersecting area of the resiliency trapezoid, the system can be more resilient. One of the solutions to minimize the area is to install ESUs across the distribution grid. However, the methodologies applied for ESU planning in the literature mainly focuses on the survivability of critical loads. Furthermore, since most of these methodologies do not evaluate the vulnerability of electrical infrastructure, the installed ESUs may fail during the event. Therefore, a generalized methodology is proposed which can enhance both the flexibility and resiliency of the distribution grid. With the input parameters like load uncertainty, weather data, location of critical loads, budget limitations, and other grid parameters in the proposed model; the proposed methodology will enhance the overall system performance during extreme conditions.

Chapter 4

Distribution System Modeling

This chapter introduces the fundamental necessity of modeling the uncertainty and vulnerability associated with the distribution system towards the optimal planning of ESU. Furthermore, the uncertainty followed to model the distribution system is elaborated. In addition, Monte-Carlo based probabilistic disaster hazard model developed to identify the vulnerable components of the distribution system like substations and distribution lines is discussed. Finally, with a case study, the procedure followed to model the derived uncertainty using DigSILENT PowerFactory is discussed. This chapter is based on the journal publication [131, 132].

4.1 Introduction

In any planning activity, it is essential to model the uncertainties associated with the decision variables to end up with feasible solutions. As discussed in chapter 2, REPs and ESUs are integrated into the distribution system to achieve various purposes as stated in Table 2.1. It is a recognized fact that any renewable generations, especially wind and solar, are substantially uncertain; and in the literature, ESUs are placed along with REPs to cater to these uncertainties. In [38, 88], REPs and ESUs are optimally placed in a distribution network using meta-heuristic algorithm to face the uncertainty of REPs and to tackle the demand response. In [133], a novel multistage model is proposed for distribution system planning considering the uncertainties introduced due to wind turbines. Here, the uncertainties are modelled based on the operational parameters such as limits of current and voltage by framing chance constraints. It is also expressed here that assuming a single probability distribution to address wind uncertainty may not be realistic; therefore, the wind uncertainty is represented using ‘*distributionally robust*’ chance constraints. In [134], the uncertainty of wind generation is addressed based on various probability distributions using the Kullback – Leibler divergence measure. On the other side, clustering techniques are used to decrease the complexity of problems with high renewable uncertainty [135]. Since ESUs are directly integrated into the distribution system, it is essential to determine its size

and location mainly based on the uncertainties associated with load and power generation from REPs.

Similar to uncertainty, it is equally significant to identify the vulnerable substations and distribution lines of a distribution system. The REPs or ESUs installed in the distributed network can serve the required demand as developed; however, it is possible only if the substation to which it is connected and the distribution line connecting this substation and the demand are in operation. Therefore, the operation of critical electrical infrastructures like substations and distribution lines are essential during and after the event (natural disaster) to serve the demand. To ensure the operation of these critical components, it is essential to derive its vulnerability towards natural disasters. This can be achieved from the vulnerability assessment of the distribution network. In [29], ESUs are planned to satisfy the partial demand of critical loads considering the effect of earthquakes on distribution lines. As mentioned earlier in chapter 1, the natural disaster in this study is earthquakes. Therefore, in this chapter, the vulnerability analysis of electrical infrastructures like substations and distribution lines against earthquakes is discussed.

4.2 Uncertainty Modeling

The ESU planning is a decision-making problem and therefore it is essential to consider the uncertainties related to load growth, load fluctuations, power fluctuations of REPs, the growth rate of grid-tied REPs, and influx of electric vehicles. The parameters like load fluctuation and power fluctuations of REPs can be modelled using a probability distribution function. However, in real-world scenarios, the growth rate parameters are system dependent. Therefore, it is essential to initially decide the system for which the planning is performed.

Once the distribution system is identified, the following data are essential to identify the growth rate of general load, the penetration rate of REPs, and the influx of electric vehicles on the distribution grid considering a time period.

- number of electric vehicles introduced into the distribution grid each year.
- charging time.
- density of electric vehicles across the distribution grid.
- number of grid-tied solar power plants installed each year along with its capacity.

Parameters like the number of electric vehicles in operation (year-wise), the source and time of the day (TOD) for charging, the power rating of electric vehicles, and number of grid-tied REPs (here solar PV is

considered) in operation (year-wise) are derived from the above data. With these parameters, the average growth rate factors for grid-tied solar PV, electric vehicles, and load demand are calculated using the equation 4.1. In this equation, x represents the data corresponding to the number of electric vehicles in operation, total demand, and total grid-tied REPs installed at k_{th} year. Using this growth rate factor (GF), the future value (FV) of these parameters are found using the equation 4.2.

$$GF = \frac{1}{n} \sum_{k=1}^n \frac{x_k}{x_{k-1}} \quad (4.1)$$

$$FV(x_{pre}) = GF \times x_{pre}^{f_n} \quad (4.2)$$

In this equation, x_{pre} represents the present value, f_n represents the future number of years for which the estimated FV needs to be calculated. To verify the reliability of the model represented by the equation 4.1 and equation 4.2, the data is divided into two sets, where one set (70%) is used to develop the GF and the other set (30%) is used to test FV. There is a possibility for a significant difference in the electric vehicle density and the distribution of grid-tied solar PV across the distribution grid. These differences are found because of various reasons such as population density, economic status, load density, etc. Therefore, it is essential to incorporate these factors into the optimization model. Here the uncertainties of REPs and load are modelled on their probabilistic behaviour.

4.2.1 Uncertainty of Solar PV Generation

The output power of the solar power plant majorly depends on the solar irradiance. This parameter is modelled using a beta distribution function as given by the equation 4.3.

$$PDF_{PV}(x_i) = \begin{cases} \frac{1}{B(\alpha, \beta)} \times x_i^{\alpha-1} \times (1 - x_i)^{\beta-1}, & \text{if } x_i \in [0, 1] \\ 0, & \text{otherwise} \end{cases} \quad (4.3)$$

where x_i is the solar irradiance at the i_{th} location in W/m^2 , B is the beta function and α and β are the shape parameters of the probability density function taking values greater than zero.

4.2.2 Uncertainty of Load

Load variations are mostly modelled using a normal probability distribution. In this study, the real power demand is distributed using a normal probability distribution, whereas the reactive power is calculated using the average power factor of i_{th} location (obtained from the repository/survey). The probability distribution function of real power

demand located at the i_{th} bus is calculated using the equation 4.4. The influx of electric vehicles into distribution is increasing with the market scenario and environmental policies. In this study, the number of electric vehicles connected to the distribution network (or the corresponding demand) is distributed within a region using the normal probability distribution given by the equation 4.5.

$$PDF_D(P_i) = \frac{1}{\sigma[P_i]\sqrt{2\pi}} \times e^{-\left(\frac{P_i - E[P_i]}{\sigma[P_i]\sqrt{2\pi}}\right)^2} \quad (4.4)$$

$$PDF_{EV}(P_{EV}) = \frac{1}{\sigma[P_{EV}]\sqrt{2\pi}} \times e^{-\left(\frac{P_{EV} - E[P_{EV}]}{\sigma[P_{EV}]\sqrt{2\pi}}\right)^2} \quad (4.5)$$

where P_i represents the real power demand at the i_{th} bus, P_{EV} represents the total electric vehicle demand in a particular region/cluster, $E[\]$ and $\sigma[\]$ denote the expected or mean value and standard deviation respectively.

4.3 Vulnerability Assessment against Earthquakes

The procedure to perform vulnerability assessment against earthquakes is shown in Figure 4.1. Here, the historical earthquake data is obtained from the seismic activity catalogue. From this, the moment magnitude of the earthquake, its location (latitude and longitude), and the distance from the epicentre to the hypocentre are derived. The effect of ground acceleration due to an earthquake gets attenuated as it travels along various soil types. Therefore, it is also essential to consider the soil type in the seismic model. Here, to assess the effect of seismic activity on electrical infrastructure (both substation and distribution lines), an analytical relationship is characterized based on peak ground acceleration (PGA). The algorithm proposed to estimate the potential risk due to seismic hazard is as follows:

1. From the seismic catalog of the chosen region, categorize the severe earthquake magnitude (M_w).
2. Determine the soil type, distance from the epicenter to the hypocenter, and location of infrastructure, respectively.
3. Based on the historical data of the chosen region, develop a regression model that reflects the relationship of attenuation.
4. From the standard fragility curves developed by the Federal Emergency Management Agency (FEMA) for electrical infrastructure, and the developed regression model, estimate the potential damage probability.

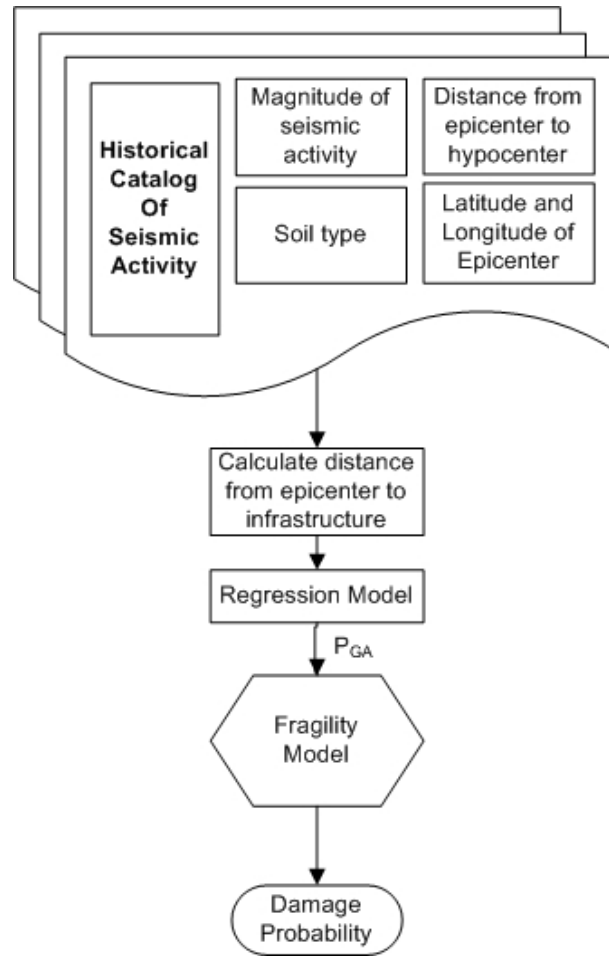


Figure 4.1: Procedure to perform Vulnerability Assessment against Earthquakes

4.3.1 Modeling seismic activity

The estimation of seismic hazard is very essential for any infrastructure planner. PGA is the most common tool for better estimation of seismic hazard. The earthquake intensity varies from the hypocentre to the point of a particular location due to the attenuation. It has been broadly accepted that the soil type and geotechnical characteristics are the major factors for the occurrence of high ground acceleration during earthquakes. In general, the attenuation is modelled using regression analysis, which includes the parameters such as the intensity of the earthquake, distance from the surface (at the epicentre) to the hypocentre commonly known as depth, and the distance between the equipment and the epicentre (fault location), etc. A general regression model for attenuation is shown in the equation 4.6 [136].

$$\ln(X) = c_0 + c_1 F_1(R) + c_2 F_2(D) + c_3 F_3(M_w) \quad (4.6)$$

where X is the peak ground acceleration or spectral displacement in gals [g], R is the distance between the epicentre and the location of the equipment,

D is the distance between the epicentre and the hypocentre, M_w is the moment magnitude and c_0, c_1, c_2 & c_3 are regression coefficients.

4.3.2 Fragility Model

Fragility models can be derived through various means such as (i) by expert's viewpoint, (ii) statistical models built from a large failure record database, (iii) experimental or simulation-based characterization of specific equipment under a series of shocks of various intensities, and (iv) mixed model by combining the above methods [137]. The outcome of. This model provides the probability of failure of the equipment (electrical infrastructure) under the potential intensity of a hazard or disaster. To derive better solutions, the damage caused on the infrastructure is classified into none, minor, moderate, extensive, and complete; depending on the intensity of the seismic activity. For a given level of seismic activity (X), the level of damage is obtained through lognormal fragility curves, which reflect the probability of attaining or surpassing a damaged state. The fragility curve corresponding to the damage state is defined by its median value of spectral displacement and lognormal standard deviation (β_{d_s}) [138]. This probability of attaining or surpassing a particular damage state (d_s) is given in the equation 4.7.

$$P[d_s|S_d] = \phi \left[\frac{1}{\beta_{d_s}} \ln \left(\frac{S_d}{\overline{S_{d,d_s}}} \right) \right] \quad (4.7)$$

where S_d is the spectral displacement, $\overline{S_{d,d_s}}$ is the median value of spectral displacement, β_{d_s} , is the standard deviation of the lognormal of spectral displacement for a damage state d_s , and ϕ is the standard normal cumulative distribution function. In this thesis, the fragility model is derived for electrical substations and distribution lines; the corresponding fragility curves are shown in Figure 4.2(a) and 4.2(b) respectively.

4.3.3 Damage Probability of Electrical Infrastructure

For a maximum value of PGA, the probability of damage caused to the electrical infrastructure is to be quantified. Estimation of the unavailability of the substation due to the earthquake is equally important as the estimation of the unavailability of overhead distribution lines which carry power to the end-users; the reason being, the large-scale ESUs will be connected to the grid via substations. Henceforth, in this thesis, the overall damage probability of both substation and the distribution lines is quantified based on the fragility curves corresponding to five different damage states such as none, minor, moderate, extensive and complete. The damage probability of each state of both substation and distribution line can be defined as:

$$P(d_s = no|X)_{SS|DL} = P_{no} + P_{mi} + P_{mo} + P_{ex} + P_{co} = 1 \quad (4.8)$$

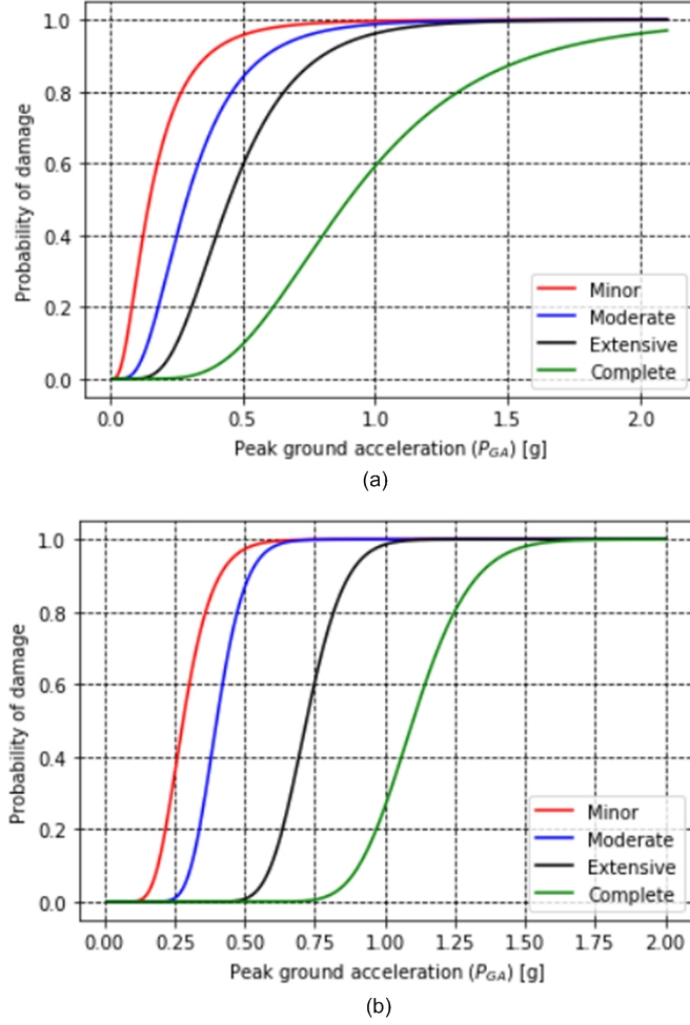


Figure 4.2: The Fragility curves of (a) Electrical substation (b) Distribution line

$$P(d_s = mi|X)_{SS|DL} = P_{mi} + P_{mo} + P_{ex} + P_{co} \quad (4.9)$$

$$P(d_s = mo|X)_{SS|DL} = P_{mo} + P_{ex} + P_{co} \quad (4.10)$$

$$P(d_s = ex|X)_{SS|DL} = P_{ex} + P_{co} \quad (4.11)$$

$$P(d_s = co|X)_{SS|DL} = P_{co} \quad (4.12)$$

where the subscripts *no*, *mi*, *mo*, *ex* and *co* represents the damage state such as none, minor, moderate, extensive and complete respectively.

4.4 Monte-Carlo based Probabilistic Earthquake hazard Model

The occurrence of earthquakes at any location is purely a random event and therefore modelling earthquakes using the probabilistic approach might be more realistic. For better infrastructure planning, it is essential to consider all possible earthquake scenarios and therefore a Monte-Carlo based probabilistic approach is developed in this thesis to evaluate the vulnerability of substations and distribution lines. The procedure followed to develop this model is explained as follows:

1. From the historical seismic catalogue, parameters such as moment magnitude, its location (latitude and longitude), and distance from the epicentre to the hypocentre are derived.
2. Using the data derived in step 1, evaluate the parameters such as mean, standard deviation, and variance for the variables such as earthquake magnitude, its location, and source to chosen site distance.
3. Based on the statistical data obtained from step 2 characterize the earthquake probability distribution function (PDF) for parameters such as earthquake magnitude M_w , its location (Loc), source to chosen site distance (R) as shown in the equation 4.13, 4.14, and 4.15 respectively.

$$PDF_{M_w}(M_w) = \frac{1}{\sigma[M_w]\sqrt{2\pi}} \times e^{-\left(\frac{M_w - E[M_w]}{\sigma[M_w]\sqrt{2\pi}}\right)^2} \quad (4.13)$$

$$PDF_{Loc}(Loc) = \frac{1}{\sigma[Loc]\sqrt{2\pi}} \times e^{-\left(\frac{Loc - E[Loc]}{\sigma[Loc]\sqrt{2\pi}}\right)^2} \quad (4.14)$$

$$PDF_R(R) = \frac{1}{\sigma[R]\sqrt{2\pi}} \times e^{-\left(\frac{R - E[R]}{\sigma[R]\sqrt{2\pi}}\right)^2} \quad (4.15)$$

4. With the PDF of earthquake parameters, generate n number of possible earthquake scenarios for the chosen region using a Monte-Carlo based approach.
5. Having the outcomes of step 4 as input parameters to the seismic activity model, the spectral displacement or PGA in gals [g] is evaluated.
6. With PGA as input to the fragility model of substation and distribution line, all possible failure likelihoods of substations and distribution lines are evaluated.

The seismic activity model discussed in section 4.3.1 and the fragility curves discussed in section 4.3.2 are used to derive the PGA values and failure probabilities respectively for the Monte-Carlo based probabilistic hazard model.

4.5 DigSILENT PowerFactory Model of Distribution Grid – A Case Study

In this thesis, modelling of distribution system and performing optimization studies are performed using DigSILENT PowerFactory 2019 SP2 (x64) and Python 3.7. As mentioned earlier, the 156-bus practical distribution system of Dehradun district, Uttarakhand, India, is chosen for all case studies. With the line data and bus data, the distribution system is modelled using PowerFactory and the same is shown in Figure 4.7 [139]. Once the PowerFactory model of the distribution system is developed, it is essential to introduce the variations and uncertainties of parameters such as loads (both general and EV load), and power generation from REPs. The load variation considered in this study during summer and winter is shown in Figure 4.3 and the power variation of REPs (solar PV) due to the variation in irradiance is shown in Figure 4.4. As mentioned earlier, to recognize the uncertainty of the essential parameters, a survey has been conducted. From this survey, it is observed that the electric vehicles are regularly charged between 9 PM to 7 AM (for about 10 hours). For that reason, the hourly scaling factor of EVs is given as $EV_{sh} \in [0, 1] \forall h = 1, 2, \dots, 7 \& 21, 22, \dots, 24$. These variations are introduced into the PowerFactory model by using the time characteristics tool available in PowerFactory. For example, the Figure 4.5 (a) represents the time characteristics tool through which the load variations during summer or winter of ‘ACraft’ load connected to ‘Selaqui’ bus is modelled as shown in Figure 4.5 (b). As discussed earlier, to introduce the uncertainty, probability distribution function corresponding to the variables such as power generation from REPs, general load, and EV load mentioned in equations 4.3 to 4.5 is utilized. This factor is introduced into the PowerFactory model using the project distribution tool available in PowerFactory. For example, the uncertainty of ‘ACraft’ load connected to ‘Selaqui’ bus is modelled using normal distribution tool as shown in Figure 4.6 (a) with the values of mean and standard deviation obtained from survey as shown in Figure 4.6 (b). Similar procedure is followed to introduce the uncertainty of other parameters into the PowerFactory model. These variations can be introduced into the PowerFactory model using either scaling factor variation or the demand/generation (in MW) variation.

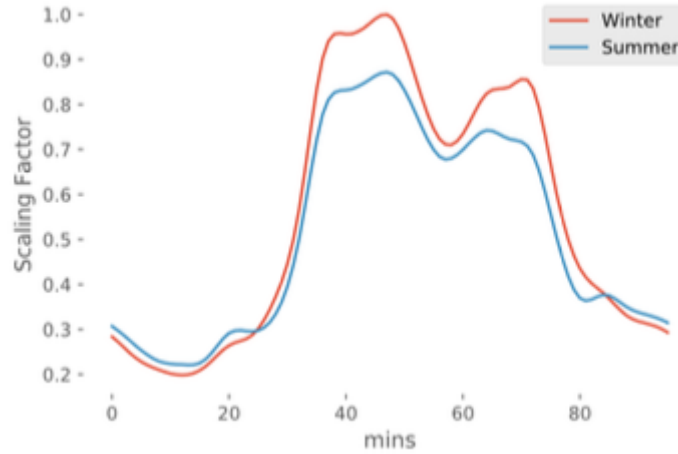


Figure 4.3: Scaling factor of General Load during Summer and Winter

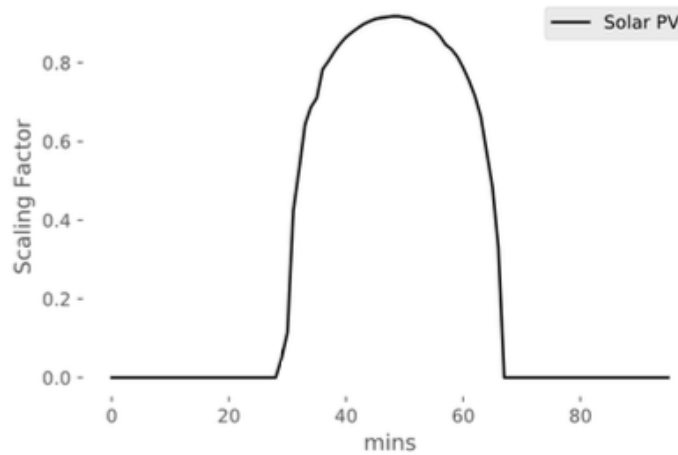
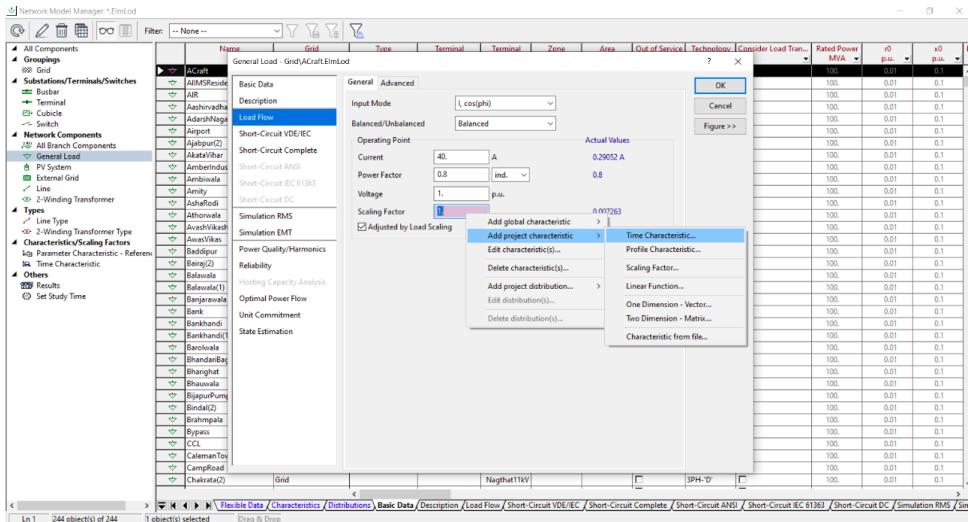


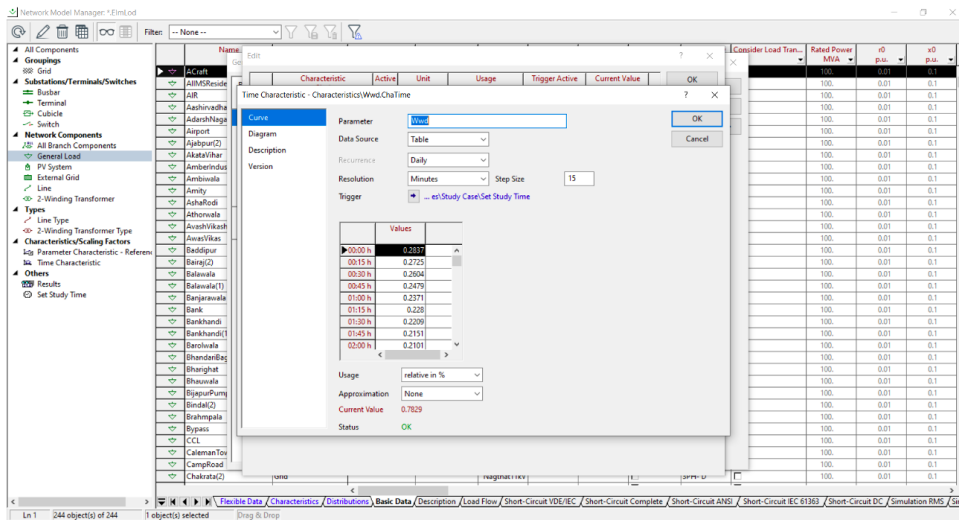
Figure 4.4: Scaling factor of Solar Power Plant

4.6 Closing Remarks

In this chapter, the necessity for distribution system modelling with the uncertainties of REPs & load, and the vulnerability of the distribution system components are presented. For ESU planning in any chosen system, it is essential to identify the parameters which introduce the uncertainty and vulnerability of system components for a particular earthquake activity. It is also essential to make the ESUs placed by the planning methodology to withstand the earthquake and serve the defined load. Therefore, it is essential to place it either with increased structural strength in a vulnerable zone or to avoid placing in the vulnerable zone. To identify the vulnerable location for the components like substation and distribution lines, it is essential to characterize the earthquake. In this thesis, considering the randomness of the event, a Monte-Carlo based probabilistic earthquake hazard model is proposed. Modelling the outcome of this model in the distribution grid, i.e., identifying the nodes and distribution lines along with



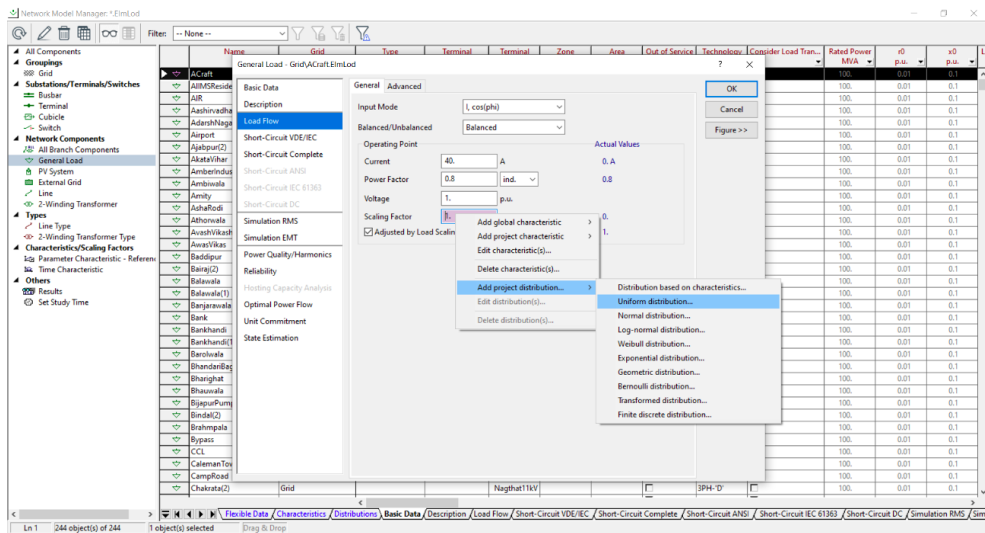
(a)



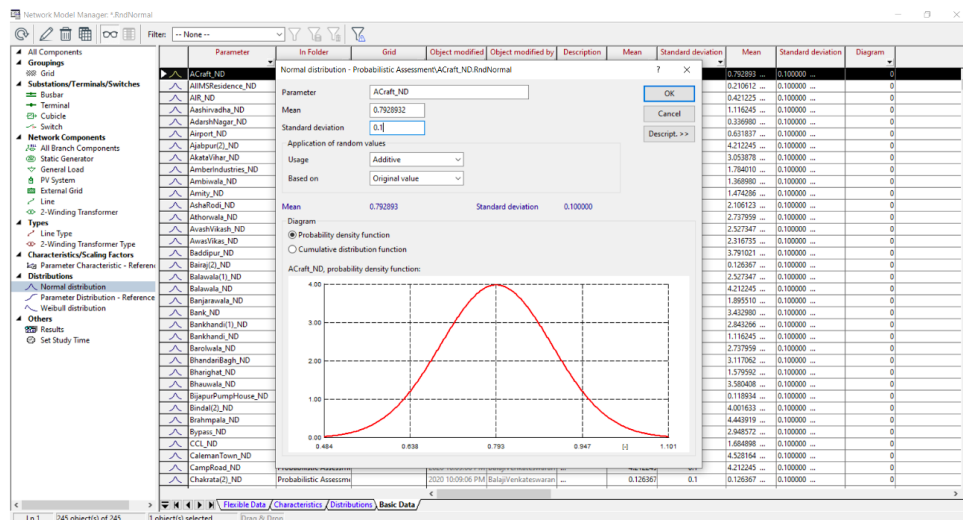
(b)

Figure 4.5: Procedure to Introduce load variations in PowerFactory model

its probability of failure corresponding to an earthquake can lead to derive the better optimal planning of ESUs. Modelling of uncertainty introduced by REPs and load including general load and EV load is discussed.



(a)



(b)

Figure 4.6: Procedure to introduce uncertainty in PowerFactory model

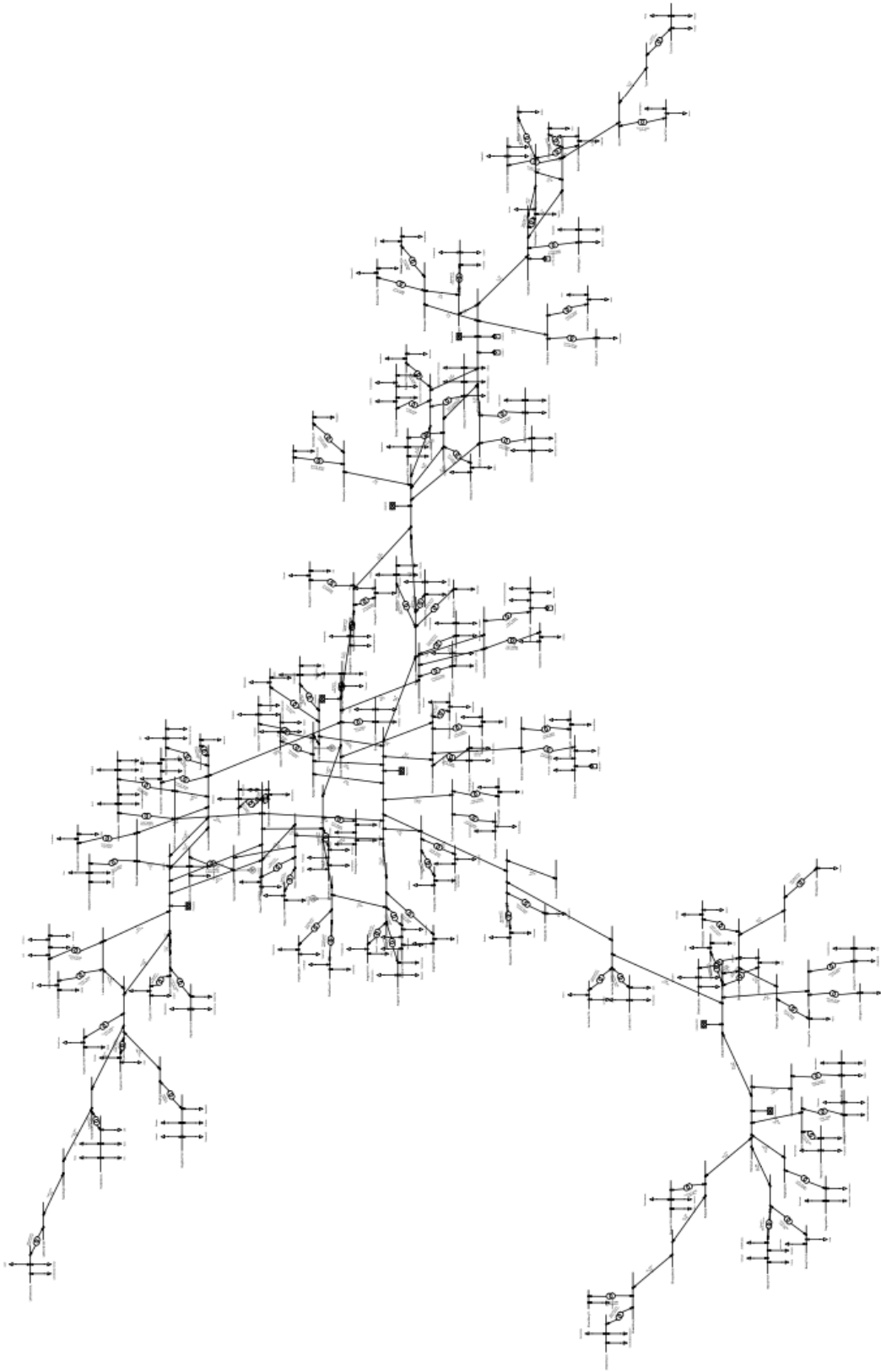


Figure 4.7: DigSILENT PowerFactory Model of Dehradun Distribution Grid

Chapter 5

Practically Constrained Optimal Planning of Energy Storage Units

This chapter typically focuses on the optimal planning of ESUs in a distribution network to improve the grid flexibility. Here, the objective function of the optimization problem is formulated by considering the real-world scenarios that may affect the location and size of ESU such as (i) environmental impact, (ii) land requirement and its associated cost for ESU installation and (iii) renewable purchase obligation (RPO) on top of grid performance parameters. Here, the ESUs are optimally configured to frame HESUs to minimize the overall environmental impact due to ESUs. Furthermore, the uncertainty related to decision variables is modelled in the objective function. This chapter is based on the journal publication [131].

5.1 Introduction

The world is witnessing climate change, an increase in environmental pollution, and global warming, mainly due to the exploitation of energy from fossil fuels. On the other hand, the trend of fossil fuel exploration is decreasing, which makes to search for pollution less alternative. One such way to produce energy is through renewables. This made people across the world to invest in renewable technologies for power generation. The integration of renewables into the grid introduces many challenges because of its intermittent nature. Therefore, many researchers proposed the integration of ESUs along with renewables can increase the flexibility of both REPs and the distribution grid. Later, recognizing the benefits of direct integration of ESUs like peak management, effective management of renewables, and power quality, and considering the capital cost involved, ESUs are optimally placed across the distribution system. As mentioned in chapter 2, the methods proposed in the literature considers mainly the electrical parameters, ignoring the practical variables and constraints. In reality, the optimal locations obtained with these

methods may be unsuitable for the installation of ESUs because of many practical constraints; one such constraint is land availability. For a densely populated country like India, it is always a direct challenge to obtain the space for placing electrical equipment mainly in a densely populated location. Therefore, formulating the optimization problem inevitably leaving behind these practical constraints may not lead to better planning. This chapter elaborates the optimal ESU planning problem formulation by considering the practical parameters and the methodology proposed to solve the same. In this study, a practical 156-bus distribution system of Dehradun district, India elaborated in chapter 4 is considered.

5.2 System Modeling

As mentioned in chapter 4, the distribution system is modelled considering the uncertainty introduced by Solar PV, general load and EV. To estimate the growth rate of parameters as discussed in section 4.2, a survey is conducted across Dehradun district to identify (a) the number of electric vehicles introduced into the distribution grid each year, (b) charging time, (c) the density of electric vehicles across the district and (d) the number of grid-tied solar power plants installed each year along with its capacity. From the survey, there is a significant difference in the electric vehicle density and the distribution of grid-tied solar PV across the district. These differences were found because of various reasons such as population density, economic status, load density, etc. Therefore, it is essential to incorporate these factors into the optimization model. The distribution network chosen for this study is spread-out on a mixed terrain which consists of both plain and hilly areas, which also creates various challenges of its own for ESU planning. Since the operational constraints differ with respect to the terrain, population and specific activities in the location, the network is clustered. In the forthcoming subsections, the network clustering and selection of ESU technology to frame HESU were discussed.

5.2.1 Clustering of Distribution Network

Based on the survey, electric vehicles are rarely found at places of high altitude and mostly found within city limits (at low altitudes). From the experts' suggestions, and considering the economic status of people, the possibility of electric vehicles at high and medium-altitude regions of the district are low. Therefore, this aspect should be modelled in the system for which planning is to be performed. To introduce this, the chosen distribution system is clustered based on latitude, longitude, mean sea level (MSL), population, tourism index (TI), and load density using the k-means algorithm [140]. Here, TI takes the value 1 if the i_{th} location is an identified tourist spot and 0 otherwise. Applying k-means clustering is

effective for large datasets. However, the major drawback of the k-means algorithm is the number of clusters for the clustering procedure has to be provided in prior. Therefore, to address this issue, the cluster quality index (CQI) is formulated as given by the equation 5.1, based on popular quality measuring indices for clustering such as Silhouette index (SI) and Davies – Bouldin index (DBI) [141]. Here, $w_1, w_2 \in [0, 1]$ represents the importance factor of SI and DBI, respectively. To get the optimal number of clusters for a given data set, a methodology is followed as mentioned in the flowchart shown in Figure 5.1.

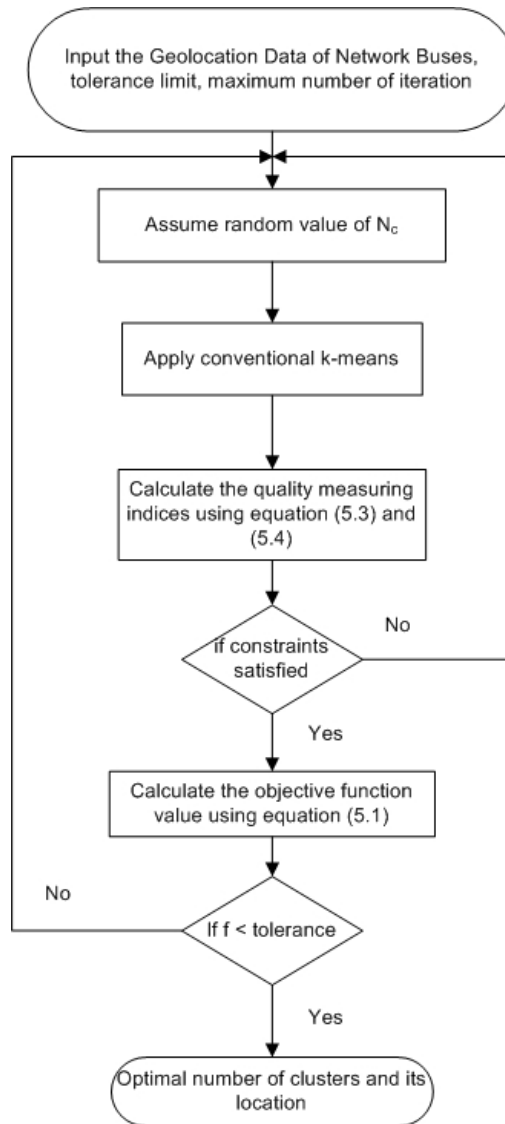


Figure 5.1: Flowchart of the clustering method for mixed terrain network

$$CQI = SI^{-w_1} DBI^{w_2} \quad s.t. SI, DBI \in [0, 1] \quad (5.1)$$

The indices represented in the equation 5.1 are calculated using the equations given below:

$$S(j) = \frac{y(j) - x(j)}{\max(x(j), y(j))} \quad (5.2)$$

where $x(i)$ is the average distance between the i_{th} location and all other locations within the cluster C_k and $y(i)$ is the minimum average distance between the i_{th} location and all other locations in different clusters. Therefore, the overall Silhouette index is calculated by using the equation 5.3.

$$SI = \frac{1}{L_{tot}} \sum_{i=1}^{L_{tot}} \left(\frac{1}{N_c} \sum_{j=1}^{N_c} S(j) \right) \quad (5.3)$$

$$DBI = \frac{1}{L_{tot}} \sum_{i=1}^{L_{tot}} \max_{i \neq j} \left(\frac{X(i) + X(j)}{d_{ij}} \right) \quad (5.4)$$

where L_{tot} is the total number of locations in a given set and N_c is the number of clusters. The DBI index is calculated using 5.4. Where $X(i)$ and $X(j)$ is the average distance between each location of cluster i & j and centroid of that cluster respectively; d_{ij} is the distance between the centroids of cluster i and cluster j .

5.2.2 Selection of ESU Technology

Estimates from expert reveals that nearly 55% of ESUs installed in the world for peak management is mainly based on lithium-ion technology considering its round trip efficiency, depth of discharge (DOD), and energy to power ratio [8]. In general, the choice of ESU technology is only considered based on the electrical requirement, ignoring the environmental impact created by it while planning ESU [9, 142]. However, the ecological impact due to Li-ion technology compared to other technologies is significant. Therefore, it is essential to consider the climatic impact parameter for ESU planning along with other parameters mentioned in Table 1.1. It is evident from Table 1.1 that; Li-ion battery can deliver high power to meet the peak management requirements. However, the CO₂ emission of Li-ion solvent is 12.5 kg CO_{2-eg} , whereas for Na-S battery, the CO₂ emission level is 1.2 CO_{2-eg} indicating high environmental damage [143]. Since both battery technologies are commercially available in the market, it is essential to redesign the ESU planning problem based on environmental constraints. Therefore, it is required to find a hybrid combination of battery technologies, which can satisfy the electrical requirement with a minimized impact on the environment. Thus, in this case, ESU technology is modelled with a hybrid configuration of Li-ion and Na-S.

5.3 Problem Formulation

5.3.1 REPs and Load Modelling

For better accuracy in optimal planning, it is essential to combine time variation, GF, and uncertainty to create RES and load models. Here, the hourly time variation of general load and solar PV are introduced by scaling factors constructed using the historical data. The real power of the general load and power generated from the solar PV plant connected at the i^{th} location (bus) at hour h of the day in f_n^{th} year is given by equation 5.5 and 5.6 respectively. As mentioned earlier, the reactive power is calculated using the power factor. Moreover, it is assumed that the solar power plants are operated at a constant power factor.

$$P_D^{i,h,f_n} = PDF_D (FV(P_{pre}^D(i)) \times L_{s_h}) \quad (5.5)$$

$$P_{PV}^{i,h,f_n} = PDF_{PV} (FV(P_{pre}^{PV}(i)) \times PV_{s_h}) \quad (5.6)$$

where $P_{pre}^D(i)$ and $P_{pre}^{PV}(i)$ represents the present value of real power demand and power generated from solar power plants, respectively, at the i_{th} location, L_{s_h} and PV_{s_h} represents the hourly scaling factor of general load and solar PV respectively. As mentioned earlier, the distribution of electric vehicle load on the distribution system depends on the clustering. From the survey and the outcome of clustering, it is apparent that the cluster with a higher population and load density has comparatively more electric vehicles. Therefore, in this case, the electric vehicle loads are distributed in the cluster having a high population and load density as given by the equation 5.7.

$$P_{EV}^{i,h,f_n} = PDF_{EV} (FV(P_{pre}^{EV}(i_{N_c})) \times EV_{s_h}) \quad (5.7)$$

where $P_{pre}^{EV}(i_{N_c})$ represents the present value of electric vehicle power demand at i_{N_c} location, EV_{s_h} represents the hourly scaling factor of electric vehicle load, and C_h represents the charging hours of EV . This power is distributed within a cluster about the EV distribution index (EV_{DI}). As mentioned earlier, this index is the ratio of the number of EV s in operation for the selected cluster to the total number of EV s in operations. It is assumed that the electric vehicle load is operated at a constant power factor.

5.3.2 Optimization Problem

The objective function formulated for the optimization problem comprises of five parameters, namely, the capital investment of HESU, operation and maintenance cost of HESU, the land required to install the optimal HESU and its associated cost, the price of environmental impact due to HESUs and the grid performance parameters such as voltage deviation cost, cost

of line loading, cost of apparent power loss are represented by equation 5.8 to 5.17.

$$P_{Obj} = [C_I^{HESU} + C_{OM}^{HESU} + C_{land}^{HESU} + C_{env}^{HESU} + C_P^G] \times 365 \quad (5.8)$$

where

$$C_I^{HESU} = \sum_{i=1}^{N_{ESU}} C_{PI}^{ESU,i} + C_{EI}^{ESU,i} + C_{FI}^{ESU,i} \quad (5.9)$$

$$C_{OM}^{HESU} = \sum_{i=1}^{N_{ESU}} \sum_{t=1}^{N_t} [[P_{Sell,t} \times T_{Sell,t} - P_{Pur,t} \times T_{Pur,t}] + C_{FOM}^{ESU} \times P_{rated}^{ESU}] \quad (5.10)$$

$$P_{rated}^{HESU} = \sum_{i=1}^{N_{ESU}} [P^{ESU,i}] \quad (5.11)$$

$$C_{land}^{HESU} = \sum_{i=1}^{N_{ESU}} LCI^{N_b} \times C_{land}^{N_b} \times A^{ESU,i} \forall N_b \quad (5.12)$$

$$C_{env}^{HESU} = \sum_{i=1}^{N_{ESU}} \sum_{t=1}^{N_t} [P_{dis,t}] \times \gamma_{emi}^{ESU,i} \times \mathbb{k}_{env} \quad (5.13)$$

$$C_P^G = C_{VD}^{N_b} + C_{LL}^{N_l} + C_{SP}^{N_l} \quad (5.14)$$

$$C_{VD}^{N_b} = \sum_{b=1}^{N_b} |V_{Rated} - V_b^{HESU}| \times \mathbb{k}_{VD} \quad (5.15)$$

$$C_{LL}^{N_l} = \left(\sum_{l=1}^{N_l} \%LL^{HESU} \right) \times \mathbb{k}_{LL} \quad (5.16)$$

$$C_{SP}^{N_l} = \sqrt{\sum_{l=1}^{N_l} (P_{Loss,l}^2 + Q_{Loss,l}^2)} \times \mathbb{k}_{Loss} \quad (5.17)$$

The first term of the objective function presents the installation cost of HESU, which includes power rating cost in $\$/kW - day$, energy rating cost in $\$/kW - day$ and fixed installation cost in $\$/kW - day$. The second term presents the operation and maintenance cost of HESU, which comprises two components, such as the cost of energy trade and the fixed price. The energy trade cost (in $\$/day$) is defined as the difference in cost between the energy sold and the energy purchased at any time t of a day. As the city or an area witnesses the development, the value of the land and its availability plays a vital role in the installation of HESUs, which is represented in the third term of the objective function. The same is calculated based on the price of the land in $\$/sq.m$ multiplied by the physical size of HESU in sq.m. The value and the availability

of the land are modelled with land cost index (LCI), which denotes the category for the location of the land. Here, the original data of land cost (in $\$/sq.m$) is considered [144]. A significant part of the economy of a country is spent on compensating the climate-driven damage [145]. Therefore, it is essential to consider the cost of environmental damage created by HESUs, which is represented in the fourth element as the cost of damage created by CO_2 emissions from HESUs in $\$/day$. The last term of the objective function deals with the cost involved in HESU affecting the grid performance. The time limit considered here is one day on f_n^{th} year, and the operation cost is calculated for one day with an interval of 15 minutes. However, the total cost is calculated for f_n^{th} year.

The proposed objective function is subjected to the following constraints:

Operational Constraints

The operational constraints of the distribution network are given from equation 5.18 to equation 5.23, which includes the real and reactive power balance, power flow equations, voltage limit, and line loading limits.

$$P_D^{i,t,f_n} + P_{EV}^{i_{Nc},t,f_n} = P_{PV}^{i,t,f_n} + P_{HESU}^{i,t} + P_{grid}^{i,t} + P_{loss}^t \quad \forall t = 1, \dots, N_t \ \& \ i = 1, \dots, N_b \quad (5.18)$$

$$Q_D^{i,t,f_n} + Q_{EV}^{i_{Nc},t,f_n} = Q_{PV}^{i,t,f_n} + Q_{HESU}^{i,t} + Q_{grid}^{i,t} + Q_{loss}^t \quad \forall t = 1, \dots, N_t \ \& \ i = 1, \dots, N_b \quad (5.19)$$

$$P_{flow}^{i,t} = V^{i,t} \times \sum_{i,j \in N_b} V^{j,t} (G_{ij} \cos \theta_{ij,t} + B_{ij} \sin \theta_{ij,t}) \quad (5.20)$$

$$Q_{flow}^{i,t} = V^{i,t} \times \sum_{i,j \in N_b} V^{j,t} (G_{ij} \sin \theta_{ij,t} - B_{ij} \cos \theta_{ij,t}) \quad (5.21)$$

$$V_{min} < V_t^b < V_{max} \quad \forall b = 1, 2, 3, \dots, N_b \quad (5.22)$$

$$LL_t^l < LL_{max}^l \quad \forall l = 1, 2, 3, \dots, N_l \quad (5.23)$$

HESU Constraints

The absorbed or injected power from HESU depends on its mode of operation, namely charging and discharging mode [146]. This mode of operation is constrained concerning the energy capacity limits, charging power and discharging power limits, limits of the state of charge (SOC), apparent power to be delivered, the maximum budget allocated, and the energy to power ratio of individual ESU. Then the summation of these constraints is considered as the constraints of HESU. Therefore, the constraints of HESU are modelled as: both the charging and discharging

mode of operation are represented by the equation 5.24 to equation 5.37, and budget limits, energy to power ratio and apparent power are represented by equation 5.38, 5.39 and 5.40 respectively.

Charging Mode:

$$E_{t+1}^{HESU} = \sum_{i=1}^{N_{ESU}} E_{t+1}^{ESU,i} \quad \forall t = 1, \dots, N_t \quad (5.24)$$

$$E_{t+1}^{ESU,i} = \min \left(\left(E_t^{ESU,i} - \Delta t \times P_t^{ESU,i} \times \eta_{ch,i} \right), E_{max}^{ESU,i} \right) \quad \forall t = 1, \dots, N_t \quad (5.25)$$

$$P_{min}^{ESU,i} < P_t^{ESU,i} < P_{max}^{ESU,i} \quad \forall t = 1, \dots, N_t \quad (5.26)$$

$$E_{min}^{ESU,i} < E_t^{ESU,i} < E_{max}^{ESU,i} \quad \forall t = 1, \dots, N_t \quad (5.27)$$

Discharging Mode:

$$E_{t+1}^{HESU} = \sum_{i=1}^{N_{ESU}} E_{t+1}^{ESU,i} \quad (5.28)$$

$$E_{t+1}^{ESU,i} = \max \left[\left(E_t^{ESU,i} - \frac{\Delta t \times P_t^{ESU,i}}{\eta_{dis,i}} \right), E_{min}^{ESU,i} \right] \quad \forall t = 1, \dots, N_t \quad (5.29)$$

$$P_{min}^{ESU,i} < P_t^{ESU,i} < P_{max}^{ESU,i} \quad \forall t = 1, \dots, N_t \quad (5.30)$$

$$E_{min}^{ESU,i} < E_t^{ESU,i} < E_{max}^{ESU,i} \quad \forall t = 1, \dots, N_t \quad (5.31)$$

where

$$P_{max}^{ESU,i} = \min \left[P_{max}^{ESU,i}, \frac{\left(E_t^{ESU,i} - E_{min}^{ESU,i} \right) \times \eta_{dis,i}}{\Delta t} \right] \quad \forall t = 1, \dots, N_t \quad (5.32)$$

$$P_{min}^{ESU,i} = \max \left[P_{min}^{ESU,i}, \frac{\left(E_t^{ESU,i} - E_{max}^{ESU,i} \right)}{\Delta t \times \eta_{ch,i}} \right] \quad \forall t = 1, \dots, N_t \quad (5.33)$$

$$SOC_{min}^{HESU} \leq SOC_t^{HESU} \leq SOC_{max}^{HESU} \quad (5.34)$$

where

$$SOC_{min}^{HESU} = \sum_{i=1}^{N_{ESU}} SOC_{min}^{ESU,i} \quad (5.35)$$

$$SOC_{max}^{HESU} = \sum_{i=1}^{N_{ESU}} SOC_{max}^{ESU,i} \quad (5.36)$$

$$SOC_t^{HESU} = \sum_{i=1}^{N_{ESU}} SOC_t^{ESU,i} \quad \forall t = 1, \dots, N_t \quad (5.37)$$

$$C_I^{HESU} \leq Budget_{max} \quad (5.38)$$

$$\frac{E_t^{ESU,i}}{P_t^{ESU,i}} = \kappa^{ESU,i} \quad (5.39)$$

$$S^{ESU,i} = \sqrt{P_{ESU,i}^2 + Q_{ESU,i}^2} \quad (5.40)$$

5.4 Methodology

HESU planning is involved with significant capital investment and therefore it is important to maximize the arbitrage cost with the available capacity. Hence, it is essential to find an optimal size and location of HESU including the arbitrage cost. To implement this, the optimization problem is divided into two sub-problems with equation 5.8 being the primary objective and equation 5.41 being the secondary objective function, where the secondary objective function deals with the arbitrage cost. The constraints of the secondary objective function are given by the equation 5.42 to equation 5.45.

$$S_{Obj} = \sum_{t=1}^{N_t} [P_{dis,t}^{HESU} \times T_{sell,t} - P_{ch,t}^{HESU} \times T_{pur,t}] + C_{FOM}^{HESU} \quad (5.41)$$

subject to

$$\sum_{t=1}^{N_t} P_{dis,t} \times D_{eff} = D_f \times \sum_{t=1}^{N_t} P_{ch,t} \times C_{eff} \quad (5.42)$$

$$\sum_{t=1}^{N_t} P_{ch,t}^{HESU} \times \Delta t \leq E_{max}^{HESU} \quad (5.43)$$

$$\sum_{t=1}^{N_t} P_{dis,t}^{HESU} \times \Delta t \leq E_{max}^{HESU} \quad (5.44)$$

$$\sum_{t=1}^{N_t} P_{dis,t} \leq E_{dem,b} \quad (5.45)$$

Equation 5.42 describes the total charging and discharging power flow into the ESU in a day must be equal. This equality constraint is relaxed by using a factor Df. The total charging and discharging energy must be less than or equal to the maximum energy capacity of ESU, represented in equation 5.43 and 5.44. Equation 5.45 represents the sum of discharging power in a day must be less than the total energy demand of that day at the bus where ESU is placed.

To optimize the stated problem (both primary and secondary objective function), a methodology is proposed as mentioned in Figure 5.2.

Although the PSO algorithm is widely applied in various optimization problems, it can get weak in finding a global optimal solution as the PSO particles may converge prematurely around the local minimum. From the literature, it is evident that the PSO algorithm fails to converge to a global minimum or ends up with premature convergence when the velocity parameter approaches a value very near to zero. In other words, if the velocity vector is very close to zero, the position vector cannot move from its previous position significantly and therefore resulting in premature convergence or settling at a local minimum. To address this problem, the average absolute value of the velocity vector is calculated at the end of every iteration and this can be utilized to improve the exploratory ability of PSO. However, to increase the strength of the exploration ability of the algorithm, it is desirable to have a high average velocity for a longer duration in the initial stage of optimization. During the ending stage of optimization, the average velocity must take a small value for a longer duration to obtain the optimal solution. Therefore to avoid such types of results, the authors have applied the methodology proposed in [147]. Here, the velocity of PSO is calculated using a nonlinear function as given below:

$$v_{new}(t) = v_{initial} \times \frac{1 + \cos\left(\frac{t\pi}{0.95 \times It_{max}}\right)}{2} \quad (5.46)$$

where v_{new} is the updated velocity for PSO particle, $v_{initial}$ is the initial velocity (generated randomly), It_{max} is the maximum number of iterations. The inertia weights of PSO are calculated using the equations 5.47 and 5.48 depending on the conditions specified.

$$w(t+1) = \max(w(t) - \Delta w, w_{min}) \text{ for } v_{avg}(t) \geq (t+1) \quad (5.47)$$

$$w(t+1) = \min(w(t) - \Delta w, w_{max}) \text{ for } v_{avg}(t) < (t+1) \quad (5.48)$$

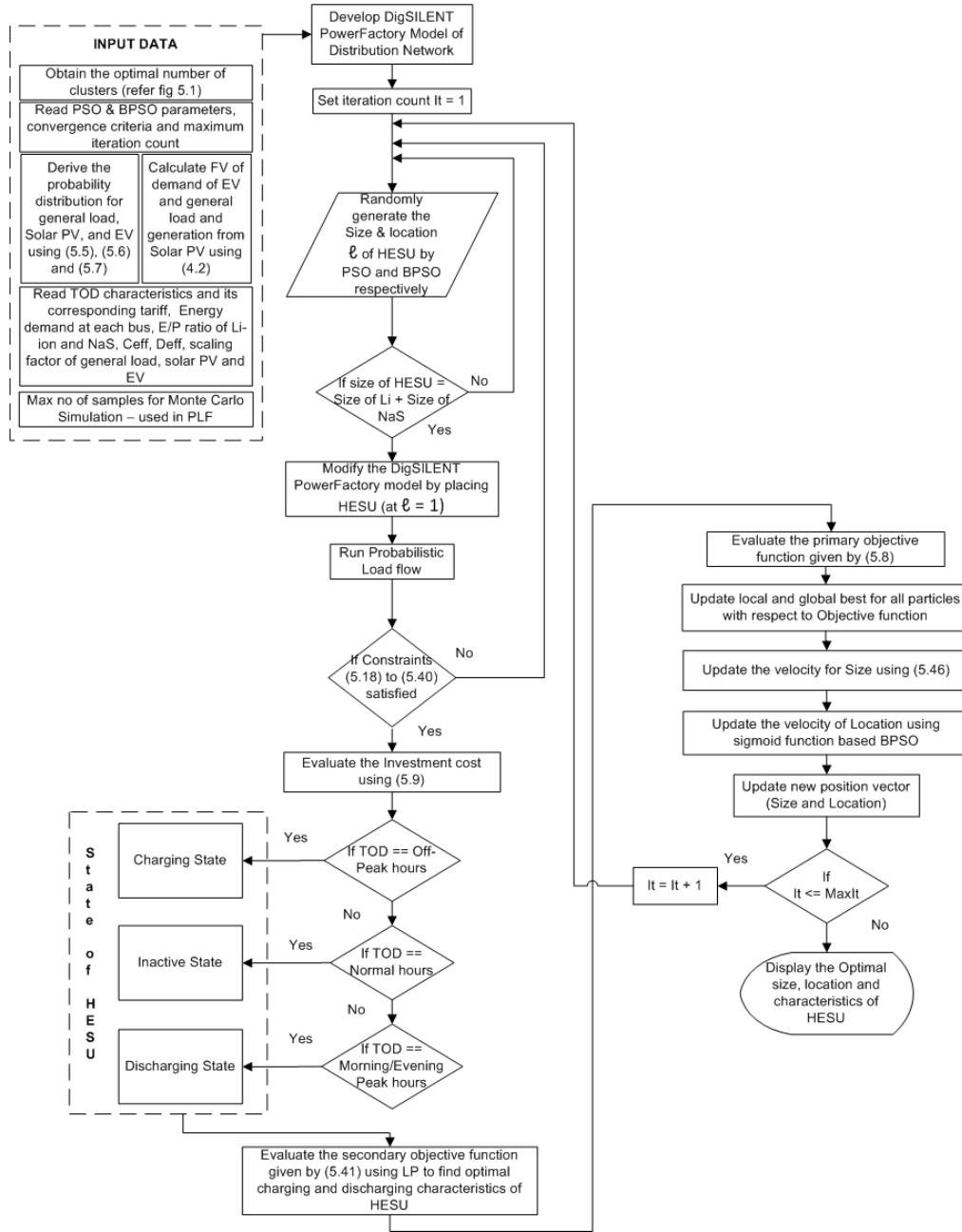


Figure 5.2: Flowchart of Proposed Methodology

5.5 Case Study Results

In this case study, the optimal planning of HESU is performed for a practical 156-bus system of Dehradun district, Uttarakhand, India. The distribution system modelling is performed as discussed in chapter 4 including the scaling factors and uncertainties of general load, EVs and solar power generation. All experiments of this study are conducted on a computer with Intel i7-4510U CPU and 8 GB RAM. Other input parameters are shown in Table 5.1. The TOD and tariff details (for summer and winter) used in this study are referred from Uttarakhand

Power Corporation Limited (UPCL) [139].

Table 5.1: Input Parameters for Optimal Planning

<i>Outcomes of Survey</i>	
GF_D	1.054
GF_{PV}	1.386
GF_{EV}	2.045
P_{pre}^D	Annexure
P_{pre}^{PV}	26.454 MWp
P_{pre}^{EV}	400 kW
<i>Parameters for Optimization</i>	
PSO parameters	$w_{min} = 0.2, w_{max} = 0.9, nDeltaw = 0.1, c-1 = c-2 = 1.5$
Maximum No of iterations	300
Population size	50
Range of HESU size	[0.1,2] in MVA
κ^{Li-ESU}	1.2
$\kappa^{NaS-ESU}$	4
k_{env}	0.0085 \$/kg CO2
k_{VD}	0.142 in \$/p.u
k_{LL}	0.503 in \$/p.u
k_{Loss}	0.265 in \$/p.u
$[V_{min}, V_{max}]$	[0.95 p.u, 1.05 p.u]
LL_{max}^l	80% of line capacity

As discussed, the electric vehicle loads are mostly distributed in regions where the population and load density are high. As mentioned before, the optimal number of clusters is obtained by CQI. After applying the methodology shown in Figure 5.2, the optimal number of clusters will be six. Consequently, the curve of CQI shown in Figure 5.5 has attained its peak value at 6, which shows that the Dehradun district is clustered into six numbers of regions. The distribution network nodes (buses) located in these clustered regions are shown in Figure 5.7. This figure also depicts the spread of the distribution network over mixed terrain. The distribution of electric vehicle load on these regions was carried out based on EVDI as shown in Table 5.3. For better understanding, the cluster color used in Figure 5.7 is presented in this table.

The characteristics of HESU charging and discharging obtained by maximizing the secondary objective function (arbitrage cost) for summer and winter are shown in Figure 5.3 and 5.4 respectively. By incorporating the input parameters (shown in Table 5.1) to the proposed methodology (shown in Figure 5.2), the optimal results obtained are shown in Table 5.4. It is evident from the cluster no represented in Table 5.4 that the

sixteen optimal locations of HESU are widely spread across the network. Since the HESUs are distributed completely throughout the network region, these can serve critical loads (or part of the load connected) in case of grid failure. After placing the HESUs at the optimal locations with the size mentioned in Table 5.4, the bus voltage profile has significantly improved. This is shown in Figure 5.8, as a comparison of bus voltage profile with and without HESU in terms of percentage. From the obtained results, the one having global minima and converging with less number of iterations is shown in Figure 5.6. From this, it is evident that the proposed methodology converges to a global minimum at around 110th iteration count.

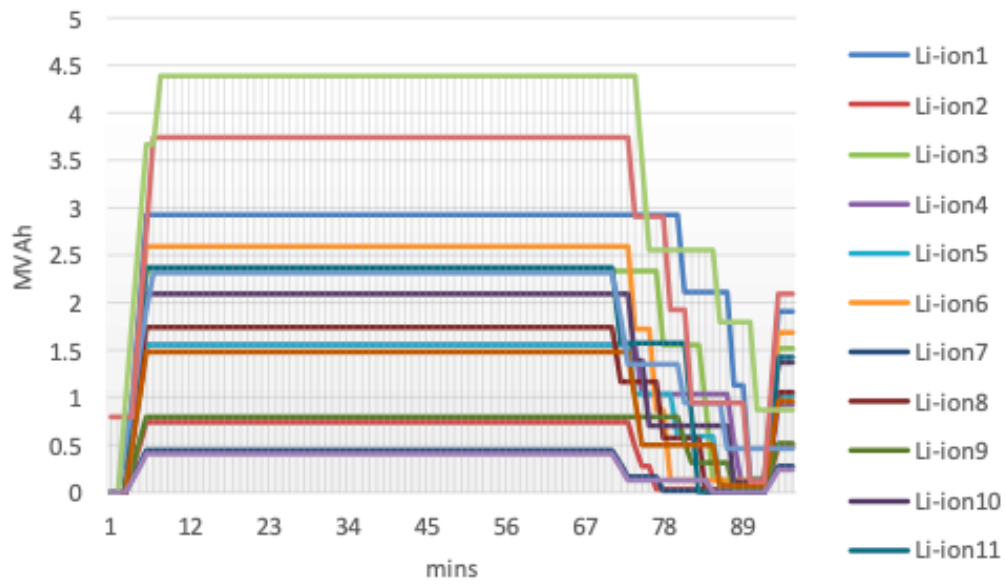
As mentioned earlier, recent studies prove that Li-ion ESU contributes to CO_2 emission significantly. Moreover, it is nearly impossible in today's scenario to completely replace this technology as it has shown promising results in terms of peak management. However, many companies have invested in other ESU technologies which have less environmental effect, one such is NaS ESU. Therefore, in this study, an optimal configuration of Li-ion and NaS ESUs are formed as HESU, which can minimize the environmental impact. This can be visualized with a comparison of damage cost due to CO_2 emission for having only Li-ion technology and the proposed hybrid configuration (HESU) is shown in Table 5.2. The CO_2 emission level is also compared and shown in Figure 5.9. It is evident from Table 5.2 that the HESU has significantly decreased the damage cost by 99548.8 dollars.

Table 5.2: Damage Cost Comparison

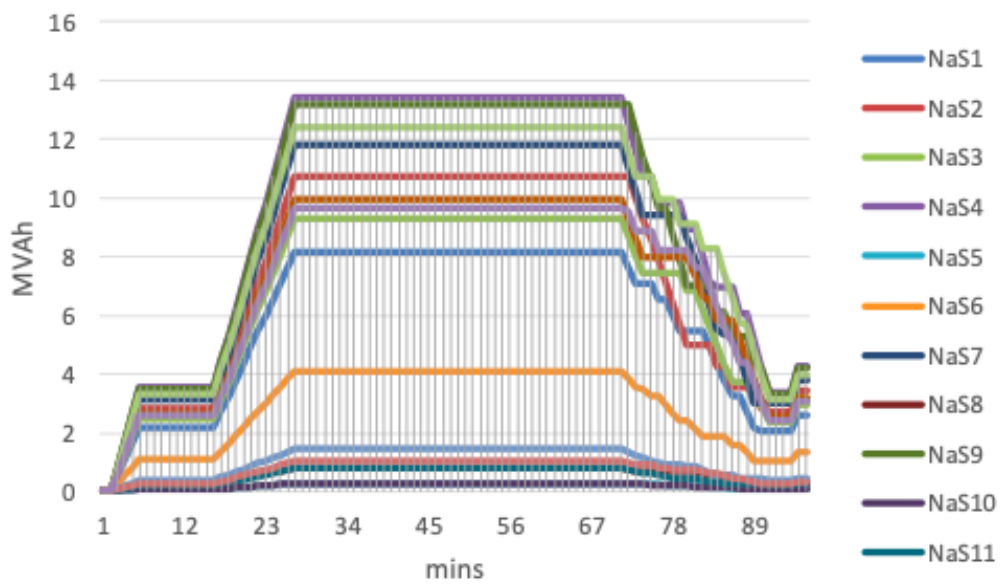
Damage cost (in \$)	Only Li-ion	HESU
	259092.7	159543.9

Table 5.3: Distribution of EVs on Optimal Clusters based on EV
Distribution Index

$f_n = 5$	Optimal No. of Clusters = 6			Total EV load on grid in f_n^{th} year = 1.85 MW		
	C_1 (blue)	C_2 (red)	C_3 (black)	C_4 (yellow)	C_5 (cyan)	C_6 (white)
EVDI	0.15	0	0.55	0	0.3	0
EVs in f_n^{th} year	278	0	1018	0	555	0



(a)

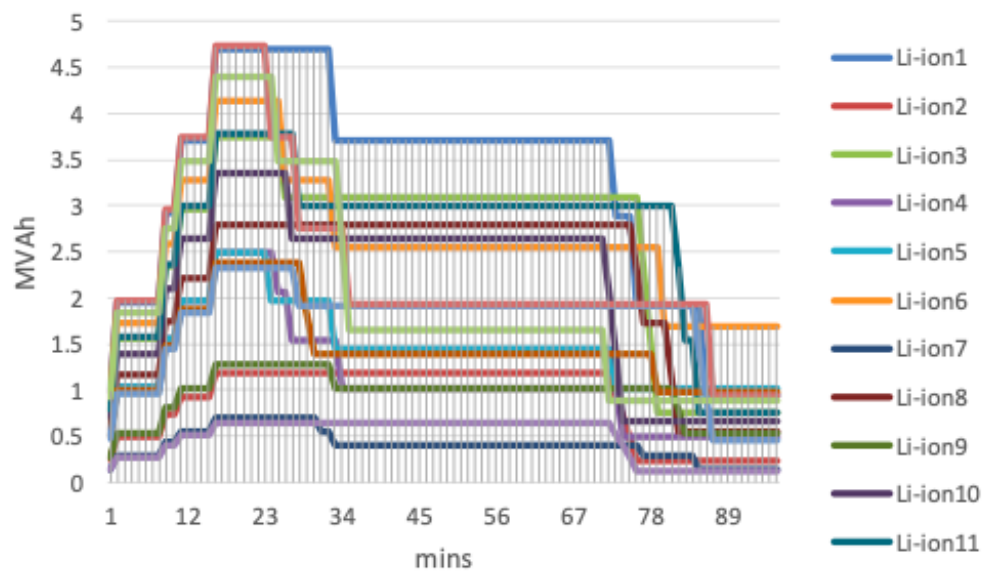


(b)

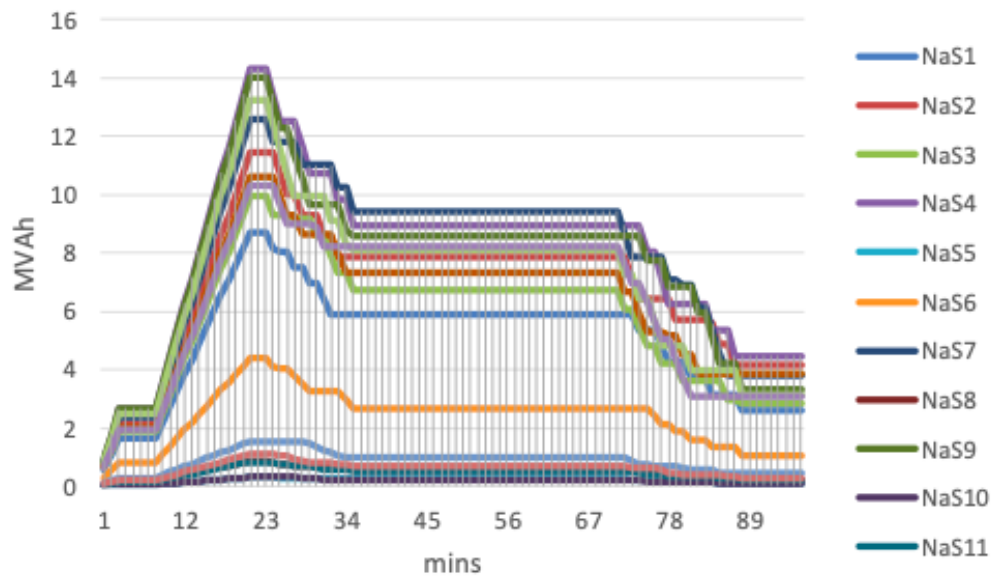
Figure 5.3: Optimal Charging and Discharging Characteristics of HESU during Summer (a) Li-ion ESU (b) Na-S ESU

Table 5.4: Size and Location of Optimal ESUs in Dehradun Distribution Grid

Optimal No of Location	Location Name	LAT	LON	Cluster No	Size of HESU	Size of Li	Size of NaS	Objective Function
	Anarwala	30.3657	78.0445	2	1.5219	0.9769	0.545	
	Araghar	30.3069	78.0499	2	0.9603	0.2452	0.7151	
	Bindal	30.3305	78.0297	2	1.4004	0.7797	0.6207	
	Dakpatti	30.3916	78.0944	3	1.4151	0.5194	0.8957	
	ITpark	30.3015	78.0583	2	0.5376	0.5188	0.0188	
	Landour	30.4555	78.1023	1	1.1377	0.8634	0.2743	
	Miyawala	30.267	78.0909	4	0.9331	0.1464	0.7867	
	Nagarpalika	30.10647	78.28156	0	0.6385	0.5835	0.055	
16	Nagthat	30.5721	77.9721	5	1.1453	0.2682	0.8771	1646388252
	Niranjanpur	30.2967	78.0141	4	0.717	0.6975	0.0195	
	Raipur	30.309	78.0948	2	0.8413	0.7894	0.0519	
	Raiwala	30.0222	78.2147	0	1.1595	0.496	0.6635	
	Sahaspur	30.3927	77.8096	4	0.579	0.4826	0.0964	
	Savra	30.82238	77.8546	5	1.0549	0.9858	0.0691	
	Tuini	30.9429	77.8496	3	1.7432	0.916	0.8272	
	Vasant Vihar	30.3226	78.0037	2	0.778	0.134	0.644	



(a)



(b)

Figure 5.4: Optimal Charging and Discharging Characteristics of HESU during Winter (a) Li-ion ESU (b) Na-S ESU

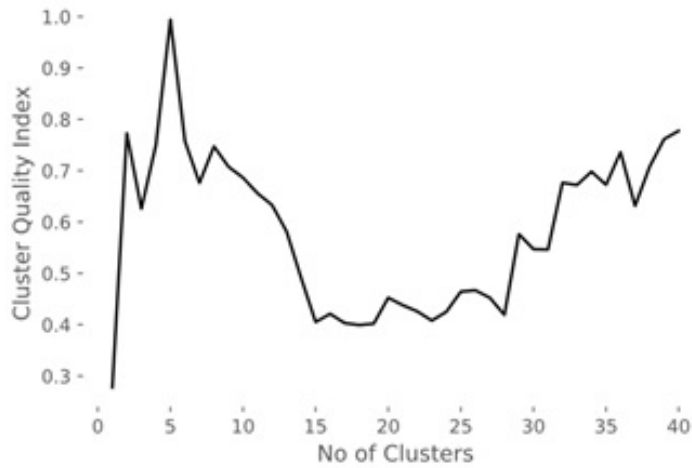


Figure 5.5: Cluster Quality Index for different number of clusters

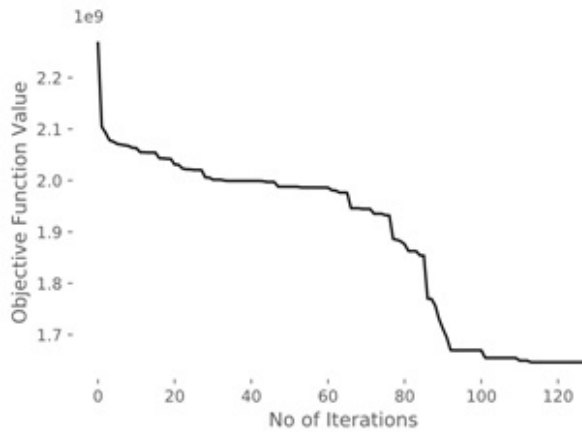


Figure 5.6: Convergence of Proposed Methodology

5.6 Closing Remarks

In this chapter, the optimal planning of HESU for an Indian mixed terrain distribution grid is discussed by modelling the problem with practical constraints such as RPO, land required to install HESU and its associated cost, CO_2 emission from ESU affecting the environment. Apart from this, the outcomes of the survey is discussed from which it is clear that the EV loads are not connected throughout the distribution network. Hence, the distribution grid is clustered based on load density, geographical data (latitude, longitude and MSL), TI, and population. After this, the EV loads are placed on clusters where both the population and load density are high. Within the cluster, the EV loads are distributed using EV_{DI} (obtained from the survey). Having these data, the distribution system is modelled in DigSILENT PowerFactory as explained in chapter 4.5 and the optimal planning of HESU is obtained from the proposed methodology.

The ESU planning in the literature did not consider the environmental

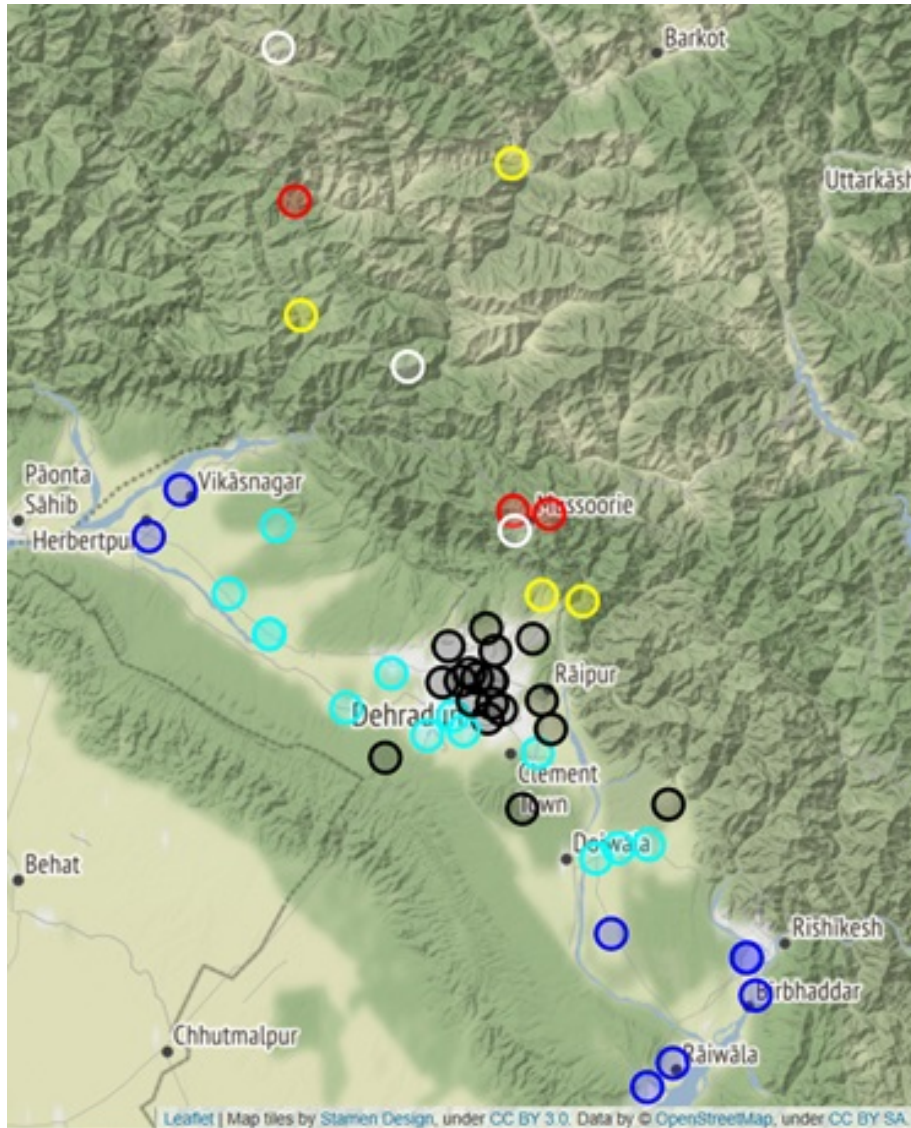


Figure 5.7: Map of Dehradun district with Optimal number of clusters

impact, but it has the utmost importance for sustainable planning. Therefore, to minimize the emission level from ESU, a hybrid combination of popular Li-ion battery along with Na-S battery technology has been implemented using the proposed methodology. The optimized results paved a way towards reduced damage cost due to CO_2 emission significantly, by considering the other components such as uncertainty (of load and solar PV), grid performance cost, land cost index, operation and maintenance cost, arbitrage cost, and capital investment. From the results obtained, it is also evident that the HESUs are widely spread across all the clusters of the distribution network. Therefore, the same HESUs can be utilized to form microgrids to satisfy critical loads during grid failure or to improve the overall resiliency of the system.

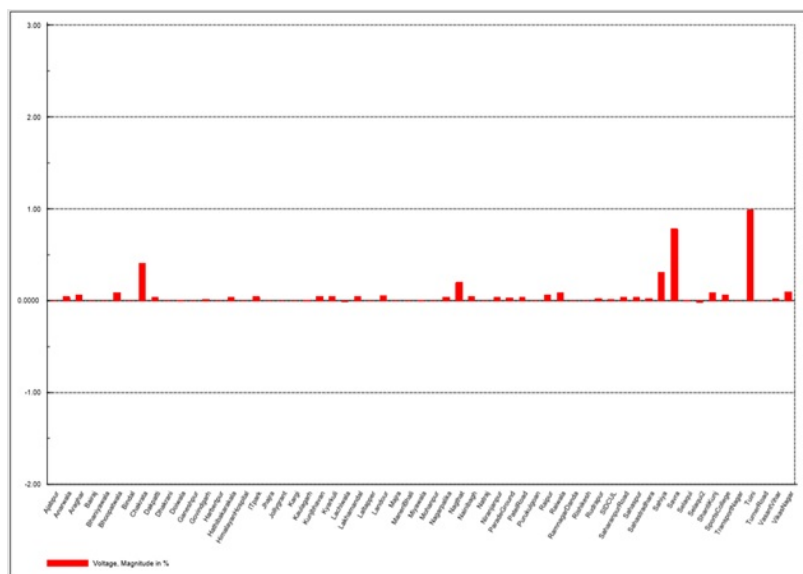


Figure 5.8: Comparison of bus voltage profile with and without HESU in percentage

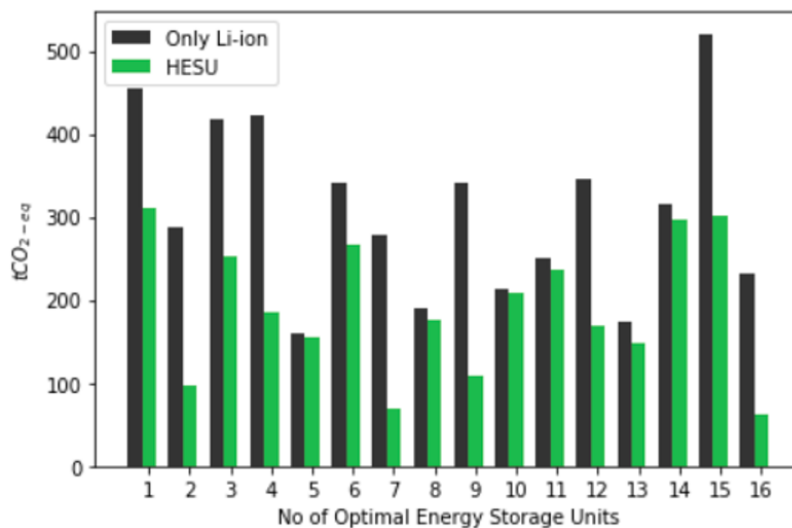


Figure 5.9: Comparison of CO2 Emission with only Li-ion and HESU

Chapter 6

Resiliency Enhancement Strategies via Optimal ESU Planning

This chapter proposes two schemes to enhance the system resiliency by applying both the grid-side and demand-side strategies. The first scheme utilizes ESUs and battery inverter set (BIS) to improve both the grid flexibility during normal condition and the grid resiliency during extreme conditions; whereas in the second scheme, a three-dimensional hardening methodology is proposed to improve the same. In both these schemes, the optimization problem is formulated considering the real-world scenarios and practical constraints including the uncertainty parameters and potential vulnerability of the distribution system components. This chapter is based on the journal publication [132].

6.1 Introduction

The electrical distribution grid is unremittingly vulnerable to natural disasters. Therefore, it is essential to increase the system resiliency by placing resilient energy sources that can serve the demand when needed. In the first scheme, a two-stage framework is proposed to enhance the resiliency of the distribution system via hardening and operational strategies against earthquakes. Here, vulnerability-constrained optimal planning of ESUs and combined operation of ESUs and BIS installed at domestic load are used to enhance hardening and operational resiliency. The vulnerability of both electrical substations and distribution lines against earthquakes is characterized using PGA and fragility curves. For better planning of ESU, the uncertainties associated with REPs and load are modelled. From the obtained results, it is evident that the combined operation of BIS and ESUs has increased the energy served during the emergency period, thereby improving the overall system performance. Moreover, increased BIS capacity can greatly decrease the capital investment for utilities toward large-scale ESUs.

As an extension of the first scheme to implement both the grid-side and demand-side strategy for overall resiliency enhancement, in the second scheme, a three-dimensional optimal hardening strategy is proposed which includes underground cables (UCs), large-scale ESUs, and home battery inverters (HBIs). Here, a Monte-Carlo based probabilistic disaster hazard model is applied as explained in section 4.4. Through this model, all possible occurrences of the disaster are identified and the failure likelihood of substations and distribution lines is established. Thenceforth, the network is clustered using a k-means algorithm based on the potential risk to identify different clusters, a MINLP problem is formulated to identify the optimal location and size of ESUs, and the overhead distribution line to be paralleled with UCs. The demand-side resilience is enhanced via developing a communication infrastructure between the HBIs spread out across the distribution network for effective operation under emergency conditions. Since the utility level hardening requires a significant initial investment, the proposed methodology deploys decision-making based on the predicted revenue generation. The effectiveness of the proposed methodology is analyzed via numerical experiments and verified by applying it to a practical distribution system.

6.2 Framework to enhance System Resiliency against Earthquakes

6.2.1 Proposed Framework

The two-stage framework for optimal planning of ESUs is shown in Figure 6.1 and is discussed in further subsections.

Resiliency enhancement via Hardening

In this stage, the system hardening is carried out by identifying the optimal locations of ESUs constrained by the vulnerability of electrical infrastructure against natural disasters on top of other practical constraints. As mentioned in Figure 6.1, the system hardening to improve both flexibility and resiliency follows a three-stride procedure as discussed below:

- **Vulnerability Assessment against Earthquakes:** The vulnerability assessment against earthquakes is carried out for critical electrical infrastructures like substations and distribution lines as mentioned in chapter 4.3. Here, the historical earthquake data is obtained from the seismic activity catalogue. From this, the moment magnitude of the earthquake, its location (latitude and longitude), and the distance from the epicentre to the hypocentre are derived. The ground acceleration due to an earthquake gets attenuated as it travels along with various soil types.

- **Distribution network modelling:** The modelling of the distribution network aligned with the chosen problem is very essential. As mentioned earlier, the proposed two-stage framework for ESU planning is suitable for both normal and extreme conditions. By connecting suitable energy resources at the demand end and ensuring its operation during the emergency condition will greatly improve the demand-side resiliency. In this scheme, it is assumed that the communication infrastructure between the BIS (connected to the domestic load center across the distribution grid) and the control center is available. Here, the BIS acts as a load during the normal condition and as a local energy resource which can serve the essential demand during emergency conditions. Therefore, the distribution system model developed consists of domestic loads (with BIS as obtained from the survey) and the uncertainties of REPs and load. The DigSILENT PowerFactory model of the distribution system along with the uncertainties of REPs and load is developed as explained in section 4.5.
- **Optimal Planning of ESUs:** The formulated optimization problem consists of the cost of investment (including installation and land cost corresponding to the location), operation and maintenance cost, environmental damage cost (created by ESUs), and the cost of grid performance. Minimizing the objective function based on the inputs from the previous stage using an algorithm that combines APSO and BPSO provides the optimal capacity and location of ESUs. Here, the deciding factor for the location of ESUs is the overall damage probability estimated using the vulnerability assessment. Therefore, instead of responding to the outages after the earthquake, the proposed framework for hardening positions the system operator to act before the occurrence of the event.

Resiliency enhancement via operational strategies

The operational strategy formulated to enhance the system resiliency follows a two-stride procedure as discussed below:

- **Clustering of the distribution network:** Following an earthquake, the distribution network is grouped into k number of clusters to restore the supply for maximum possible consumers including critical/priority-based. In other words, the formation of clusters leads to minimal overall load curtailment. Here, it is assumed that the communication link is available between the control center and BIS during the event.
- **Optimal Operation of ESUs:** Initially, the communication infrastructure derives the SOC level of BIS to the control center available within the cluster. The formulated optimization problem

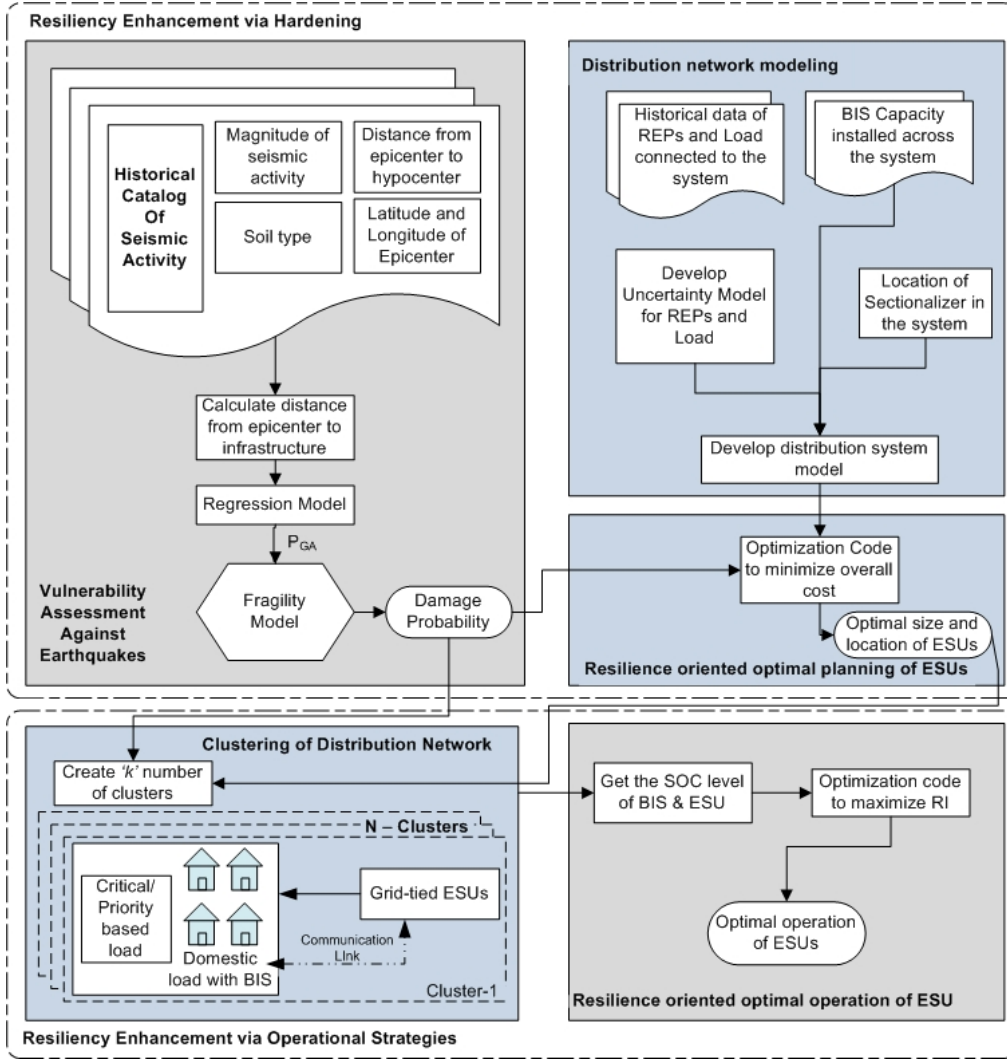


Figure 6.1: Framework to Improve Grid Flexibility and Resiliency

consists of the status of BIS (i.e., its SOC level), the power demand of the critical/priority-based load, and the demand for domestic load within the clusters. Maximizing the overall energy served by the targeted ERT using linear programming provides optimal operation of ESUs within the clusters.

The conceptual system performance to enhance system resiliency against natural disasters has been proposed in many studies of the literature [28, 148, 149]. The significance of the proposed framework to enhance system performance against the natural disaster is shown in Figure 6.2. Here, during the occurrence of an event at time t_e , the system has begun to degrade and reached a minimum level at the time t_{r1} . If the ESUs for improving the grid flexibility are deployed considering the impact of natural disaster, then not only the interruption time will be shifted to t_{r2} by a factor of ΔT_1 , but also the system performance will be improved by ΔP_{D1} . It is also evident that, by considering the effect of BIS in the system, the interruption time and the system performance will be improved by ΔT_2

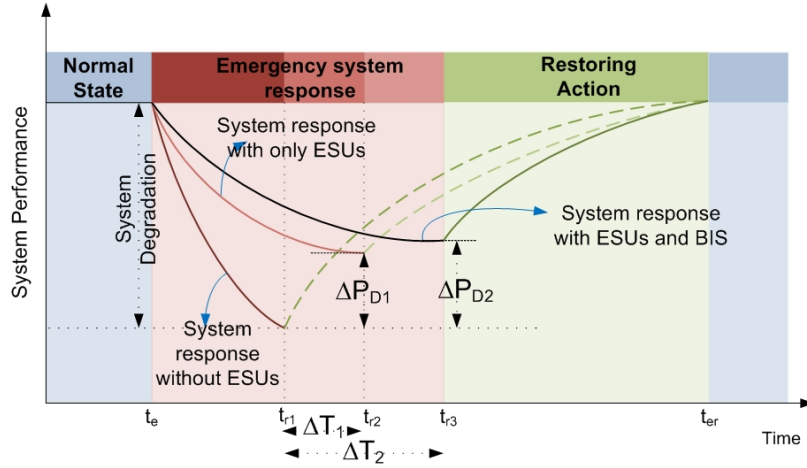


Figure 6.2: System Performance against natural disaster: without ESUs, with only ESUs, with ESUs and BIS

and ΔP_{D2} respectively. Therefore, one may recognize that, by hardening the distribution network via ESUs, it improves the system resiliency as the critical/priority-based demand is satisfied for a period of ΔT_1 during the interruption. However, by considering the BIS installed in the system along with ESUs, the performance of the system can be improved by ΔP_{D2} and the critical/priority-based demand will be satisfied for a period of ΔT_2 during the interruption. The seismic model and the fragility model are implemented as discussed in the sections 4.3.1 and 4.3.2.

6.2.2 Proposed Methodology

The proposed methodology for optimal planning of ESU combines the grid-side and demand-side resiliency strategies. As mentioned earlier, vulnerability-constrained optimal ESU improves the grid-side resiliency, and the optimal operation between ESUs and BIS improves the demand-side resiliency.

Selection of Nodes for ESU Placement

The operation of electrical infrastructure such as distribution lines might get interrupted due to its partial/complete damage followed by an earthquake. Therefore, while planning ESUs, it is essential to choose the candidate bus such that the electrical infrastructure suffers from null or minimal damage. In this scheme, an algorithm based on vulnerability assessment is proposed to define the set of nodes for ESU planning shown in Figure 6.3

Algorithm - I - Selection of Nodes for ESU Placement Input: N_b , distribution lines connected to the bus N_b worst case and frequent seismic hazard.

Step 1. **for** $i = 1:N_b$

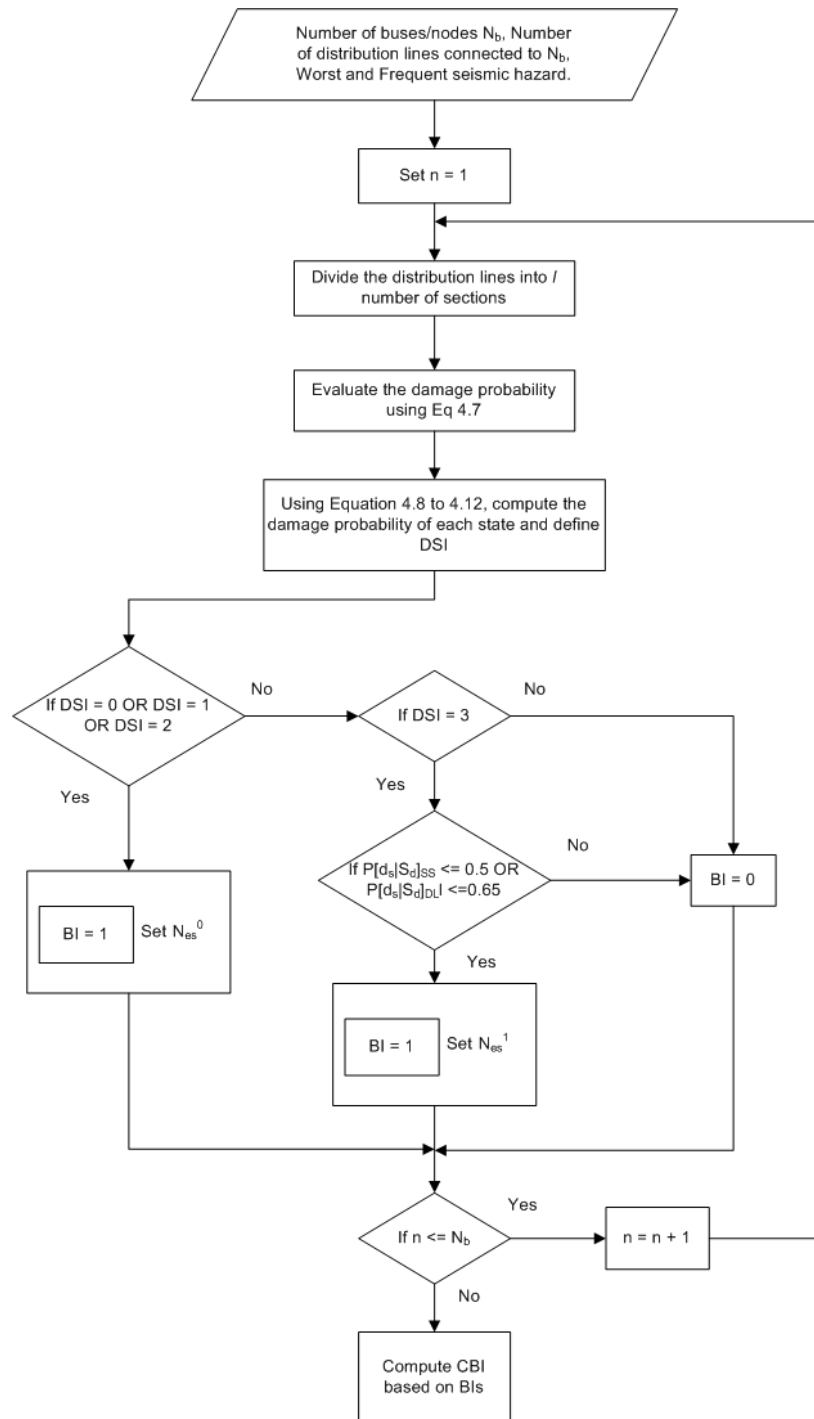


Figure 6.3: Flowchart of Algorithm I: Selection of Nodes for ESU Placement against worst and frequent Seismic hazard

- Step 2. Divide the distribution line into l number of sections
- Step 3. Evaluate the damage probability of substation and the distribution lines connected to the bus i using the equation 4.7.
- Step 4. Using equation 4.8 to 4.12, compute the damage probability of each state for the substation and the distribution line sections. Moreover, define its damage state index (DSI) as 0,1,2,3, and 4 corresponding to none, minor, moderate, extensive, and complete.
- Step 5. Define binary index (BI) for each substation and the distribution line section as given below:

- i. **if** $DSI_{SS|DL_i} = 0$ **OR** $DSI_{SS|DL_i} = 1$ **OR** $DSI_{SS|DL_i} = 2$:
 $BI_{SS|DL_i} = 1 \in N_{es}^0$
- ii. **if** $DSI_{SS|DL_i} = 3$
if $P[d_s|S_d]_{SS} \leq 0.5$ **OR** $P[d_s|S_d]_{DL_i} \leq 0.65$
 $BI_{SS|DL_i} = 1 \in N_{es}^1$
else
 $BI_{SS|DL_i} = 0$
- iii. **if** $DSI_{SS|DL_i} = 4$
 $BI_{SS|DL_i} = 0$

Step 6. **end for**

Step 7. Compute the combined binary index (CBI) as : $CBI_i = BI_{SS_i} \times [BI_{DL1} + BI_{DL2} + \dots + BI_{DLl}]_i$

In the above equation of CBI_i , the symbol $+$ represents logical **OR** and the symbol \times represents logical **AND**.

Optimal sizing and siting of ESUs

The distribution network model is developed by incorporating the uncertainty of REPs and load (modelled using beta and normal distribution function respectively) [131]. As mentioned earlier, the location of ESU will be decided using a binary vector given by the equation 6.1.

$$CBI_i = \begin{cases} 1, & \text{place ESU at location } i \in N_{es} \\ 0, & \text{otherwise} \end{cases} \quad (6.1)$$

The optimal size and location of ESUs to enhance both flexibility and resiliency is obtained by minimizing the formulated objective function given in the equation 6.2.

$$Obj = C_{I|L}^{ESU} + C_{OM}^{ESU} + C_{Env}^{ESU} + C_p^{Grid} \quad (6.2)$$

where

$$C_{I|L}^{ESU} = \sum_{i=1}^{N_{ESU}} \left[C_{PI}^{ESU,i} + C_{EI}^{ESU,i} + C_{FI}^{ESU,i} + (LCI^{N_{es}} \times C_{land}^{N_{es}} \times A^{ESU,i} \forall N_{es}^0, N_{es}^1 \in N_{es}) \right] \quad (6.3)$$

$$C_{OM}^{ESU} = \sum_{i=1}^{N_{ESU}} [C_{FOM}^{ESU} \times P_{rated}^{ESU}] \quad (6.4)$$

$$C_{env}^{ESU} = \sum_{i=1}^{N_{ESU}} P_{rated}^{ESU} \times \gamma^{ESU,i} \times \kappa_{env} \quad (6.5)$$

$$C_p^{Grid} = \sum_{b=1}^{N_b} |V_{Rated} - V_b^{ESU}| \times \mathbb{k}_{VD} + \left(\sum_{l=1}^{N_l} \%LL^{ESU} \right) \times \mathbb{k}_{LL} + \sqrt{\left(\sum_{l=1}^{N_l} (P_{Loss,l}^2 + Q_{Loss,l}^2) \right) \times \mathbb{k}_{Loss}} \quad (6.6)$$

In the equation 6.2, the first term represents the installation cost of ESU, which includes investment cost (consisting of the cost of fixed installation in \$/kW-day, the cost of power rating in \$/kW-day and the cost of energy rating in \$/kWh-day) and variable land cost (as the area witnessed the development, its land availability plays a major role in the installation of ESUs). The variable land cost is calculated based on the physical size of ESU in sq.m times the price of the land in \$/sq.m. Here, the LCI signifies the category of land by which its cost variation is addressed. The second term denotes the fixed operation and maintenance cost of ESU concerning its power rating. Considering the need to shift towards environmentally friendly technology, here the cost of environmental damage created by CO_2 emissions from ESU is reflected in the fourth term. The last term represents the cost involved in ESU affecting the grid performance. In the equation 6.3, if the ESU is to be placed in a candidate bus $\in N_{es}^1$, then the fixed investment cost is increased by a factor α to improve the structural stability.

Optimization Constraints

The demand in the power system at any time t must be satisfied. This real power balance is represented in equation 6.7. The operational constraints of the distribution system such as real and reactive power flow, voltage limits, the limit of maximum loading of the distribution lines are represented in equations 6.8 – 6.11 respectively. The operational constraints of ESU such as the real power limit, energy capacity limit, limit of SOC, apparent power, and budget limit are represented in the equations 6.12 – 6.16 respectively.

$$P_{D,t} = P_t^{SPP} + P_t^{ESU} + P_t^{Grid} \quad \forall t = 1, \dots, N_t \quad (6.7)$$

$$P_f^{i,t} = V^{i,t} \times \sum_{i,j \in N_b} V^{j,t} (G_{ij} \cos \theta_{ij,t} + B_{ij} \sin \theta_{ij,t}) \quad (6.8)$$

$$Q_f^{i,t} = V^{i,t} \times \sum_{i,j \in N_b} V^{j,t} (G_{ij} \sin \theta_{ij,t} - B_{ij} \cos \theta_{ij,t}) \quad (6.9)$$

$$V_{min} < V_t^b < V_{max} \quad \forall b = 1, \dots, N_b \quad (6.10)$$

$$LL_t^l < LL_{max}^l \quad \forall l = 1, 2, 3, \dots, N_l \quad (6.11)$$

$$P_{min}^{ESU,i} < P_t^{ESU,i} < P_{max}^{ESU,i} \quad \forall t = 1, \dots, N_t \quad (6.12)$$

$$E_{min}^{ESU,i} < E_t^{ESU,i} < E_{max}^{ESU,i} \quad \forall t = 1, \dots, N_t \quad (6.13)$$

$$SOC_{min}^{ESU} \leq SOC_t^{ESU} \leq SOC_{max}^{ESU} \quad (6.14)$$

$$S^{ESU,i} = \sqrt{P_{ESU,i}^2 + Q_{ESU,i}^2} \quad (6.15)$$

$$C_I^{ESU} \leq Budget_{max} \quad (6.16)$$

Formation of clusters in the distribution network

The distribution system is clustered into k number of clusters by minimizing the overall demand curtailment (ODC). The proposed algorithm for cluster formation is shown below:

Algorithm II – Clustering of distribution network

Input: $DSI_{SS|DL_t}, P_{ESU,i}$

Step 1. **for** each possible cluster:

Step 2. Evaluate the ODC (sum of disconnected demands) for each cluster

Step 3. Store the values of ODC in an array

Step 4. **end for**

Step 5. **Sort** each cluster based on its ODC and the cluster with minimal ODC is chosen.

Optimal ESU operation during ERT

Following an event (or disaster), the performance of the system degrades as shown in Figure 6.2. As mentioned earlier, the communication link between the control center and BIS is in operation during ERT. To improve the system performance during ERT, it is essential to maximize the resiliency index (RI), defined as the ratio of energy served during ERT to the expected energy demand. For the maximum value of RI within the cluster during ERT, it is essential to find the optimal power output from ESU for a given SOC level of BIS. Maximizing the objective function given by the equation 6.17 constrained with equations 6.18 to 6.23 using LP leads to the optimal power output of ESU during ERT. In the case of equation 6.17, the difference between t_e and t_{r_3} gives the value of ERT.

$$RI = \sum_{t=t_e}^{t_{r_3}} \left(P_{D,t}^{C|P,k} + P_{D,t}^{do,k} \right) / P_{D,t}^{Exp,k} \quad \forall k \quad (6.17)$$

$$P_{D,t}^{C|P,k} + P_{D,t}^{do,k} = P_t^{ESU} + P_t^{BIS} \quad \forall t = 1, \dots, E_t \quad (6.18)$$

$$\sum_{t=t_r}^{t_{r_3}} P_t^{ESU} \leq E_D^{C|P} \quad (6.19)$$

$$\sum_{t=t_r}^{t_{r_3}} P_t^{ESU} \times \Delta t \leq E_{max}^{ESU} \quad (6.20)$$

$$SOC_{min}^{ESU} \leq SOC_t^{ESU} \leq SOC_{max}^{ESU} \quad (6.21)$$

$$0 \leq P_t^{ESU} \leq P_{max}^{ESU} \quad (6.22)$$

$$0 \leq E_t^{ESU} \leq E_{max}^{ESU} \quad (6.23)$$

where, $P_{D,t}^{C|P,k}$ and $P_{D,t}^{do,k}$ represents the power demand of critical/priority-based load and domestic load in k_{th} cluster respectively at time t , $E_D^{C|P}$ represents the expected energy demand from a critical/priority-based load during the emergency period (E_t), P_t^{ESU} represents the power output from ESU at time t and E_t^{ESU} represents the energy demand satisfied by ESU at time t .

6.2.3 Case Study Results

The system modelled in section 4.5 is considered to analyze the proposed framework of ESU planning against earthquakes. Based on the seismic catalogue of the chosen region, the moment magnitude of the earthquake ranges between $3.5 \leq M_w \leq 5.3$ and the equation 6.24 represents its corresponding regression model [136].

$$\ln(PGA) = c_0 + c_1 \ln(R) + c_2 M_w - c_3 \ln(R + 15) \quad (6.24)$$

The value of seismic regression coefficients c_0, c_1, c_2, c_3 considered in this study are 2.29, 1.95, 2.07 and 4.03, respectively. From the survey conducted across the system, 60

$$PDF_D(P_{BIS}) = \frac{1}{\sigma[P_{BIS}]\sqrt{2\pi}} \times e^{-\left(\frac{P_{BIS}-E[P_{BIS}]}{\sigma[P_{BIS}]\sqrt{2\pi}}\right)^2} \quad (6.25)$$

Here, the Na-S battery technology is chosen for ESU because it has the least climatic impact of $30kgCO_{2-eq}/kWh$ [150]. In this scheme, the cases considered to study the proposed framework are *caseA* : worst case seismic faults and *caseB* : the most frequent seismic fault occurred in the region. Here, based on equation 6.26 derived from the seismic study performed in the chosen region [136], and the normalized (by a factor 100) frequency of occurrence data (for the past five years) is shown in Figure 6.4, representing the historical catalogue of seismic activity, it is evident that the most frequent seismic fault in the chosen region is of 3.3 moment magnitude. The frequent earthquake of moment magnitude 3.3 occurs in eight different locations across the region of study.

$$\text{Log}_{10}N = 5.7 - 0.71M \quad (6.26)$$

where M is the moment magnitude of the earthquake and N is the number of earthquakes with moment magnitude M . Table 6.1 shows the predicted critical/priority-based load which includes hospitals, water pump houses, VIP/VVIP across the distribution system. Table 6.2 shows the median and lognormal standard deviation of the fragility curves corresponding to the different damage states considered in this study.

Table 6.1: Predicted Peak Values of Critical/Priority-Based Loads

Location	Load in MVA	Location	Load in MVA
Anarwala	0.3964	Govindgarh	0.6442
Araghar	3.3698	HimalayanHospital	0.9911
Bhaniyawala	0.7434	Jollygrant	0.5451
Bindal	0.8672	Kunjbhavan	1.4867
Dakpatti	1.9822	Natraj	0.0991

Based on the historical seismic catalogue, the seismic fault occurred in the location ($30.45^\circ N 77.92^\circ E$) with a moment magnitude of 5.4 is the worst-case seismic fault stricken in the region of study.

Set of Nodes & Lines for ESU placement

As described in section 6.2.2, *Algorithm – I*, based on the vulnerability assessment described in section 6.2, derives the set of nodes and distribution

Table 6.2: Median and β_{d_s} Values Of Electrical Infrastructures For Different Damage States

Electrical Infrastructure	Damage State	Median [g]	β_{d_s}
Substation	Minor	0.15	0.7
	Moderate	0.29	0.55
	Extensive	0.45	0.45
	Complete	0.9	0.45
Distribution Lines	Minor	0.28	0.3
	Moderate	0.4	0.2
	Extensive	0.72	0.15
	Complete	1.1	0.15

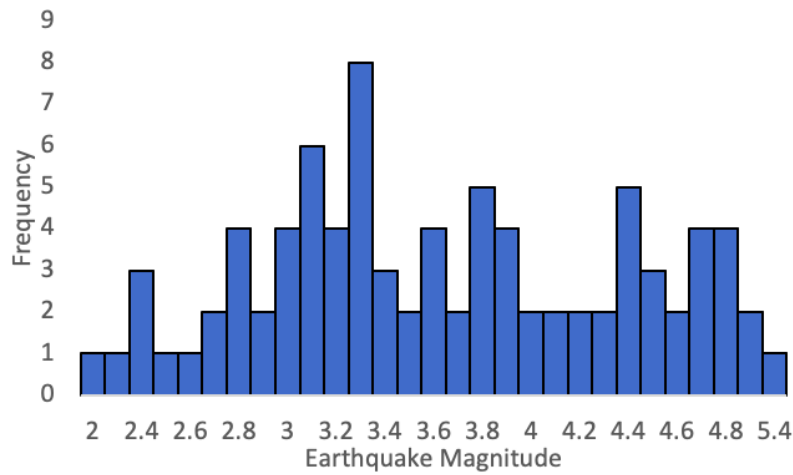


Figure 6.4: Normalized Occurrence frequency of earthquakes in the region of study

lines for ESU placement. Step 4 of *Algorithm – I* descend the accessible substations and distribution lines against an earthquake scenario via the binary vector DSI obtained using equations 4.8 to 4.12. Table 6.3 and Table 6.4 show the accessible distribution lines and substations followed by the worst-case seismic fault, respectively (*caseA*). As described in step 7 of the *Algorithm – I*, the binary vector DSI derives CBI vector which denotes the set of feasible locations for ESU placement with null or minimal damage due to earthquakes. Followed by the most frequent earthquakes analysed for all eight different locations in the region of study, all substations and distribution lines are accessible as per the *Algorithm – I*. Therefore, the identification of the optimal solution for case B is like ESU planning for the normal condition (as explained in chapter 5).

Table 6.3: Accessible Distribution Lines Followed by Worst Case Seismic Fault

Line Section	Damage Probability	DSIDL	Line Section	Damage Probability	DSIDL
L08	0.5114	1	L60	0.6411	3
L09	0.8922	0	L61	0.6411	3
L10	0.5156	1	L63	0.5213	3
L11	0.8975	0	L64	0.7461	2
L12	0.5213	2	L65	0.8338	0
L19	0.6428	3	L66	0.646	0
L20	0.5558	3	L67	0.8006	0
L32	0.5401	1	L68	0.8673	2
L33	0.5293	1	L69	0.8004	0
L34	0.4371	2	L70	0.8409	0
L42	0.601	3	L72	0.5024	3
L48	0.7887	2	L73	0.6601	0
L49	0.9027	2	L75	0.5878	3
L56	0.6258	3	L76	0.5932	3
L57	0.6258	3			

Table 6.4: Accessible Substations Followed by Worst Case Seismic Fault

Substation	Damage Probability	DSISS	Substation	Damage Probability	DSISS
Araghar	0.488396	3	ManeriBhali	0.293203	1
Bairaj	0.331563	1	Nagarpalika	0.292999	1
Bhaniyawala	0.107374	2	Raiwala	0.340927	1
Bhoopatwala	0.378232	1	Ramnagar Danda	0.11555	2
Doiwala	0.103981	2	Rishikesh	0.302965	1
Himalayan Hospital	0.112021	2	Savra	0.167859	2
Jollygrant	0.128834	2	ShantiKunj	0.349822	1
Lachiwala	0.486559	3	Transport Nagar	0.479541	3
Lakhamandal	0.346177	3	Tuini	0.339201	1
Laltapper	0.179293	1			

Results of Optimal Sizing and Siting of ESUs

Having the CBI vector derived from *Algorithm – I*, the objective function given by the equation 6.2 constrained with equations 6.7 to 6.16 derives the optimal size and location of ESUs, which can improve the grid flexibility during the normal condition and the system resiliency during emergency condition. The results of the optimal solution shown in Table 6.5 reflect the global minima obtained using an algorithm that combines APSO and BPSO [131]. During normal conditions, the optimal ESU improves the bus voltage profile of the distribution system. This is evident from Figure 6.5, which represents the percentage comparison of bus voltage profile for cases with and without ESUs.

Table 6.5: Optimal Results of Distribution System Hardening

No of ESUs	Location Name	Lat(oN)	Lon(oE)	Size of ESU	Objective Function
14	Bhaniya wala	30.3657	78.0445	0.5601	442388953.2
	Bhoopat wala	30.3069	78.0499	1.1191	
	Jollygrant	30.3305	78.0297	0.6001	
	Lachiwala	30.3916	78.0944	0.9977	
	Lakha mandal	30.3015	78.0583	1.0158	
	Laltapper	30.4555	78.1023	0.6393	
	Maneri	30.267	78.0909	0.9557	
	Bhali				
	Nagar palika	30.1064	78.2815	1.6935	
	Raipur	30.5721	77.9721	1.6228	
	Ramnagar	30.2967	78.0141	1.9725	
	Danda				
	ShantiKunj	30.309	78.0948	0.5136	
	Transport Nagar	30.0222	78.2147	1.2547	
Bhaniya wala	30.3927	77.8096	0.9243		
Bhoopat wala	30.8223	77.8546	1.133		

Results of Optimal Operation of ESUs

As mentioned earlier, clustering the network to minimize the overall load curtailment (using *Algorithm – II*) defines the demand and available storage capacity in the cluster. Table 6.6 shows the results of the optimal

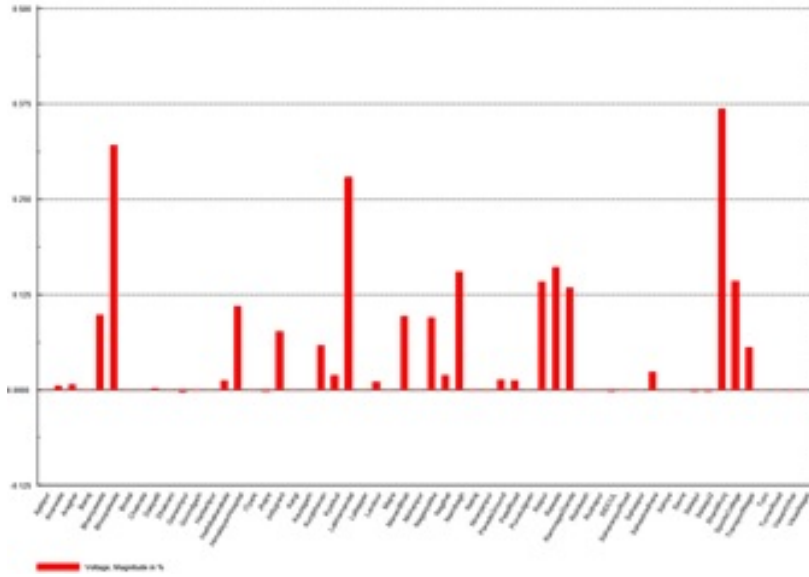


Figure 6.5: Bus Voltage Profile Comparison - with and without ESU in percentage

clusters with the available capacity of ESU and BIS. Having this, the objective function given by the equation 6.17 constrained with equations 6.18 to 6.23 solved using LP derives the optimal operation of ESUs within the cluster by assuming two SOC levels for BIS such as 0% and 100%. Figure 6.6 shows the maximized value of RI by the optimal operation of ESUs along with BIS for various targeted ERTs.

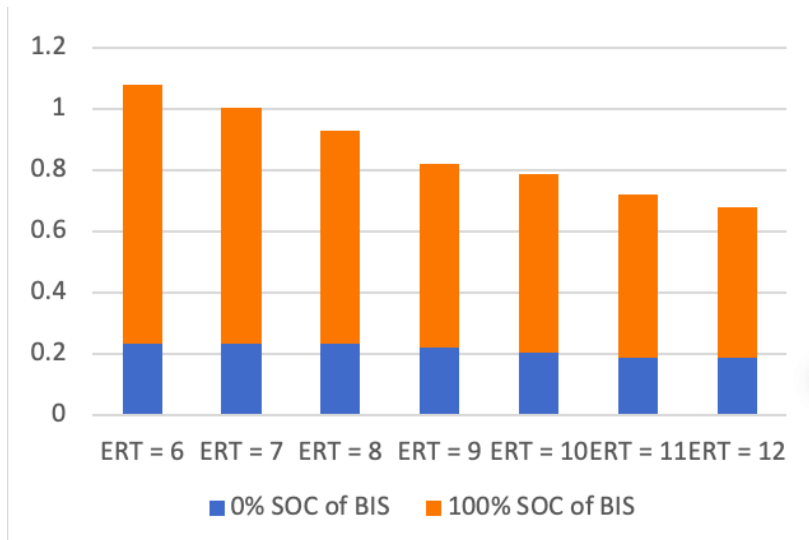


Figure 6.6: Resiliency Index for various SOC levels of BIS

Validation of the Proposed Framework

This section elaborates on the critical findings of this scheme and compares the system performance between various strategies (as mentioned in Figure

Table 6.6: Total Size of ESU, BIS and Critical/Priority-Based Load In Optimal Clusters

	No of ESUs	Total ESU Capacity	Total BIS Capacity	Total Priority Load
Cluster 1	1	0.6393	0.3091	1.0927
Cluster 2	10	10.0026	2.9604	12.4682
Cluster 3	2	3.1055	29.0675	29.9163
Cluster 4	1	1.2547	4.6117	4.7107

6.2) such as without ESUs, with only ESUs and the proposed framework to validate the effectiveness of this work. Section 6.2.3 presents the results obtained from numerical experiments based on two earthquake scenarios (such as the worst seismic fault and the most frequent seismic fault occurred in the chosen region) to validate the proposed framework. The system chosen for this study is situated on a mixed terrain (situated on both hilly and plain regions) comprised of fifty-nine 33kV nodes and seventy-six 33kV lines. From the results obtained for *caseA*, it is evident that out of fifty-nine 33kV nodes only nineteen nodes and out of seventy-six 33kV lines only twenty-nine lines are accessible (shown in Figure 6.7) whereas, for *caseB*, all nodes and lines are accessible. Therefore, any framework which applies to the normal condition is suitable for *caseB*. However, the results obtained for the *caseA* proves that the system may not withstand a high impact low probability (HILP) seismic hazard, i.e., the worst seismic hazard.

From the Figure 6.7, it is apparent that ESU placement obtained for *caseA* also improves the bus voltage profile of the system during normal conditions. For any resiliency enhancement framework, it is essential to minimize the load curtailment during ERTs. From Table 6.6, it is evident that clustering the network concerning *Algorithm – II* minimizes the overall curtailment of critical/priority-based loads within the cluster. It is also clear that maximizing equation 6.17 constrained with equations 6.18 to 6.23 effectively utilizes the presence of BIS and channelizes the ESUs to meet the overall demand with minimized curtailment. Figure 6.6 shows that having 0% SOC of BIS (or without BIS), the ESUs can satisfy approximately 20% of the identified critical/priority-based loads for all targeted ERTs, however, having 100% SOC of BIS (with BIS), the ESUs can satisfy approximately 50% to 80% of the identified load for ERTs ranging from six to twelve hours. This contribution of BIS directly decreases the initial investment of ESUs for utilities. Table 6.8 compares the investment and operation and maintenance costs for having only ESUs and the combination of ESUs and BIS to satisfy the identified critical/priority-based loads. Table 6.7 shows the comparison of system performance based on RI for a system without ESUs, with only ESU and with the proposed framework. From this, it is evident that using this

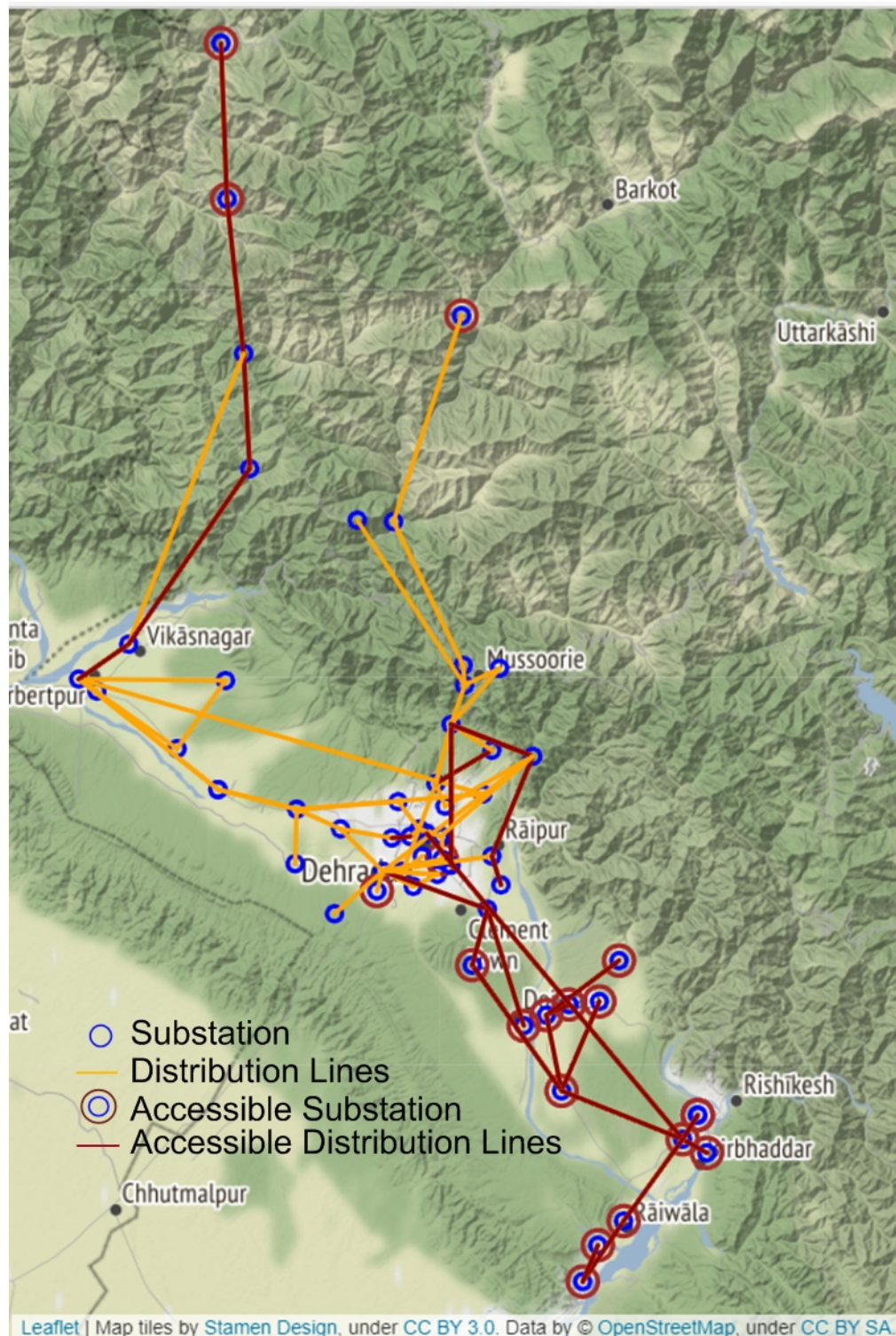


Figure 6.7: Accessible substations and distribution lines derived from Algorithm – I for Case A

proposed scheme, the RI has improved by 60% compared to the strategy of having only ESUs.

Table 6.7: Comparison of RI for various Resiliency Enhancement Strategies

Resiliency Index (RI)	Without ESUs	With Only ESU	Proposed Framework
	0.0659	0.2135	0.6462

Table 6.8: Cost Comparison with Only ESUs and with BIS

	Cost of Investment (\$)	Cost of O&M (\$)
Only ESUs	24624626.57	249363.3
ESU & BIS	7110995.4	72010.08

6.3 Three-Dimensional Optimal Hardening Strategy for Distribution Grid against Natural Disaster

In this scheme, a three-dimensional optimal hardening strategy is proposed based on two mainstays for building resiliency such as grid hardening and demand-side resilience; which includes underground cables, large-scale energy storage units (ESUs), and home battery inverters (HBIs). Here, a Monte-Carlo based probabilistic disaster hazard model is applied as explained 4.4 . Through this model, all possible occurrences of the disaster are identified and the failure likelihood of substations and distribution lines is established. Thenceforth, the network is clustered using a k-means algorithm based on the potential risk to identify different vulnerable zones of the network. To enhance the resiliency via grid hardening, for different clusters, a mixed-integer non-linear problem is formulated to identify the optimal location and size of ESUs and the over-head distribution line to be paralleled with underground cables. The second mainstay – demand-side resilience is enhanced via developing a communication infrastructure between the HBIs spread out across the distribution network for effective operation under emergency conditions. Since the utility level hardening requires a significant initial investment, the proposed methodology deploys the decision-making based on the predicted revenue generation. The effectiveness of the proposed methodology is analysed via numerical experiments and verified by applying it to a practical distribution system.

6.3.1 Concept of HBI

The demand side resiliency can be established by developing a communication infrastructure for coordinated operation. The communication infrastructure applied in this case for HBIs is shown in Figure 6.8. In modern days, the installation of resources and storage systems such as solar standalone rooftops ranging from 1 kWp to 5 kWp and BIS with a size ranging from 850VA to 1150VA respectively are increasing with an idea to become energy independent demand [139, 151]. However, due to the initial investment, these are generally installed to serve the essential demands.

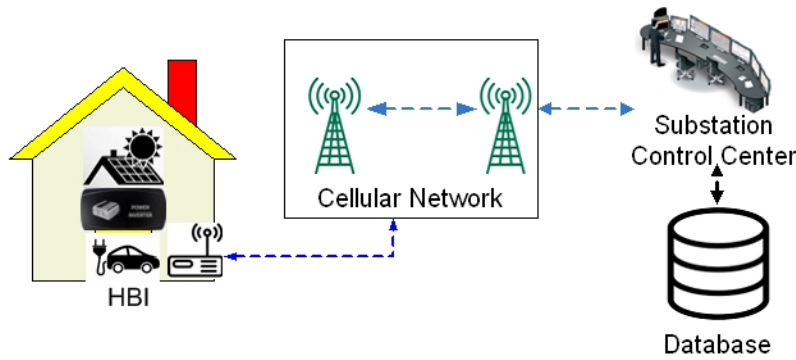


Figure 6.8: Communication Infrastructure for HBIs

6.3.2 Optimization Problem for Three Dimensional Hardening

The objective function consists of three components such as cost for establishing ESUs, underground cabling, and communication infrastructure for HBIs as given in equation 6.27. The costs associated with ESUs are capital investment (which includes energy rating cost, power rating cost, and fixed installation cost), land required to install ESU and its allied cost, operation, and maintenance cost of ESUs, and grid performance cost due to ESUs (which includes voltage deviation cost, line loading cost and cost of power loss) which are represented from equations 6.28 to 6.31. The costs associated with cabling are the capital investment of underground cabling (which includes cable cost per km and its fixed cost) and maintenance cost of underground cables which is represented in equation 6.32. The cost associated with HBIs is the capital investment of communication infrastructure for HBIs represented in equation 6.33. As mentioned earlier, the presence of HBI components may differ between load points and this aspect is reflected using the binary variables such as b_{BIS} , b_{PV} , and b_{EV} for BIS, standalone solar-rooftop, and electric vehicles respectively in equation 6.33.

$$C_{obj} = C_I^{ESU} + C_{land}^{ESU} + C_{OM}^{ESU} + C_{GP}^{ESU} + C_I^{UC} + C_{OM}^{UC} + C_I^{HBI} \quad (6.27)$$

where

$$C_I^{ESU} = \sum_{i=1}^{N_{ESU}} [C_{PI}^{ESU} + C_{EI}^{ESU} + C_{FI}^{ESU}] \quad (6.28)$$

$$C_{land}^{ESU} = \sum_{i=1}^{N_{ESU}} C_{land}^{N_b} \times A^{ESU} \quad \forall N_b \quad (6.29)$$

$$C_{OM}^{ESU} = \sum_{i=1}^{N_{ESU}} \sum_{t=1}^T [P_{Sell,t} \times T_{Sell,t} - P_{Pur,t} \times T_{pur,t}] + C_F^{ESU} \times P_{rated}^{ESU} \quad (6.30)$$

$$C_{GP}^{ESU} = \sum_{n=1}^{N_n} |V_{target} - V_b^{ESU}| \times \mathbb{k}_{VD} + \left(\sum_{l=1}^{N_L} \%LL^{HESU} \right) \times \mathbb{k}_{LL} + \sqrt{\sum_{l=1}^{N_L} (P_{Loss,l}^2 + Q_{Loss,l}^2)} \times \mathbb{k}_{Loss} \quad (6.31)$$

$$C_I^{UC} = \sum_{i=1}^{N_{UC}} L_{UC,i} \times C_{ipk}^{UC} \quad (6.32)$$

$$C_I^{HBI} = \sum_{i=1}^{N_{HBI}} b_{BIS} \times C_{ci}^{BIS} + b_{PV} \times C_{ci}^{PV} + b_{EV} \times C_{ci}^{EV} + C_{FI}^{HBI} \quad (6.33)$$

Optimization Constraints

In the modern distribution system, the real and reactive power demand of general load, electric-vehicle, and BIS at any time t at i^{th} bus must be satisfied by the power from the REPs, the power absorbed or injected from ESUs, the power grid, and the power losses. This balance in real and reactive power is represented by equation 6.34 and 6.35. The operational constraints governing the real and reactive power flow is given by equation 6.36 and equation 6.37. When REPs and large-scale ESUs are integrated into the grid, its performance will be affected. To ensure this, limits of the node voltage and line loading (of already installed lines) are considered as given in equation 6.38 and 6.39.

$$P_D^{i,t} + P_{EV}^{i,t} + P_{BIS}^{i,t} = P_{PV}^{i,t} + P_{ESU}^{i,t} + P_{grid}^{i,t} + P_{loss}^t \quad \forall t = 1, \dots, T \ \& \ n = 1, \dots, N_n \quad (6.34)$$

$$Q_D^{i,t,f_n} + Q_{EV}^{i_{Nc},t,f_n} = Q_{PV}^{i,t,f_n} + Q_{HESU}^{i,t} + Q_{grid}^{i,t} + Q_{loss}^t \quad \forall t = 1, \dots, N_t \ \& \ i = 1, \dots, N_b \quad (6.35)$$

$$P_{flow}^{i,t} = V^{i,t} \times \sum_{i,j \in N_b} V^{j,t} (G_{ij} \cos \theta_{ij,t} + B_{ij} \sin \theta_{ij,t}) \quad (6.36)$$

$$Q_{flow}^{i,t} = V^{i,t} \times \sum_{i,j \in N_b} V^{j,t} (G_{ij} \sin \theta_{ij,t} - B_{ij} \cos \theta_{ij,t}) \quad (6.37)$$

$$V_{min} < V_t^b < V_{max} \quad \forall b = 1, 2, 3, \dots, N_b \quad (6.38)$$

$$LL_t^l < LL_{max}^l \quad \forall l = 1, 2, 3, \dots, N_l \quad (6.39)$$

The power absorbed or injected by ESUs depends on its mode of operation such as charging or discharging. The mode of operation is mainly decided by the state of charge (SOC) of ESU. Since the main objective of this case is to operate ESUs under the emergency response period, only discharging mode is shown. Therefore, the constraints corresponding to ESUs are limits of discharging power and energy from ESUs, limits of SOC of ESUs, and apparent power which is given by equations 6.40 to 6.43. As mentioned earlier, underground cables are installed to increase the strength of load connectivity during the emergency response period. Therefore, it is essential to consider the loading capacity of these cables as given in equation 6.44. Apart from all the technical constraints, budget allocation for hardening is the major constraint which is given by equation 6.45.

$$P_{min}^{ESU} < P_t^{ESU} < P_{max}^{ESU} \quad \forall t = 1, \dots, N_t \quad (6.40)$$

$$E_{min}^{ESU} < E_t^{ESU} < E_{max}^{ESU} \quad \forall t = 1, \dots, N_t \quad (6.41)$$

$$SOC_{min}^{ESU} \leq SOC_t^{ESU} \leq SOC_{max}^{ESU} \quad (6.42)$$

$$S^{ESU} = \sqrt{P_{ESU}^2 + Q_{ESU}^2} \quad (6.43)$$

$$LL_t^{UC} < LL_{max}^{UC} \quad \forall UC = 1, \dots, N_{UC} \quad (6.44)$$

$$C_I^{ESU} + C_I^{UC} + C_I^{HBI} \leq Budget_{max} \quad (6.45)$$

6.3.3 Proposed Methodology

The problem formulated includes both the grid side and demand side hardening to enhance the overall system performance during the emergency period. Since hardening is a planning activity, the distribution network is modeled by considering the uncertainty of REPs and load using beta and normal distribution function respectively [131]. A bi-level approach is proposed to solve this optimization problem as discussed below. In the first level, optimal clusters reflecting the possible vulnerable zones of the distribution network are identified. In the second level, the objective

function 6.27 is minimized constrained with equations 6.28 to 6.45 using the hybrid algorithm.

First Level Optimization

The main objective of the utilities is to ensure the power supply for all the loads during both normal and extreme conditions. However, there are many practical challenges faced by the utilities to supply power during extreme conditions. These challenges can be streamlined if the vulnerable zones of the distribution network are identified. Also, these challenges may vary across the distribution network depending on load density. Therefore, to identify the vulnerable zones, the distribution network is clustered based on the outcome of the probabilistic earthquake hazard model, the density of HBIs, and load density using the k-means algorithm. Since the number of clusters is provided as an input for the k-means algorithm, a methodology based on the Silhouette index (SI) and Davies Bouldin index (DI) given in equation 6.46 and 6.47 respectively is applied to find the optimal number of clusters. The flowchart of the clustering methodology is shown in Figure 6.9.

$$SI = \frac{1}{N_{tot}} \sum_{i=1}^{N_{tot}} \left(\frac{1}{N_c} \sum_{j=1}^{N_c} S(j) \right) \quad (6.46)$$

$$DBI = \frac{1}{N_{tot}} \sum_{i=1}^{N_{tot}} \max_{i \neq j} \left(\frac{X(i) + X(j)}{d_{ij}} \right) \quad (6.47)$$

where N_{tot} is the total number of nodes in a given set, N_c is the number of clusters and $S(j)$ represents the ratio of the difference between the minimum average distance and the average distance between j_{th} node and all other nodes to the maximum of both, $X(i)$ and $X(j)$ are the average distance between each location of cluster i & j and centroid of that cluster respectively, d_{ij} is the distance between the centroids of cluster i and cluster j .

Second Level Optimization

In this section, the proposed methodology to optimize the overall hardening is discussed. The flowchart of the proposed methodology is shown in Figure 6.10. In this methodology, the set of buses/nodes and the lines which belong to the search space of the optimization algorithm is derived using Algorithm – III shown in Figure 6.11. Here, the nodes for B is chosen such that they do not fall on vulnerable zones. The lines for L is chosen based on step 8 and step 9 of the Algorithm – III. Here, the distance matrix API is imported from cloud service to calculate the distance between the given two nodes (CS_{dis}). The parameters d and m mentioned in step 7 of the Algorithm – III are constants which are chosen based on line loading and the budget. Generally, the effect of earthquakes on substations and distribution lines is calculated based on PGA and for the underground cables, it is calculated

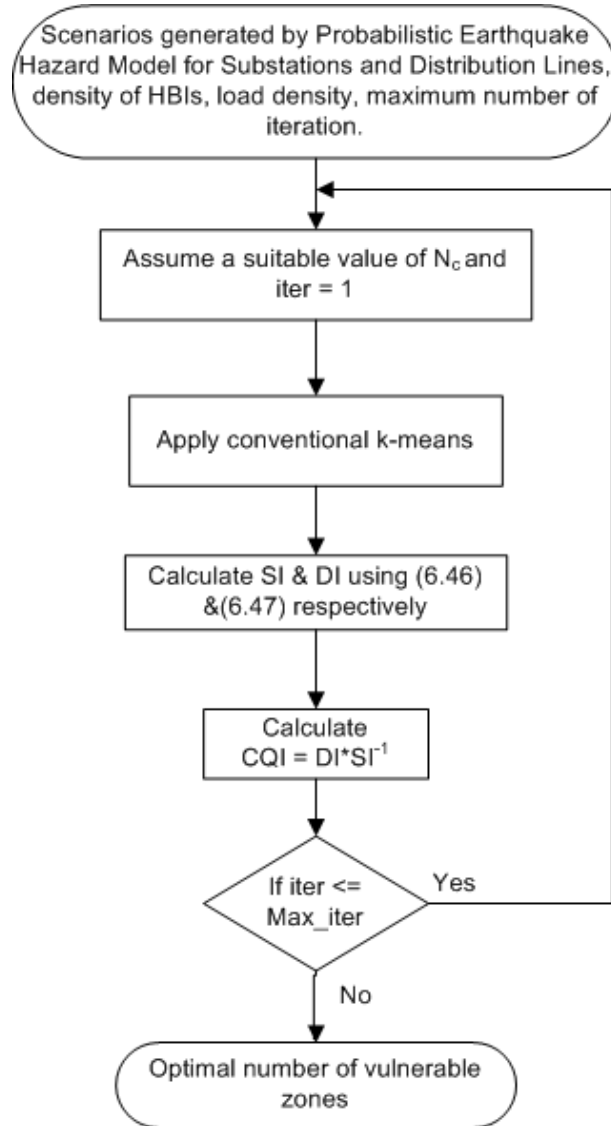


Figure 6.9: Flowchart of the clustering method for optimal vulnerable zones

using peak ground velocity (PGV). The expression for PGV applied is given by equation 6.48 [152]. The worst-case PGV mentioned in Figure 6.10 is obtained by calculating PGV for the worst earthquake magnitude.

$$\ln(PGV) = \begin{cases} -0.6615 + 0.3463 \times M_w - 0.0262 \times R - 0.0021 \times D, & \text{firm soil} \\ -1.1646 + 0.4299 \times M_w - 0.0159 \times R - 0.003 \times D, & \text{soft soil} \\ -0.7649 + 0.3729 \times M_w - 0.0229 \times R - 0.0044 \times D, & \text{soil} \end{cases} \quad (6.48)$$

Algorithm - III - Selection of Set of buses/nodes and lines

Input: Vulnerable zones and its index of the network, N_n, N_L and location of substations and lines (i.e. latitude, longitude and mean sea level)

Step 1. **for** $n = 1$ to N_n :

Step 2. **if** i does not fall under vulnerable zone:

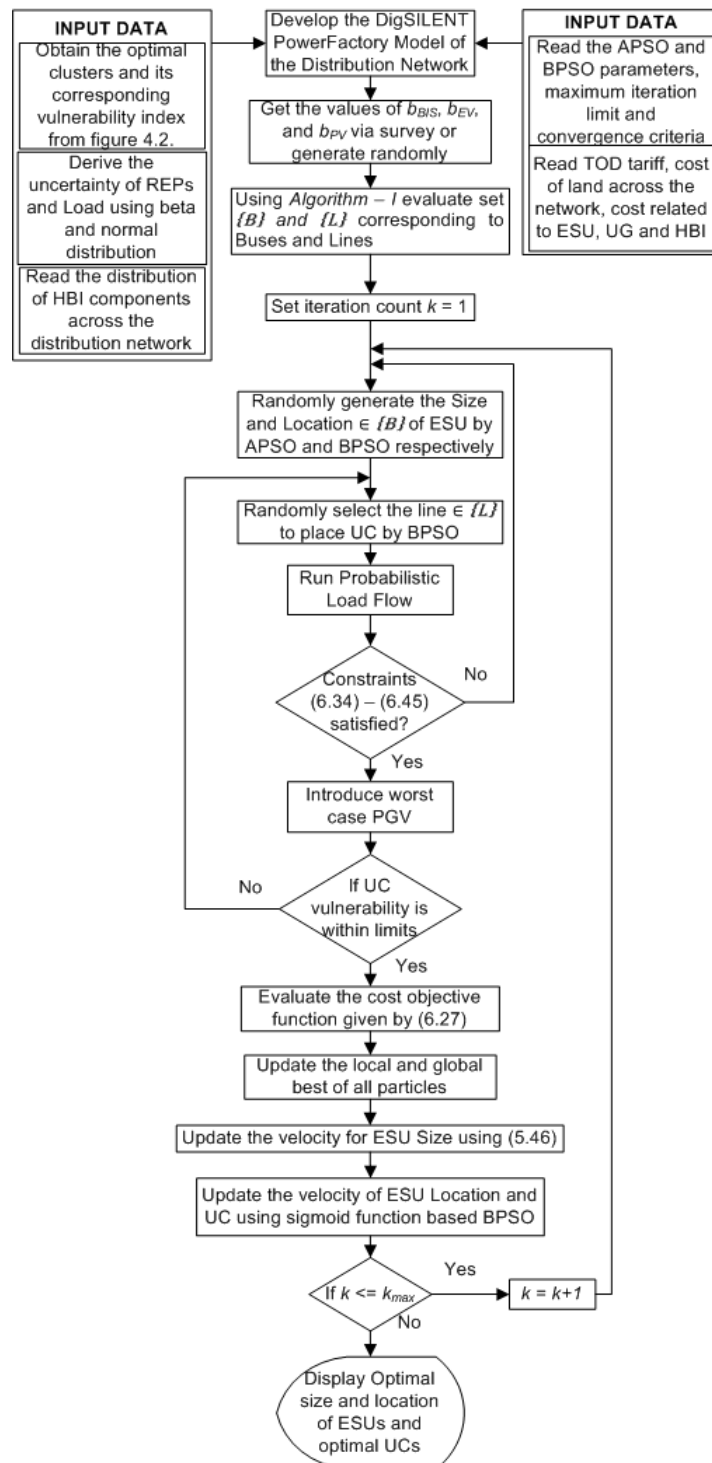


Figure 6.10: Flowchart of the clustering method for optimal vulnerable zones

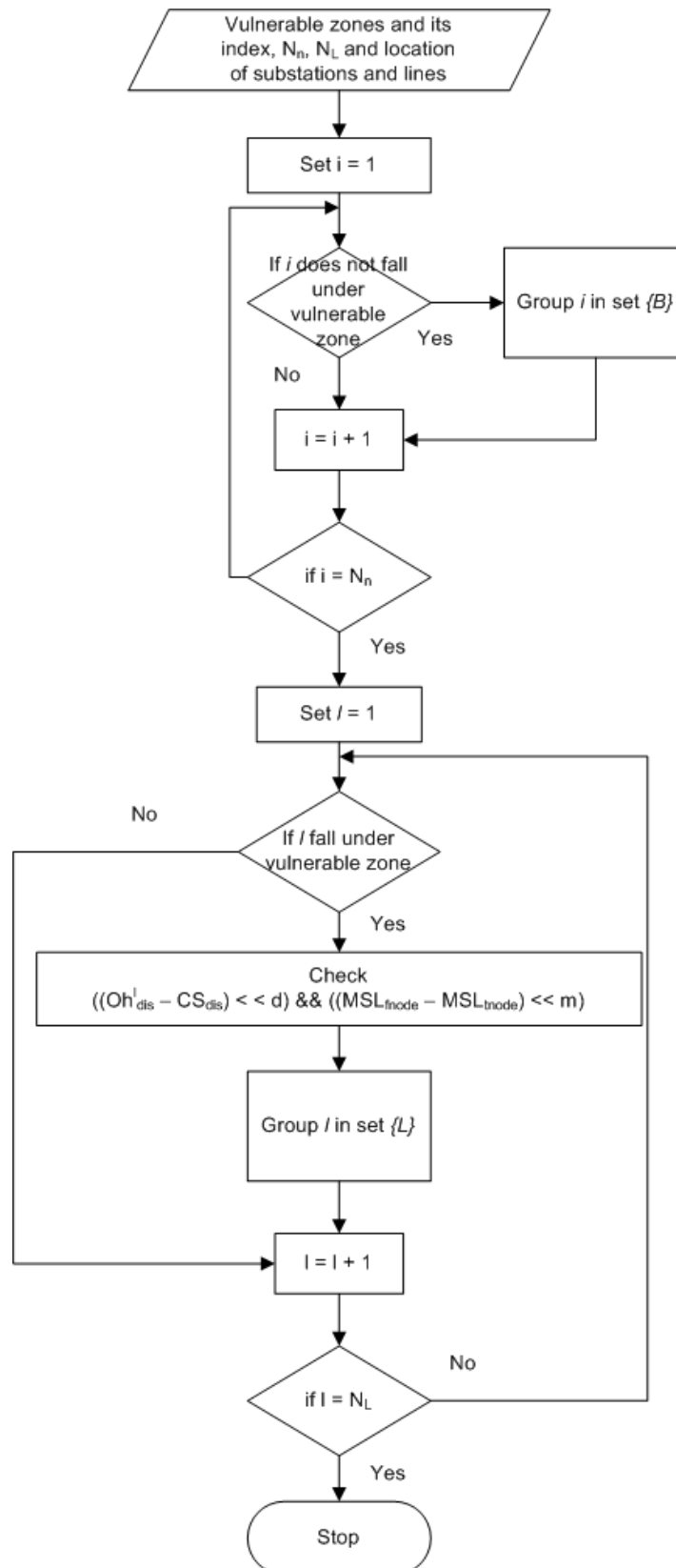


Figure 6.11: Flowchart of Algorithm III: Selection of Set of Buses and Lines

Step 3. $n \in B$

Step 4. **end for**

Step 5. **for** $n = 1$ to N_L :

Step 6. **if** l falls under vulnerable zone:

Step 7. **if** $((OH_{dis}^l - CS_{dis}) \ll d) \&\& ((MSL_{fnode} - MSL_{tnode}) \ll m)$:

Step 8. $l \in L$

Step 9. **end for**

6.3.4 Results of Case Study

The proposed methodology for optimal hardening of distribution network against earthquakes is applied on a practical 156-bus distribution system of Dehradun district, Uttarakhand, India. The historical data of earthquakes in the selected region is obtained from [153]. All the numerical experiments in this study are conducted on a computer with Intel i7-4510U CPU with 8 GB RAM. A survey is conducted to understand the distribution of HBIs across the distribution network. It is observed that the average percentage of BIS installed under the domestic load center across the distribution network is 60%. Since it was very difficult to find the PVs and EVs presence in the domestic load center, the PVs and EVs with a capacity of (3 x 10) kWp and 30kW respectively are installed using the normal distribution in the distribution network model of DigSILENT PowerFactory. The Time of Day (TOD) and its corresponding tariff is obtained from [139]. With these data, the proposed bi-level approach is applied to obtain the optimal hardening solution. After obtaining the optimal hardening, the effectiveness of this solution during the extreme condition is tested for two cases. Case A: by considering the complete load connected to the system, Case B: by considering only the critical loads of the system (which is mentioned in Table 6.1).

As discussed, the distribution network is clustered to obtain its vulnerable zones. The major components of the distribution network considered in this study are substations and distribution lines. Here the vulnerability of buses/nodes (substations) and the distribution lines are derived using the Monte-Carlo earthquake hazard model as explained in section 4.4. Since the fragility of substations and distribution lines are different for the same earthquake activity [139], individual clustering of substations and distribution lines is performed. Using the clustering methodology mentioned in Figure 6.9, the optimal number of vulnerable zones are obtained for substations and distribution lines. From Figure 6.12 and Figure 6.13, it is evident that the optimal number of clusters for substations and distribution lines are two and four respectively. The optimal number of vulnerability zones and the possibility of risk are shown in Table 6.9.

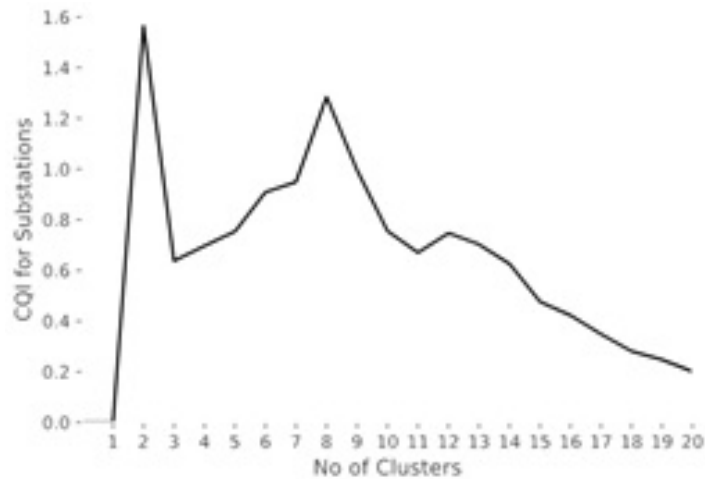


Figure 6.12: Cluster Quality Index of Substation for different number of clusters

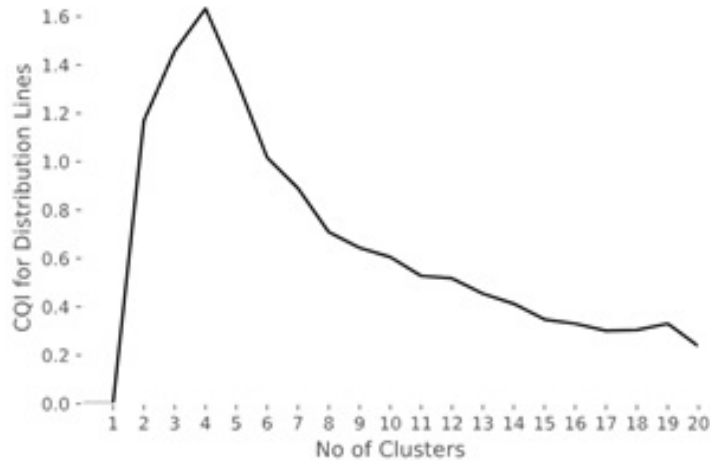


Figure 6.13: Cluster Quality Index of Distribution Lines for different number of clusters

By applying the *Algorithm-III*, twenty, and thirty-one number of buses/nodes and distribution lines are obtained for B and L respectively shown in Figure 6.15. In this figure, the substations and the distribution lines in the set B and L are represented by a red circle and red lines respectively. With the derived input data for second-level optimization, the optimized cost obtained is 508847398.68 dollars with the optimal size and location of ESUs are shown in Table 6.10 and the optimal location of UCs is shown in Table 6.11. The hardening methodology must improve the system performance both under normal and extreme conditions to reduce the overall investments. During the normal condition, placing ESUs at optimal locations with optimal size has significantly improved the bus voltage profile. The same can be evident from Figure 6.14, where the percentage comparison of bus voltage profile for cases, with and without ESUs is shown. To test the effectiveness of the proposed methodology under

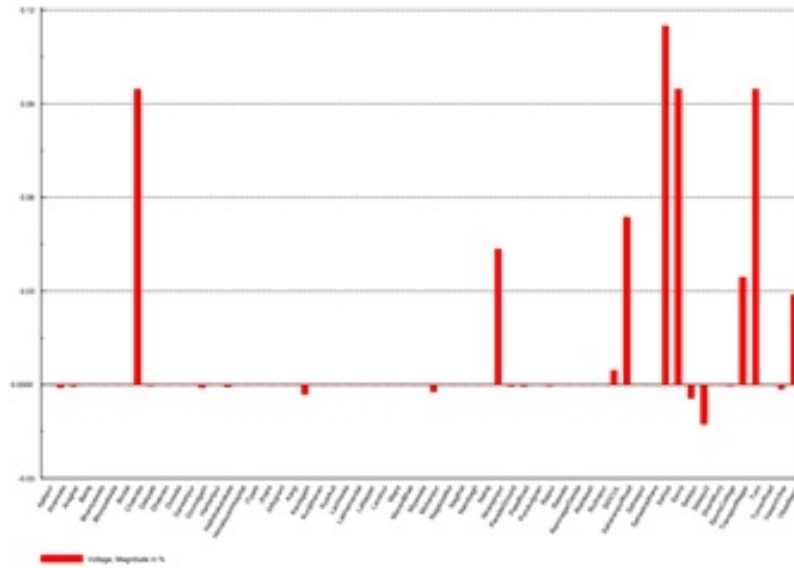


Figure 6.14: Bus Voltage Profile Comparison - with and without ESU in percentage

Table 6.9: Optimal Clusters and its Risk Possibility of Substations and Distribution Lines

Substations	Optimal Clusters = 2			
<i>Possibility of Risk</i>	<i>Cluster 1</i>			<i>Cluster 2</i>
	High			Low
Distribution Lines	Optimal Clusters = 4			
<i>Possibility of Risk</i>	<i>Cluster 0</i>	<i>Cluster 1</i>	<i>Cluster 2</i>	<i>Cluster 3</i>
	High	Nil	Medium	Low

emergency condition, a worst-case seismic fault occurred in the location ($30.45^{\circ}N, 77.92^{\circ}E$) with a moment magnitude of 5.4 is applied. A resiliency index (RI) is defined to measure the overall system performance for both the cases A & B during the emergency period given by equation 6.17.

Case A

Considering the complete load connected to the distribution system, the values of RI are calculated using the equation 6.17. A comparison is made with RIs for various conditions such as without hardening, with only ESUs and with the proposed methodology shown in Table 6.12. From this, it is evident that the proposed methodology has improved the overall energy served by three times of the case without any hardening measures and 1.5 times of the case with only ESUs.

Table 6.10: Optimal Size and Location of ESUs

Optimal ESUs	Location			Size in MVA
	<i>Latitude</i>	<i>Longitude</i>	<i>MSL</i>	
5	30.448	77.7195	439	1.3848
	30.3306	77.9574	610	1.1914
	30.30925	78.031806	640	1.5593
	30.6115	77.8753	1049	0.7573
	30.2811	77.9903	601	0.7208

Case B

Considering only the critical loads of the distribution system as mentioned in Table 6.1, the values of RI are calculated using the equation 6.17 against various emergency response periods. A comparison is made with RIs for various conditions such as with only ESUs and with the proposed methodology shown in Table 6.13. From this, it is apparent that the proposed methodology has significantly improved the energy served during the emergency period.

The obtained hardening results can improve the overall system performance during normal conditions. Apart from that, the results obtained for both the cases A & B, shows the proposed methodology can effectively improve the energy served during the emergency condition.

6.4 Closing Remarks

In this chapter, two schemes to improve the overall system resiliency during both normal and extreme conditions by considering both the grid-side and demand-side resiliency strategies are discussed. In the first scheme, a novel framework is proposed which combines the grid-side and demand-side resiliency enhancement strategies for optimal planning of ESUs to improve the flexibility and resiliency during normal and extreme conditions. In this two-stage framework, the first stage elaborates the three-stride procedure for hardening the grid via ESU planning and in the second stage, a two-stride procedure to improve the system resiliency via optimal operation of BIS and ESU is elaborated. Since large-scale ESUs are commonly integrated via substations, this framework investigates the resiliency enhancement by considering the vulnerability of both substations and distribution lines. Here, the numerical experiments were performed considering two cases like worst and the most frequent seismic fault occurred in the region. Initially, by minimizing the cost objective function, the optimal size and location of ESUs is derived which is less prone to seismic hazards. Later, the RI is maximized

Table 6.11: Optimal Locations of UCs

Optimal Number of UCs	From Bus	To Bus	Cluster	Distance in km
16	Anarwala	Hathibakarakala	2	5.3
	Bindal	Anarwala	2	6.7
	Bindal	Kaulagarh	2	4.8
	Bindal	Niranjanpur	2	8.2
	Bhaniyawala	HimalayanHospital	2	2.7
	Bhoopatwala	ShantiKunj	3	5.5
	Dhakrani	Harbertpur	3	2.8
	Dhakrani	VikasNagar	3	8.2
	Jhajra	Selaqui	2	7.8
	Laltapper	Bhaniyawala	0	7.4
	Majra	Mohanpur	0	11.1
	Majra	Niranjanpur	2	3.6
	Majra	TransportNagar	2	2.4
	Rishikesh	Laltapper	2	24.9
	Rishikesh	ManeriBhali	0	7
	Rishikesh	Raiwala	0	10.4

Table 6.12: Comparison of Resiliency Index for Case A

Resiliency Index (RI)	Without hardening	Only ESU	Proposed Hardening
	0.0659	0.1258	0.1887

by combining the usage of ESUs and BIS to satisfy the identified critical/priority-based load with minimal curtailment. From the results, it is evident that the ESU planning constrained by the vulnerability of electrical infrastructure on top of grid performance parameters will improve both grid flexibility and resiliency. In addition, by considering BIS in optimal planning will enhance the operational resiliency of the system and can majorly decrease the capital investment for utilities towards ESUs.

In the second scheme (as an extension of first scheme), a three-dimensional hardening methodology is proposed to improve the overall system performance against earthquakes. The occurrence of earthquakes is a purely random event. Therefore, in this thesis, a Monte-Carlo based earthquake hazard model is proposed to generate the possible earthquake scenarios in the chosen region of study. Later, the PGA and fragility model is applied to identify the failure likelihood of electrical infrastructure. With the possibility of failure, the optimal vulnerable zone of the network is derived by clustering the network using the proposed clustering

Table 6.13: Comparison of Resiliency Index for Case B

ERT	Resiliency Index (RI)	
	With only ESU	Proposed Hardening
8	0.2335	0.6935
9	0.2179	0.6013
10	0.2024	0.5857
11	0.1868	0.5318
12	0.1664	0.4935

methodology; which is termed as first level of optimization. Later, with reference to the vulnerable zones, the ESUs, UCs, and communication infrastructure are placed optimally using the second level optimization. The proposed methodology is evaluated for two cases such as (i) considering the complete load connected to the system, and (ii) considering only the critical loads of the system using RI. From the results, it is evident that the proposed three-dimensional hardening has significantly improved the system performance both during normal and emergency conditions.

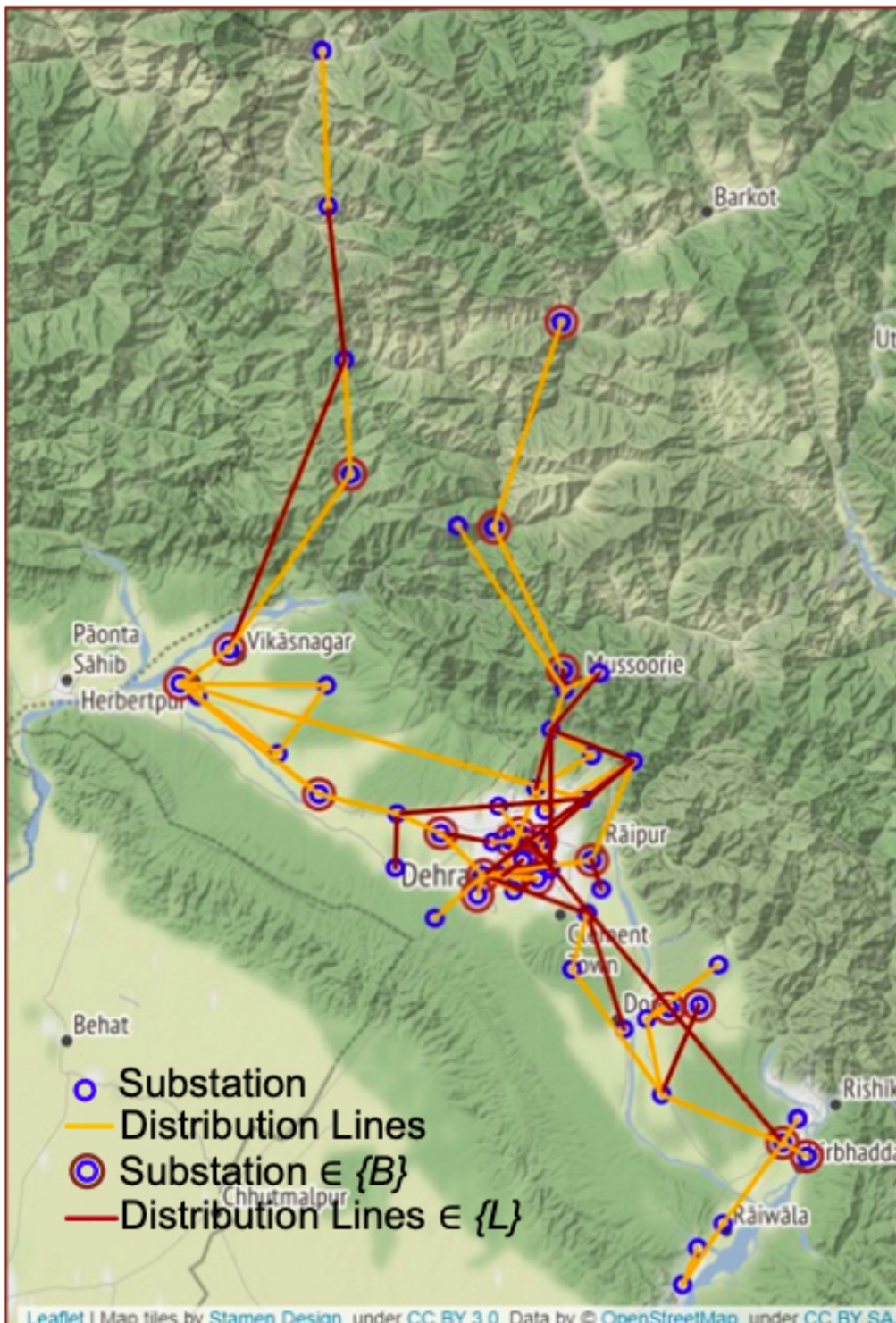


Figure 6.15: Set of Substations and Distribution Lines derived from Algorithm – III

Chapter 7

Closure of Thesis

This chapter summaries the major conclusions of this thesis and possible future directions.

7.1 Summary

Integration of large-scale ESUs is a promising solution to improve grid flexibility and resiliency. However, considering the capital investment, ESUs are optimally placed in the system to improve system performance. In planning the ESUs for the distribution system many researchers proposed optimization problem and methodologies to improve system conditions. However, these methodologies were developed mainly by considering the electrical parameters leaving behind the practical parameters and constraints. This thesis proposes novel ways to formulate the optimization and problem, quantify the system performance against short and long term resiliency by considering both grid side and demand side resiliency to improve system performance during emergency conditions. Since the distribution system modeling plays a major role for planning activity, most possible practical parameters such as RPOs, uncertainty of REPs, general load, EV load and the practical constraints such as land availability and environmental damage caused by ESUs are formulated in the distribution system via modeling the distribution network. The effect of modeling the natural disaster into the distribution system is very crucial to develop strategies for improving system resiliency. To address this a Monte-Carlo based probabilistic hazard model is integrated into the distribution system to identify the vulnerable components of the distribution system against earthquake activity. These concepts are simulated by considering three cases such as optimal planning of HESUs to improve the grid flexibility with minimized environmental impact, optimal planning of ESUs considering BISs in the network and three dimensional hardening to improve both system flexibility and resiliency.

7.2 Conclusions

The HESU planning is carried out by modeling the problem with practical constraints such as RPO, land required to install HESU & its associated cost, CO_2 emission from ESU affecting the environment. Apart from this, a survey is conducted from which the uncertainty parameters related to general load, EV load, and Solar PV generation are calculated and introduced in the model. From the survey, it was concluded that the EV loads are not connected throughout the distribution network. Therefore, the distribution network is clustered based on load density, geographical data (latitude, longitude, and MSL), TI, and population. After this, the EV loads are placed on clusters where both the population and load density are high. Within the cluster, the EV loads are distributed using EVDI (obtained from the survey). Having these data, the distribution system is modeled in DigSILENT PowerFactory and the optimal planning of HESU is obtained from the proposed methodology. Albeit the ESU planning in literature did not consider the environmental impact, but it has the utmost importance for sustainable planning. To minimize the emission level from ESU, a hybrid combination of popular Li-ion battery along with Na-S battery technology has been implemented using the proposed methodology. The optimized results paved a way towards reduced damage cost due to CO_2 emission significantly, by considering the other components such as uncertainty (of load and solar PV), grid performance cost, land cost index, operation and maintenance cost, arbitrage cost, and capital investment. From the results obtained, it is also evident that the HESUs are widely spread across all the clusters of the distribution network. Therefore, the same HESUs can be utilized to form microgrids to satisfy critical demand during grid failure.

A framework is proposed for optimal planning of ESUs to improve flexibility and resiliency during normal and extreme conditions. A two-stage framework is proposed in which the first stage elaborates the three-stride procedure for hardening the grid via optimal planning of ESU and in the second stage, a two-stride procedure to improve the system resiliency via optimal operation of BIS & ESU. Generally, large-scale grid-tied ESU is placed in the substation. Therefore, to improve the overall resiliency of the system, the vulnerability of both substations and distribution lines must be assessed. To address this, a set of candidate bus is identified from the overall damage probability (including substation and distribution lines). In this second-stride of the first stage, the distribution system is modeled by considering the uncertainty of REPs and load and also practical constraints. By minimizing the cost objective function, the optimal size and location of ESUs are obtained in which the damage probability against earthquake is null/minimal. In the second-stride of the second stage, the combination of BIS & ESUs is used to satisfy the expected demand with minimal curtailment. From the results obtained, it is evident that:

- ESU planning constrained with the vulnerability of electrical

infrastructure on top of grid performance parameters will improve both grid flexibility and resiliency.

- Considering BIS in optimal planning will enhance the operational resiliency of the system and also can majorly decrease the capital investment for utilities towards ESUs.
- The combined operation of ESUs & BIS has improved the energy served during emergency response period and the system performance followed by an earthquake.

A three-dimensional hardening methodology is proposed to improve the overall system performance against earthquakes. Since the occurrence of earthquakes is purely a random event, probabilistic modeling of the earthquake will lead near to practicality. Therefore, all possible scenarios of earthquakes are generated using a Monte-Carlo based earthquake hazard model. Hereinafter, the PGA of all the generated scenarios is derived using the seismic activity model and thereby the failure likelihood is obtained using the fragility curves of substations and distribution lines. With the possibility of failure, optimal vulnerable zones of the network i.e. optimal vulnerable substations and distribution lines are derived by clustering the network using the proposed clustering methodology; which is termed under the first-level optimization. Later, concerning the vulnerable zones, the ESUs, UCs, and communication infrastructure are placed optimally using the second level optimization. To test the effectiveness of this methodology, the performance of the system under normal and extreme conditions is evaluated. Concerning to extreme condition, the performance of the proposed methodology is evaluated for two cases such as (i) considering the complete load connected to the system, and (ii) considering only critical loads of the system using RI. From the results obtained, it is evident that the proposed three-dimensional hardening has significantly improved the system performance both during normal and emergency conditions. It is also evident from the results that the resiliency index has significantly improved in both the cases by using the proposed methodology.

To validate all the proposed methodologies, various numerical experiments were conducted on a real-world 156-bus distribution system of Dehradun district, Uttarakhand, India.

7.3 Future Directions

This thesis mainly present the novel ways to formulate the optimization problem for optimal planning of ESUs in distribution system considering both grid flexibility and resiliency. The methodologies mainly focus on the planning part of ESUs considering the presence of HBIs in the distribution system. In this thesis, the methodologies were developed mainly by considering the earthquakes. Therefore, the question still remains if they hold for other natural disasters. Since it is known that the strategies to

improve resiliency is disaster and system dependent, it is very difficult to formulate a more generalized methodology however the skeleton of the methodology remains same.

The main opportunities for further research are as follows:

- In this thesis, at a time the occurrence of single disaster is considered. However, multiple disaster like landslides and earthquakes may occur and in such cases there is a scope of improvement in the proposed methodology.
- In this thesis, it was assumed that all the load center having the any of the HBI components are willing to accept the communication network for HBIs. In practice, it is very difficult to answer because of the societal acceptance which may vary from place to place and time to time.
- The optimal size and location of ESUs considering HBIs were obtained. With this, there are opportunities to develop a better control scheme to achieve synchronous operation amongst ESUs and HBIs.
- In this thesis, it is assumed that the ESUs and HBIs synchronously operate with the individual status available from the communication infrastructure thereby the energy can be served to non-HBI customers from ESUs. However, this situation can be improved by formulating a business model to encourage the participation of HBIs to supply non-HBI customers and thereby improve system resiliency.
- In this thesis, the ESUs are assumed to be based on battery technology. However, there are many other technologies to explore on grid-scale storage which might be viable to mitigate the uncertainty and variability associated with intermittent, non-dispatchable renewable energy resources.
- The massive spread of distributed renewable energy resources in distribution systems, intrinsically uncertain and non-programmable, together with the new trends in electric demand, often unpredicted, require a paradigm change in grid planning for properly lead with the uncertainty sources and the distribution system operators (DSOs) should learn to support such changes. However, the DSO perspective methodologies may introduce high computational efforts which can be addressed via quantum computing.
- The ramification of incoming changes brought by the energy transition will require additional flexibility capabilities. This gives an opportunity to explore various scenarios applicable for national grid, which can be evaluated up to 2050.

Bibliography

- [1] Ministry of New and Renewable Energy, “Office Orders & Memorandums.” [Online]. Available: <https://mnre.gov.in/public-information/office-orders>
- [2] “European Distribution System Operators.” [Online]. Available: <https://www.edsoforsmartgrids.eu/>
- [3] A. W. Bizuayehu, A. A. Sanchez de la Nieta, J. Contreras, and J. P. S. Catalao, “Impacts of Stochastic Wind Power and Storage Participation on Economic Dispatch in Distribution Systems,” *IEEE Transactions on Sustainable Energy*, vol. 7, no. 3, pp. 1336–1345, jul 2016. [Online]. Available: <http://ieeexplore.ieee.org/document/7440864/>
- [4] A. Karimi, F. Aminifar, A. Fereidunian, and H. Lesani, “Energy storage allocation in wind integrated distribution networks: An MILP-Based approach,” *Renewable Energy*, vol. 134, pp. 1042–1055, apr 2019. [Online]. Available: <https://linkinghub.elsevier.com/retrieve/pii/S0960148118313533>
- [5] TPDDL, “10 MW energy storage system at Tata Power Delhi Distribution’s Rohini Substation.” [Online]. Available: <https://www.tatapower.com/media/PressReleaseDetails/1617>
- [6] G. Celli, S. Mocci, F. Pilo, and M. Loddo, “Optimal integration of energy storage in distribution networks,” *2009 IEEE Bucharest PowerTech: Innovative Ideas Toward the Electrical Grid of the Future*, pp. 1–7, 2009.
- [7] A. Balakrishnan, E. Brutsch, A. Jamis, W. Reyes, M. Strutner, and W. Reyes, “The Environmental Impacts of Utility-Scale Battery Storage in California Authors,” Ph.D. dissertation, Bren School of Environmental Science & Management, University of California, Santa Barbara, 2018. [Online]. Available: <https://www.bren.ucsb.edu/research/2018Group{-}Projects/documents/SolarStash{-}FinalGPReportredacted.pdf>
- [8] T. J. Myers, “Mitigating Hazards in Large-Scale Battery Energy Storage Systems,” Exponent, Tech. Rep., 2019.

- [9] P. Lazzeroni and M. Repetto, "Optimal planning of battery systems for power losses reduction in distribution grids," *Electric Power Systems Research*, vol. 167, pp. 94–112, feb 2019. [Online]. Available: <https://doi.org/10.1016/j.epsr.2018.10.027><https://linkinghub.elsevier.com/retrieve/pii/S0378779618303432>
- [10] D. M. R. Abbas A. Akhil, Georgianne Huff, Aileen B. Currier, Benjamin C. Kaun, Stella Bingqing Chen, Andrew L. Cotter, Dale T. Bradshaw, and W. D. Gauntlett, "DOE/EPRI 2013 Electricity Storage Handbook in Collaboration with NRECA, Sandia National Laboratories, USA," Sandia National Laboratories, Tech. Rep. July, 2013. [Online]. Available: <http://www.sandia.gov/ess/publications/SAND2013-5131.pdf>
- [11] M. Baumann, J. F. Peters, M. Weil, and A. Grunwald, "CO₂ Footprint and Life-Cycle Costs of Electrochemical Energy Storage for Stationary Grid Applications," *Energy Technology*, vol. 5, no. 7, pp. 1071–1083, jul 2017. [Online]. Available: <http://doi.wiley.com/10.1002/ente.201600622>
- [12] "Disaster Data & Statistics." [Online]. Available: <https://ndma.gov.in/en/>
- [13] Y. Lin, Z. Bie, and A. Qiu, "A review of key strategies in realizing power system resilience," *Global Energy Interconnection*, vol. 1, no. 1, pp. 70–78, 2018. [Online]. Available: <https://doi.org/10.14171/j.2096-5117.gei.2018.01.009>
- [14] S. Nikkhah, K. Jalilpoor, E. Kianmehr, and G. B. Gharehpetian, "Optimal wind turbine allocation and network reconfiguration for enhancing resiliency of system after major faults caused by natural disaster considering uncertainty," *IET Renewable Power Generation*, vol. 12, no. 12, pp. 1413–1423, 2018.
- [15] D. P. Birnie, "Optimal battery sizing for storm-resilient photovoltaic power island systems," *Solar Energy*, vol. 109, pp. 165–173, nov 2014. [Online]. Available: <https://linkinghub.elsevier.com/retrieve/pii/S0038092X14003934>
- [16] A. Soroudi, "Energy Storage Planning for Resiliency enhancement against Renewable Energy Curtailment," in *IET International Conference on Resilience of Transmission and Distribution Networks (RTDN 2017)*. Institution of Engineering and Technology, 2017, pp. 1–5. [Online]. Available: <https://digital-library.theiet.org/content/conferences/10.1049/cp.2017.0330>
- [17] J. M. Boggess, G. W. Becker, and M. K. Mitchell, "Storm & flood hardening of electrical substations," *Proceedings of the IEEE Power Engineering Society Transmission and Distribution Conference*, pp. 1–5, 2014.

- [18] A. M. Salman, Y. Li, and M. G. Stewart, "Evaluating system reliability and targeted hardening strategies of power distribution systems subjected to hurricanes," *Reliability Engineering and System Safety*, vol. 144, pp. 319–333, 2015. [Online]. Available: <http://dx.doi.org/10.1016/j.ress.2015.07.028>
- [19] N. J. Anuranj, R. K. Mathew, S. Ashok, and S. Kumaravel, "Resiliency based power restoration in distribution systems using microgrids," *2016 IEEE 6th International Conference on Power Systems, ICPS 2016*, pp. 1–5, 2016.
- [20] K. Balasubramaniam, P. Saraf, R. Hadidi, and E. B. Makram, "Energy management system for enhanced resiliency of microgrids during islanded operation," *Electric Power Systems Research*, vol. 137, pp. 133–141, 2016. [Online]. Available: <http://dx.doi.org/10.1016/j.epsr.2016.04.006>
- [21] C. Yuan, M. S. Illindala, and A. S. Khalsa, "Modified viterbi algorithm based distribution system restoration strategy for grid resiliency," *IEEE Transactions on Power Delivery*, vol. 32, no. 1, pp. 310–319, 2017.
- [22] A. Hussain, V.-h. Bui, and H.-m. Kim, "Fuzzy Logic-Based Operation of Battery Energy Storage Systems (BESSs) for Enhancing the Resiliency of Hybrid Microgrids," *Energies*, vol. 10, no. 3, p. 271, feb 2017. [Online]. Available: <http://www.mdpi.com/1996-1073/10/3/271>
- [23] S. Liu, X. Wang, and P. X. Liu, "A Stochastic Stability Enhancement Method of Grid-Connected Distributed Energy Storage Systems," *IEEE Transactions on Smart Grid*, vol. 8, no. 5, pp. 2062–2070, sep 2017. [Online]. Available: <http://ieeexplore.ieee.org/document/7394194/>
- [24] A. Hussain, V. H. Bui, and H. M. Kim, "A proactive and survivability-constrained operation strategy for enhancing resilience of microgrids using energy storage system," *IEEE Access*, vol. 6, pp. 75 495–75 507, 2018.
- [25] M. Khederzadeh and S. Zandi, "Enhancement of Distribution System Restoration Capability in Single/Multiple Faults by Using Microgrids as a Resiliency Resource," *IEEE Systems Journal*, vol. 13, no. 2, pp. 1796–1803, jun 2019. [Online]. Available: <https://ieeexplore.ieee.org/document/8616854/>
- [26] J. Zhu, Y. Yuan, and W. Wang, "An exact microgrid formation model for load restoration in resilient distribution system," *International Journal of Electrical Power and Energy Systems*, vol. 116, no. August 2019, p. 105568, 2020. [Online]. Available: <https://doi.org/10.1016/j.ijepes.2019.105568>

- [27] M. A. Gilani, A. Kazemi, and M. Ghasemi, "Distribution system resilience enhancement by microgrid formation considering distributed energy resources," *Energy*, vol. 191, p. 116442, 2020. [Online]. Available: <https://doi.org/10.1016/j.energy.2019.116442>
- [28] V. Balaji Venkateswaran, D. K. Saini, and M. Sharma, "Approaches for optimal planning of the energy storage units in distribution network and their impacts on system resiliency," *CSEE Journal of Power and Energy Systems*, 2020. [Online]. Available: <https://ieeexplore.ieee.org/stamp/stamp.jsp?tp={&}arnumber=9098154>
- [29] M. Nazemi, M. Moeini-Aghtaie, M. Fotuhi-Firuzabad, and P. Dehghanian, "Energy Storage Planning for Enhanced Resilience of Power Distribution Networks Against Earthquakes," *IEEE Transactions on Sustainable Energy*, vol. 11, no. 2, pp. 795–806, apr 2020. [Online]. Available: <https://ieeexplore.ieee.org/document/8674596/>
- [30] Tamilnadu Electricity Regulatory Commission, "Amendment in Renewable Purchase Obligation," 2016.
- [31] M. Farhoodnea, A. Mohamed, H. Shareef, and H. Zayandehroodi, "Power quality impacts of high-penetration electric vehicle stations and renewable energy-based generators on power distribution systems," *Measurement: Journal of the International Measurement Confederation*, vol. 46, no. 8, pp. 2423–2434, 2013. [Online]. Available: <http://dx.doi.org/10.1016/j.measurement.2013.04.032>
- [32] V. H. M. Quezada, J. R. Abbad, and T. G. San Román, "Assessment of energy distribution losses for increasing penetration of distributed generation," *IEEE Transactions on Power Systems*, vol. 21, no. 2, pp. 533–540, 2006.
- [33] N. Miller and Z. Ye, "Report on Distributed Generation Penetration Study," NREL, Tech. Rep., 2003. [Online]. Available: <file:///D:/Studies/PhD/Review/ReviewPaper/34715.pdf>
- [34] NREL, "DG Power Quality, Protection and Reliability Case Studies Report," NREL, Tech. Rep., 2003. [Online]. Available: <https://www.nrel.gov/docs/fy03osti/34635.pdf>
- [35] G. Carpinelli, G. Celli, S. Mocci, F. Mottola, F. Pilo, and D. Proto, "Optimal Integration of Distributed Energy Storage Devices in Smart Grids," *IEEE Transactions on Smart Grid*, vol. 4, no. 2, pp. 985–995, jun 2013. [Online]. Available: <http://ieeexplore.ieee.org/document/6476054/>
- [36] N. Jayasekara, P. Wolfs, and M. A. S. Masoum, "An optimal management strategy for distributed storages in distribution networks with high penetrations of PV," *Electric*

- Power Systems Research*, vol. 116, pp. 147–157, nov 2014. [Online]. Available: <http://dx.doi.org/10.1016/j.epsr.2014.05.010><https://linkinghub.elsevier.com/retrieve/pii/S0378779614001989>
- [37] H. Nazaripouya, Y. Wang, P. Chu, H. R. Pota, and R. Gadh, “Optimal sizing and placement of battery energy storage in distribution system based on solar size for voltage regulation,” in *2015 IEEE Power & Energy Society General Meeting*. IEEE, jul 2015, pp. 1–5. [Online]. Available: <http://ieeexplore.ieee.org/document/7286059/>
- [38] E. Hooshmand and A. Rabiee, “Robust model for optimal allocation of renewable energy sources, energy storage systems and demand response in distribution systems via information gap decision theory,” *IET Generation, Transmission and Distribution*, vol. 13, no. 4, pp. 511–520, 2019.
- [39] S. Barghi, M. A. Golkar, and A. Hajizadeh, “Effect of distribution system specifications on voltage stability in presence of wind distributed generation,” *16th Conference on Electrical Power Distribution Networks (EPDC)*, no. 2, pp. 1–6, 2011. [Online]. Available: <https://ieeexplore.ieee.org/document/5876379>
- [40] J. Yang, G. Li, D. Wu, and Z. Suo, “The impact of distributed wind power generation on voltage stability in distribution systems,” in *2013 IEEE PES Asia-Pacific Power and Energy Engineering Conference (APPEEC)*. IEEE, dec 2013, pp. 1–5. [Online]. Available: <http://ieeexplore.ieee.org/document/6837205/>
- [41] M. Alotaibi, A. Almutairi, and M. M. A. Salama, “Effect of wind turbine parameters on optimal DG placement in power distribution systems,” in *2016 IEEE Electrical Power and Energy Conference (EPEC)*. IEEE, oct 2016, pp. 1–4. [Online]. Available: <http://ieeexplore.ieee.org/document/7771708/>
- [42] M. Amiri, B. Bagen, and A. M. Gole, “Probabilistic analysis of the effect of wind speed variations on power quality of power systems,” in *2016 International Conference on Probabilistic Methods Applied to Power Systems (PMAPS)*. IEEE, oct 2016, pp. 1–6. [Online]. Available: <http://ieeexplore.ieee.org/document/7764134/>
- [43] T. Sarkar, A. K. Dan, and S. Ghosh, “Effect of X/R ratio on low voltage distribution system connected with constant speed wind turbine,” in *2016 2nd International Conference on Control, Instrumentation, Energy & Communication (CIEC)*. IEEE, jan 2016, pp. 417–421. [Online]. Available: <http://ieeexplore.ieee.org/document/7513780/>
- [44] S. K. Sharma, A. Chandra, M. Saad, S. Lefebvre, D. Asber, and L. Lenoir, “Voltage Flicker Mitigation Employing Smart

- Loads With High Penetration of Renewable Energy in Distribution Systems,” *IEEE Transactions on Sustainable Energy*, vol. 8, no. 1, pp. 414–424, jan 2017. [Online]. Available: <http://ieeexplore.ieee.org/document/7553516/>
- [45] E. A. Feilat, S. Azzam, and A. Al-Salaymeh, “Impact of large PV and wind power plants on voltage and frequency stability of Jordan’s national grid,” *Sustainable Cities and Society*, vol. 36, pp. 257–271, jan 2018. [Online]. Available: <http://dx.doi.org/10.1016/j.scs.2017.10.035><https://linkinghub.elsevier.com/retrieve/pii/S2210670717308557>
- [46] P. Kritharas, L. Ochoa, K. Papastergiou, and G. Harrison, “Evaluating the Effects of High Penetrations of Roof-Top Wind Turbines on Secondary Distribution Circuits,” in *2006 IEEE/PES Transmission & Distribution Conference and Exposition: Latin America*, vol. 00. IEEE, 2006, pp. 1–6. [Online]. Available: <http://ieeexplore.ieee.org/lpdocs/epic03/wrapper.htm?arnumber=4104707>
- [47] Y. M. Atwa and E. F. El-Saadany, “Optimal Allocation of ESS in Distribution Systems With a High Penetration of Wind Energy,” *IEEE Transactions on Power Systems*, vol. 25, no. 4, pp. 1815–1822, nov 2010. [Online]. Available: <http://ieeexplore.ieee.org/document/5438853/>
- [48] M. Ghofrani, A. Arabali, M. Etezadi-Amoli, and M. S. Fadali, “A Framework for Optimal Placement of Energy Storage Units Within a Power System With High Wind Penetration,” *IEEE Transactions on Sustainable Energy*, vol. 4, no. 2, pp. 434–442, apr 2013. [Online]. Available: <http://ieeexplore.ieee.org/document/6400274/>
- [49] M. Yang, C. Chen, B. Que, Z. Zhou, and Q. Yang, “Optimal Placement and Configuration of Hybrid Energy Storage System in Power Distribution Networks with Distributed Photovoltaic Sources,” in *2018 2nd IEEE Conference on Energy Internet and Energy System Integration (EI2)*. IEEE, oct 2018, pp. 1–6. [Online]. Available: <https://ieeexplore.ieee.org/document/8582007/>
- [50] N. Yan, B. Zhang, W. Li, and S. Ma, “Hybrid Energy Storage Capacity Allocation Method for Active Distribution Network Considering Demand Side Response,” *IEEE Transactions on Applied Superconductivity*, vol. 29, no. 2, pp. 1–4, 2019.
- [51] M. R. Jannesar, A. Sedighi, M. Savaghebi, and J. M. Guerrero, “Optimal placement, sizing, and daily charge/discharge of battery energy storage in low voltage distribution network with high photovoltaic penetration,” *Applied Energy*, vol. 226, no. May, pp. 957–966, sep 2018. [Online]. Available: <https://doi.org/10.1016/j.apenergy.2018.06.036><https://linkinghub.elsevier.com/retrieve/pii/S0306261918309061>

- [52] S. Salee and P. Wirasanti, "Optimal siting and sizing of battery energy storage systems for grid-supporting in electrical distribution network," in *2018 International ECTI Northern Section Conference on Electrical, Electronics, Computer and Telecommunications Engineering (ECTI-NCON)*. IEEE, feb 2018, pp. 100–105. [Online]. Available: <https://ieeexplore.ieee.org/document/8378290/>
- [53] D. Hu, M. Ding, R. Bi, X. Liu, and X. Rong, "Sizing and placement of distributed generation and energy storage for a large-scale distribution network employing cluster partitioning," *Journal of Renewable and Sustainable Energy*, vol. 10, no. 2, p. 25301, mar 2018. [Online]. Available: <http://aip.scitation.org/doi/10.1063/1.5020246>
- [54] O. Babacan, W. Torre, and J. Kleissl, "Siting and sizing of distributed energy storage to mitigate voltage impact by solar PV in distribution systems," *Solar Energy*, vol. 146, pp. 199–208, apr 2017. [Online]. Available: <http://dx.doi.org/10.1016/j.solener.2017.02.047><https://linkinghub.elsevier.com/retrieve/pii/S0038092X17301494>
- [55] S. Avril, G. Arnaud, A. Florentin, and M. Vinard, "Multi-objective optimization of batteries and hydrogen storage technologies for remote photovoltaic systems," *Energy*, vol. 35, no. 12, pp. 5300–5308, dec 2010. [Online]. Available: <http://dx.doi.org/10.1016/j.energy.2010.07.033><https://linkinghub.elsevier.com/retrieve/pii/S0360544210004081>
- [56] M. Sedghi, A. Ahmadian, and M. Aliakbar-Golkar, "Optimal Storage Planning in Active Distribution Network Considering Uncertainty of Wind Power Distributed Generation," *IEEE Transactions on Power Systems*, vol. 31, no. 1, pp. 304–316, jan 2016. [Online]. Available: <http://ieeexplore.ieee.org/document/7052416/>
- [57] M. K. Rafique, K. Khalid Mehmood, S.-J. Lee, Z. M. Haider, C.-H. Kim, and S. U. Khan, "Optimal sizing and allocation of battery energy storage systems with wind and solar power DGs in a distribution network for voltage regulation considering the lifespan of batteries," *IET Renewable Power Generation*, vol. 11, no. 10, pp. 1305–1315, aug 2017. [Online]. Available: <https://digital-library.theiet.org/content/journals/10.1049/iet-rpg.2016.0938>
- [58] P. Meneses de Quevedo and J. Contreras, "Optimal Placement of Energy Storage and Wind Power under Uncertainty," *Energies*, vol. 9, no. 7, p. 528, jul 2016. [Online]. Available: <http://www.mdpi.com/1996-1073/9/7/528>
- [59] Y. Zheng, D. J. Hill, and Z. Y. Dong, "Multi-Agent Optimal Allocation of Energy Storage Systems in Distribution Systems," *IEEE Transactions on Sustainable Energy*, vol. 8, no. 4, pp. 1715–1725, oct 2017. [Online]. Available: <http://ieeexplore.ieee.org/document/7931653/>

- [60] D. Q. Hung and N. Mithulananthan, "Community Energy Storage and Capacitor Allocation in Distribution Systems," *21st Australasian Universities Power Engineering Conference (AUPEC)*, no. February, pp. 1–6, 2011.
- [61] M. Farrokhifar, "Optimal operation of energy storage devices with RESs to improve efficiency of distribution grids; technical and economical assessment," *International Journal of Electrical Power & Energy Systems*, vol. 74, pp. 153–161, 2016. [Online]. Available: <http://www.scopus.com/inward/record.url?eid=2-s2.0-84938528083&partnerID=tZOtx3y1>
- [62] M. Farrokhifar, S. Grillo, and E. Tironi, "Loss minimization in medium voltage distribution grids by optimal management of energy storage devices," *2013 IEEE Grenoble Conference PowerTech, POWERTECH 2013*, no. Mv, pp. 1–5, 2013.
- [63] K. Kasturi, C. K. Nayak, and M. R. Nayak, "Optimal PV & BES units integration to enhance power distribution network performance," in *2017 Second International Conference on Electrical, Computer and Communication Technologies (ICECCT)*. IEEE, feb 2017, pp. 1–6. [Online]. Available: <http://ieeexplore.ieee.org/document/8117976/>
- [64] J. M. Gantz, S. M. Amin, and A. M. Giacomoni, "Optimal mix and placement of energy storage systems in power distribution networks for reduced outage costs," in *2012 IEEE Energy Conversion Congress and Exposition (ECCE)*. IEEE, sep 2012, pp. 2447–2453. [Online]. Available: <http://ieeexplore.ieee.org/document/6342550/>
- [65] Zhong Qing, Yu Nanhua, Zhang Xiaoping, Y. You, and D. Liu, "Optimal siting & sizing of battery energy storage system in active distribution network," in *IEEE PES ISGT Europe 2013*, no. 2012. IEEE, oct 2013, pp. 1–5. [Online]. Available: <http://ieeexplore.ieee.org/document/6695235/>
- [66] E. Grover-Silva, R. Girard, and G. Kariniotakis, "Optimal sizing and placement of distribution grid connected battery systems through an SOCP optimal power flow algorithm," *Applied Energy*, vol. 219, pp. 385–393, jun 2018. [Online]. Available: <https://linkinghub.elsevier.com/retrieve/pii/S0306261917312813>
- [67] M. Nick, M. Hohmann, R. Cherkaoui, and M. Paolone, "On the optimal placement of distributed storage systems for voltage control in active distribution networks," *IEEE PES Innovative Smart Grid Technologies Conference Europe*, pp. 1–6, 2012.
- [68] T. Chaiyatham and I. Ngamroo, "Bee colony optimization of battery capacity and placement for mitigation of voltage rise by PV in

- radial distribution network,” *10th International Power and Energy Conference, IPEC 2012*, pp. 13–18, 2012.
- [69] M. Nick, M. Hohmann, R. Cherkaoui, and M. Paolone, “Optimal location and sizing of distributed storage systems in active distribution networks,” in *2013 IEEE Grenoble Conference*. IEEE, jun 2013, pp. 1–6. [Online]. Available: <http://ieeexplore.ieee.org/document/6652514/>
- [70] C. K. Das, O. Bass, G. Kothapalli, T. S. Mahmoud, and D. Habibi, “Optimal placement of distributed energy storage systems in distribution networks using artificial bee colony algorithm,” *Applied Energy*, vol. 232, no. April, pp. 212–228, dec 2018. [Online]. Available: <https://doi.org/10.1016/j.apenergy.2018.07.100https://linkinghub.elsevier.com/retrieve/pii/S0306261918311358>
- [71] I. C. Martinez, C.-Y. Chen, and J.-H. Teng, “Utilising energy storage systems to mitigate power system vulnerability,” *IET Generation, Transmission & Distribution*, vol. 7, no. 7, pp. 790–798, 2013.
- [72] S. Kahrobaee and S. Asgarpour, “Reliability-driven optimum standby electric storage allocation for power distribution systems,” in *2013 1st IEEE Conference on Technologies for Sustainability (SusTech)*. IEEE, aug 2013, pp. 44–48. [Online]. Available: <http://ieeexplore.ieee.org/document/6617296/>
- [73] W. L. Ai, H. Shareef, A. A. Ibrahim, and A. Mohamed, “Optimal battery placement in photovoltaic based distributed generation using binary firefly algorithm for voltage rise mitigation,” in *2014 IEEE International Conference on Power and Energy (PECon)*, no. 2. IEEE, dec 2014, pp. 155–158. [Online]. Available: <http://ieeexplore.ieee.org/document/7062432/>
- [74] Y. Zheng, Z. Y. Dong, F. J. Luo, K. Meng, J. Qiu, and K. P. Wong, “Optimal Allocation of Energy Storage System for Risk Mitigation of DISCOs With High Renewable Penetrations,” *IEEE Transactions on Power Systems*, vol. 29, no. 1, pp. 212–220, jan 2014. [Online]. Available: <http://ieeexplore.ieee.org/document/6589173/>
- [75] A. S. A. Awad, T. H. M. EL-Fouly, and M. M. A. Salama, “Optimal ESS Allocation and Load Shedding for Improving Distribution System Reliability,” *IEEE Transactions on Smart Grid*, vol. 5, no. 5, pp. 2339–2349, sep 2014. [Online]. Available: <http://ieeexplore.ieee.org/lpdocs/epic03/wrapper.htm?arnumber=6813652>
- [76] M. Farsadi, T. Sattarpour, and A. Y. Nejadi, “Optimal placement and operation of BESS in a distribution network considering the net present value of energy losses cost,” in *2015 9th International Conference on Electrical and Electronics Engineering*

- (*ELECO*). IEEE, nov 2015, pp. 434–439. [Online]. Available: <http://ieeexplore.ieee.org/document/7394582/>
- [77] A. Narimani, G. Nourbakhsh, G. F. Ledwich, and G. R. Walker, “Storage optimum placement in distribution system including renewable energy resources,” in *2016 Australasian Universities Power Engineering Conference (AUPEC)*. IEEE, sep 2016, pp. 1–5. [Online]. Available: <http://ieeexplore.ieee.org/document/7749325/>
- [78] A. Fathy and A. Y. Abdelaziz, “Grey Wolf Optimizer for Optimal Sizing and Siting of Energy Storage System in Electric Distribution Network,” *Electric Power Components and Systems*, vol. 45, no. 6, pp. 601–614, 2017. [Online]. Available: <https://doi.org/10.1080/15325008.2017.1292567>
- [79] A. S. A. Awad, T. H. M. EL-Fouly, and M. M. A. Salama, “Optimal ESS Allocation for Benefit Maximization in Distribution Networks,” *IEEE Transactions on Smart Grid*, vol. 8, no. 4, pp. 1668–1678, jul 2017. [Online]. Available: <http://ieeexplore.ieee.org/document/7335659/>
- [80] A. Jalali and M. Aldeen, “Risk-Based Stochastic Allocation of ESS to Ensure Voltage Stability Margin for Distribution Systems,” *IEEE Transactions on Power Systems*, vol. 34, no. 2, pp. 1264–1277, mar 2019. [Online]. Available: <https://ieeexplore.ieee.org/document/8481363/>
- [81] M. Nick, R. Cherkaoui, and M. Paolone, “Optimal Planning of Distributed Energy Storage Systems in Active Distribution Networks Embedding Grid Reconfiguration,” *IEEE Transactions on Power Systems*, vol. 33, no. 2, pp. 1577–1590, mar 2018. [Online]. Available: <http://ieeexplore.ieee.org/document/8000386/>
- [82] R. LI, W. WANG, Z. CHEN, and X. WU, “Optimal planning of energy storage system in active distribution system based on fuzzy multi-objective bi-level optimization,” *Journal of Modern Power Systems and Clean Energy*, vol. 6, no. 2, pp. 342–355, mar 2018. [Online]. Available: <https://doi.org/10.1007/s40565-017-0332-x>
<https://link.springer.com/10.1007/s40565-017-0332-x>
- [83] R. C. Johnson, M. Mayfield, and S. B. M. Beck, “Optimal placement, sizing, and dispatch of multiple BES systems on UK low voltage residential networks,” *Journal of Energy Storage*, vol. 17, pp. 272–286, jun 2018. [Online]. Available: <https://linkinghub.elsevier.com/retrieve/pii/S2352152X17305509>
- [84] M. Nick, R. Cherkaoui, and M. Paolone, “Optimal Allocation of Dispersed Energy Storage Systems in Active Distribution Networks for Energy Balance and Grid Support,” *IEEE Transactions on*

- Power Systems*, vol. 29, no. 5, pp. 2300–2310, sep 2014. [Online]. Available: <http://ieeexplore.ieee.org/document/6736137/>
- [85] J. D. Watson, N. R. Watson, and I. Lestas, “Optimized Dispatch of Energy Storage Systems in Unbalanced Distribution Networks,” *IEEE Transactions on Sustainable Energy*, vol. 9, no. 2, pp. 639–650, 2018.
- [86] Y. Yang, H. Li, A. Aichhorn, J. Zheng, and M. Greenleaf, “Sizing Strategy of Distributed Battery Storage System With High Penetration of Photovoltaic for Voltage Regulation and Peak Load Shaving,” *IEEE Transactions on Smart Grid*, vol. 5, no. 2, pp. 982–991, mar 2014. [Online]. Available: <http://ieeexplore.ieee.org/document/6609116/>
- [87] A. S. A. Awad, T. H. M. EL-Fouly, and M. M. A. Salama, “Optimal ESS Allocation for Load Management Application,” *IEEE Transactions on Power Systems*, vol. 30, no. 1, pp. 327–336, jan 2015. [Online]. Available: <http://ieeexplore.ieee.org/document/6822649/>
- [88] R. Li, W. Wang, and M. Xia, “Cooperative Planning of Active Distribution System with Renewable Energy Sources and Energy Storage Systems,” *IEEE Access*, vol. 6, pp. 5916–5926, 2017.
- [89] M. Torchio, L. Magni, and D. M. Raimondo, “A mixed integer SDP approach for the optimal placement of energy storage devices in power grids with renewable penetration,” in *2015 American Control Conference (ACC)*. IEEE, jul 2015, pp. 3892–3897. [Online]. Available: <http://ieeexplore.ieee.org/document/7171937/>
- [90] A. Giannitrapani, S. Paoletti, A. Vicino, and D. Zarrilli, “Optimal Allocation of Energy Storage Systems for Voltage Control in LV Distribution Networks,” *IEEE Transactions on Smart Grid*, vol. 8, no. 6, pp. 2859–2870, nov 2017. [Online]. Available: <http://ieeexplore.ieee.org/document/7552579/>
- [91] Y. Guo, Q. Wu, H. Gao, X. Chen, J. Ostergaard, and H. Xin, “MPC-Based Coordinated Voltage Regulation for Distribution Networks With Distributed Generation and Energy Storage System,” *IEEE Transactions on Sustainable Energy*, vol. 10, no. 4, pp. 1731–1739, 2018.
- [92] S. S. Sami, M. Cheng, J. Wu, and N. Jenkins, “A virtual energy storage system for voltage control of distribution networks,” *CSEE Journal of Power and Energy Systems*, vol. 4, no. 2, pp. 146–154, 2018.
- [93] W. Hu, Q. Lu, Y. Min, and L. Zheng, “Optimal energy storage system allocation and operation for improving wind power penetration,” *IET Generation, Transmission & Distribution*, vol. 9, no. 16, pp.

- 2672–2678, dec 2015. [Online]. Available: <https://digital-library.theiet.org/content/journals/10.1049/iet-gtd.2014.1168>
- [94] B. Zhang and P. Crossley, “Reliability improvement using ant colony optimization applied to placement of sectionalizing switches,” *Energy Procedia*, vol. 142, pp. 2604–2610, 2017. [Online]. Available: <https://doi.org/10.1016/j.egypro.2017.12.199>
- [95] I. Alsaïdan, W. Gao, and A. Khodaei, “Distribution Network Expansion Through Optimally Sized and Placed Distributed Energy Storage,” *Proceedings of the IEEE Power Engineering Society Transmission and Distribution Conference*, vol. 2018-April, 2018.
- [96] K. W. Chan, X. Luo, M. Qin, T. Wu, and C. Y. Chung, “Optimal planning and operation of energy storage systems in radial networks for wind power integration with reserve support,” *IET Generation, Transmission & Distribution*, vol. 10, no. 8, pp. 2019–2025, may 2016. [Online]. Available: <https://digital-library.theiet.org/content/journals/10.1049/iet-gtd.2015.1039>
- [97] J. Xiao, L. Bai, Z. Zhang, and H. Liang, “Determination of the optimal installation site and capacity of battery energy storage system in distribution network integrated with distributed generation,” *IET Generation, Transmission & Distribution*, vol. 10, no. 3, pp. 601–607, feb 2016. [Online]. Available: <https://digital-library.theiet.org/content/journals/10.1049/iet-gtd.2015.0130>
- [98] N. Jayasekara, M. A. S. Masoum, and P. J. Wolfs, “Optimal Operation of Distributed Energy Storage Systems to Improve Distribution Network Load and Generation Hosting Capability,” *IEEE Transactions on Sustainable Energy*, vol. 7, no. 1, pp. 250–261, jan 2016. [Online]. Available: <http://ieeexplore.ieee.org/document/7321810/>
- [99] P. Fortenbacher, M. Zellner, and G. Andersson, “Optimal sizing and placement of distributed storage in low voltage networks,” in *2016 Power Systems Computation Conference (PSCC)*. IEEE, jun 2016, pp. 1–7. [Online]. Available: <http://arxiv.org/abs/1512.01218http://ieeexplore.ieee.org/document/7540850/>
- [100] S. B. Karanki and D. Xu, “Optimal capacity and placement of battery energy storage systems for integrating renewable energy sources in distribution system,” in *2016 National Power Systems Conference (NPSC)*. IEEE, dec 2016, pp. 1–6. [Online]. Available: <http://ieeexplore.ieee.org/document/7858983/>
- [101] J. Zhou, S. Tsianikas, D. P. Birnie, and D. W. Coit, “Economic and resilience benefit analysis of incorporating battery storage to photovoltaic array generation,” *Renewable*

- Energy*, vol. 135, pp. 652–662, may 2019. [Online]. Available: <https://doi.org/10.1016/j.renene.2018.12.013><https://linkinghub.elsevier.com/retrieve/pii/S0960148118314459>
- [102] D. N. Trakas and N. D. Hatziargyriou, “Optimal Distribution System Operation for Enhancing Resilience Against Wildfires,” *IEEE Transactions on Power Systems*, vol. 33, no. 2, pp. 2260–2271, 2018.
- [103] J. Najafi, A. Peiravi, A. Anvari-Moghaddam, and J. M. Guerrero, “Resilience improvement planning of power-water distribution systems with multiple microgrids against hurricanes using clean strategies,” *Journal of Cleaner Production*, vol. 223, pp. 109–126, jun 2019. [Online]. Available: <https://doi.org/10.1016/j.jclepro.2019.03.141><https://linkinghub.elsevier.com/retrieve/pii/S0959652619308327>
- [104] G. Huang, J. Wang, C. Chen, J. Qi, and C. Guo, “Integration of Preventive and Emergency Responses for Power Grid Resilience Enhancement,” *IEEE Transactions on Power Systems*, vol. 32, no. 6, pp. 4451–4463, 2017.
- [105] E. Galvan, P. Mandal, A. U. Haque, and T.-l. B. L. B. Tseng, “Optimal Placement of Intermittent Renewable Energy Resources and Energy Storage System in Smart Power Distribution Networks,” *Electric Power Components and Systems*, vol. 45, no. 14, pp. 1543–1553, aug 2017. [Online]. Available: <https://doi.org/10.1080/15325008.2017.1362605><https://www.tandfonline.com/doi/full/10.1080/15325008.2017.1362605>
- [106] A. Gabash and P. Li, “Flexible Optimal Operation of Battery Storage Systems for Energy Supply Networks,” *IEEE Transactions on Power Systems*, vol. 28, no. 3, pp. 2788–2797, aug 2013. [Online]. Available: <http://ieeexplore.ieee.org/document/6387346/>
- [107] A. Vieira Pombo, J. Murta-Pina, and V. Fernão Pires, “Multiobjective formulation of the integration of storage systems within distribution networks for improving reliability,” *Electric Power Systems Research*, vol. 148, pp. 87–96, jul 2017. [Online]. Available: <http://dx.doi.org/10.1016/j.epsr.2017.03.012>
- [108] S. Bose, D. F. Gayme, U. Topcu, and K. M. Chandy, “Optimal placement of energy storage in the grid,” in *2012 IEEE 51st IEEE Conference on Decision and Control (CDC)*. IEEE, dec 2012, pp. 5605–5612. [Online]. Available: <http://ieeexplore.ieee.org/document/6426113/>
- [109] D. I. Karadimos, A. D. Karafoulidis, D. I. Doukas, P. A. Gkaidatzis, D. P. Labridis, and A. G. Marinopoulos, “Techno-economic analysis for optimal energy storage systems placement considering stacked grid services,” in *2017 14th International Conference on the*

- European Energy Market (EEM)*. IEEE, jun 2017, pp. 1–6. [Online]. Available: <http://ieeexplore.ieee.org/document/7981898/>
- [110] A. Mohamed Abd el Motaleb, S. Kazim Bekdache, and L. A. Barrios, “Optimal sizing for a hybrid power system with wind/energy storage based in stochastic environment,” *Renewable and Sustainable Energy Reviews*, vol. 59, pp. 1149–1158, jun 2016. [Online]. Available: <http://dx.doi.org/10.1016/j.rser.2015.12.267><https://linkinghub.elsevier.com/retrieve/pii/S1364032115016500>
- [111] S. Espinoza, M. Panteli, P. Mancarella, and H. Rudnick, “Multi-phase assessment and adaptation of power systems resilience to natural hazards,” *Electric Power Systems Research*, vol. 136, pp. 352–361, 2016. [Online]. Available: <http://dx.doi.org/10.1016/j.eprsr.2016.03.019>
- [112] X. Liu, M. Shahidehpour, Z. Li, X. Liu, Y. Cao, and Z. Bie, “Microgrids for Enhancing the Power Grid Resilience in Extreme Conditions,” *IEEE Transactions on Smart Grid*, vol. 8, no. 2, pp. 589–597, 2017.
- [113] S. Mousavizadeh, M.-R. R. Haghifam, and M.-H. H. Shariatkah, “A linear two-stage method for resiliency analysis in distribution systems considering renewable energy and demand response resources,” *Applied Energy*, vol. 211, no. November 2017, pp. 443–460, feb 2018. [Online]. Available: <https://doi.org/10.1016/j.apenergy.2017.11.067><https://linkinghub.elsevier.com/retrieve/pii/S0306261917316665>
- [114] A. Stankovic. and K. Tomsovic., “The Definition and Quantification of Resilience,” Tech. Rep. April, 2018.
- [115] M. Chaudry, P. Ekins, K. Ramachandran, A. Shakoor, J. Skea, G. Strbac, X. Wang, and J. Whitaker, “Building a Resilient UK Energy System: Working paper,” : *London.*, no. UKERC Energy 2050 Working Paper (UKERC/WP/ES/2009/023), 2009.
- [116] A. R. Berkeley Iii, M. Wallace, and NIAC, “A Framework for Establishing Critical Infrastructure Resilience Goals: Final Report and Recommendations,” *Final Report and Recommendations by the Council*, pp. 1–73, 2010.
- [117] M. Carson and G. Perterson, *Arctic Council 2016. Arctic resilience report*, 2016. [Online]. Available: <http://www.arctic-council.org/arr/documents/ipyposter.pdf>
- [118] United Nations Office for Disaster Risk Reduction, “International Strategy for Disaster Reduction What is the Hyogo,” *International Strategy for Disaster Reduction (ISDR)*, no. September, p. 6, 2005.
- [119] B. Piers Blaikie; Terry Cannon; Ian Davis; Wisner, *At risk: natural hazards, people’s vulnerability and disaster*. Psychology Press, 2004.

- [120] R. Arghandeh, A. Von Meier, L. Mehrmanesh, and L. Mili, "On the definition of cyber-physical resilience in power systems," *Renewable and Sustainable Energy Reviews*, vol. 58, pp. 1060–1069, 2016. [Online]. Available: <http://dx.doi.org/10.1016/j.rser.2015.12.193>
- [121] C. Gouveia, J. Moreira, C. L. Moreira, and J. A. Peças Lopes, "Coordinating Storage and Demand Response for Microgrid Emergency Operation," *IEEE Transactions on Smart Grid*, vol. 4, no. 4, pp. 1898–1908, dec 2013. [Online]. Available: <http://ieeexplore.ieee.org/document/6509996/>
- [122] B. Zhang, P. Dehghanian, and M. Kezunovic, "Optimal Allocation of PV Generation and Battery Storage for Enhanced Resilience," *IEEE Transactions on Smart Grid*, vol. 10, no. 1, pp. 535–545, 2019.
- [123] M. Panteli, P. Mancarella, D. N. Trakas, E. Kyriakides, and N. D. Hatziargyriou, "Metrics and Quantification of Operational and Infrastructure Resilience in Power Systems," *IEEE Transactions on Power Systems*, vol. 32, no. 6, pp. 4732–4742, 2017.
- [124] K. Tierney and M. Bruneau, "A Key to Disaster Loss Reduction," pp. 14–18, 2007. [Online]. Available: <http://onlinepubs.trb.org/onlinepubs/trnews/trnews250{ }p14-17.pdf>
- [125] M. Panteli and P. Mancarella, "Operational resilience assessment of power systems under extreme weather and loading conditions," *IEEE Power and Energy Society General Meeting*, vol. 2015-Sept, 2015.
- [126] M. A. Mohamed, T. Chen, W. Su, and T. Jin, "Proactive Resilience of Power Systems against Natural Disasters: A Literature Review," *IEEE Access*, vol. 7, pp. 163 778–163 795, 2019.
- [127] A. Stankovic. and K. Tomsovic., "The Definition and Quantification of Resilience," Tech. Rep. April, 2018.
- [128] E. Yamangil, R. Bent, and S. Backhaus, "Designing Resilient Electrical Distribution Grids," sep 2014. [Online]. Available: <http://arxiv.org/abs/1409.4477>
- [129] C. Grigg, P. Wong, P. Albrecht, R. Allan, M. Bhavaraju, R. Billinton, Q. Chen, C. Fong, S. Haddad, S. Kuruganty, W. Li, R. Mukerji, D. Patton, N. Rau, D. Reppen, A. Schneider, M. Shahidehpour, and C. Singh, "The IEEE Reliability Test System-1996. A report prepared by the Reliability Test System Task Force of the Application of Probability Methods Subcommittee," *IEEE Transactions on Power Systems*, vol. 14, no. 3, pp. 1010–1020, 1999. [Online]. Available: <http://ieeexplore.ieee.org/document/780914/>
- [130] "CREST Demand Model." [Online]. Available: <https://www.lboro.ac.uk/research/crest/demand-model/>

- [131] V. B. Venkateswaran, D. K. Saini, and M. Sharma, “Environmental Constrained Optimal Hybrid Energy Storage System Planning for an Indian Distribution Network,” *IEEE Access*, vol. 8, pp. 97 793–97 808, 2020. [Online]. Available: <https://ieeexplore.ieee.org/document/9099520/>
- [132] B. Venkateswaran V, D. K. Saini, and M. Sharma, “Techno-Economic Hardening Strategies to enhance Distribution System Resilience against Earthquake,” *Reliability Engineering & System Safety*, vol. 213, no. December 2020, p. 107682, apr 2021. [Online]. Available: <https://linkinghub.elsevier.com/retrieve/pii/S0951832021002209>
- [133] A. Zare, C. Y. Chung, J. Zhan, and S. O. Faried, “A Distributionally Robust Chance-Constrained MILP Model for Multistage Distribution System Planning With Uncertain Renewables and Loads,” *IEEE Transactions on Power Systems*, vol. 33, no. 5, pp. 5248–5262, sep 2018. [Online]. Available: <https://ieeexplore.ieee.org/document/8255677/>
- [134] Y. Cao, W. Wei, J. Wang, S. Mei, M. Shafie-khah, and J. P. S. Catalao, “Capacity Planning of Energy Hub in Multi-Carrier Energy Networks: A Data-Driven Robust Stochastic Programming Approach,” *IEEE Transactions on Sustainable Energy*, vol. 11, no. 1, pp. 3–14, jan 2020. [Online]. Available: <https://ieeexplore.ieee.org/document/8510847/>
- [135] O. Z. Sehsalar, S. Galvani, and M. Farsadi, “New approach for the probabilistic power flow of distribution systems based on data clustering,” *IET Renewable Power Generation*, vol. 13, no. 14, pp. 2531–2540, 2019.
- [136] A. Joshi, A. Kumar, H. Castanos, and C. Lomnitz, “Seismic hazard of the Uttarakhand Himalaya, India, from deterministic modeling of possible rupture planes in the area,” *International Journal of Geophysics*, vol. 2013, 2013.
- [137] M. Panteli and P. Mancarella, “Modeling and Evaluating the Resilience of Critical Electrical Power Infrastructure to Extreme Weather Events,” *IEEE Systems Journal*, vol. 11, no. 3, pp. 1733–1742, sep 2017. [Online]. Available: <http://ieeexplore.ieee.org/document/7036086/>
- [138] “Multi-hazard loss estimation methodology: Earthquake model,” Department of Homeland Security, FEMA, Washington, DC, Tech. Rep., 2003. [Online]. Available: <https://www.fema.gov/hazus-mh-user-technical-manuals>
- [139] UPCL, “Uttarakhand Electricity Regulatory Commission,” Dehradun, Uttarakhand, India, Tech. Rep., 2019. [Online].

- Available: http://www.uerc.gov.in/ordersPetitions/orders/Tariff/TariffOrder/2019-20/Pressnote/PressNote-UPCL_{_}2019-20-R1.pdf
- [140] Y. Li, M. Du, W. Xie, B. Yang, C. Fang, Y. Zhang, and S. Wang, "Method for division of urban load power supply district based on cluster analysis," *IET Generation, Transmission & Distribution*, vol. 12, no. 20, pp. 4577–4581, nov 2018. [Online]. Available: <https://digital-library.theiet.org/content/journals/10.1049/iet-gtd.2018.6298>
- [141] J. Ding, Q. Zhang, S. Hu, Q. Wang, and Q. Ye, "Clusters partition and zonal voltage regulation for distribution networks with high penetration of PVs," *IET Generation, Transmission and Distribution*, vol. 12, no. 22, pp. 6041–6051, 2018.
- [142] Y. Ghiassi-Farrokhfal, C. Rosenberg, S. Keshav, and M.-b. Adjaho, "Joint Optimal Design and Operation of Hybrid Energy Storage Systems," *IEEE Journal on Selected Areas in Communications*, vol. 34, no. 3, pp. 639–650, mar 2016. [Online]. Available: <http://ieeexplore.ieee.org/document/7397853/>
- [143] A. R. Dehghani-Saniij, E. Tharumalingam, M. B. Dusseault, and R. Fraser, "Study of energy storage systems and environmental challenges of batteries," *Renewable and Sustainable Energy Reviews*, vol. 104, no. November 2018, pp. 192–208, 2019. [Online]. Available: <https://doi.org/10.1016/j.rser.2019.01.023>
- [144] D. MDDA, "Circle Rates," 2016.
- [145] K. Ricke, L. Drouet, K. Caldeira, and M. Tavoni, "Country-level social cost of carbon," *Nature Climate Change*, vol. 8, no. 10, pp. 895–900, oct 2018. [Online]. Available: <http://dx.doi.org/10.1038/s41558-018-0282-y>
- [146] B. Bahmani-Firouzi and R. Azizipanah-Abarghooee, "Optimal sizing of battery energy storage for micro-grid operation management using a new improved bat algorithm," *International Journal of Electrical Power and Energy Systems*, vol. 56, pp. 42–54, 2014. [Online]. Available: <http://dx.doi.org/10.1016/j.ijepes.2013.10.019>
- [147] G. Xu, "An adaptive parameter tuning of particle swarm optimization algorithm," *Applied Mathematics and Computation*, vol. 219, no. 9, pp. 4560–4569, jan 2013. [Online]. Available: <http://dx.doi.org/10.1016/j.amc.2012.10.067>
- [148] H. Irene, S. Sandy, T. Soudelor, and U. States, "Resilience-Oriented Pre-Hurricane Resource Allocation in Distribution Systems Considering Electric Buses," vol. 105, no. 7, 2017.

- [149] N. Bhusal, M. Abdelmalak, M. Kamruzzaman, and M. Benidris, “Power system resilience: Current practices, challenges, and future directions,” *IEEE Access*, vol. 8, no. January, pp. 18 064–18 086, 2020.
- [150] M. Baumann, J. Peters, M. Weil, C. Marcelino, P. Almeida, and E. Wanner, “Environmental impacts of different battery technologies in renewable hybrid micro-grids,” *2017 IEEE PES Innovative Smart Grid Technologies Conference Europe, ISGT-Europe 2017 - Proceedings*, vol. 2018-Janua, pp. 1–6, 2018.
- [151] A. A. Mutha, “Indian UPS and Inverter Industry Growing Slowly but Steadily,” Tech. Rep., 2014. [Online]. Available: https://www.nqr.gov.in/sites/default/files/AnnexureI_{-}4.pdf
- [152] Y. Li, Y. Zheng, D. Doermann, and S. Jaeger, “Script-independent text line segmentation in freestyle handwritten documents,” *IEEE Transactions on Pattern Analysis and Machine Intelligence*, vol. 30, no. 8, pp. 1313–1329, 2008.
- [153] National Center for Seismology, “Earthquakes in India.”

Curriculum Vitae

Education:

1. Jan 2016 - present: Pursuing Ph.D. at University of Petroleum and Energy Studies under the supervision of Dr. Madhu Sharma & Dr. Devender K. Saini
2. Jun 2011 - May 2013: M. Tech Power System at SRM University, Chennai, Tamilnadu, India.
3. Jun 2007 - May 2011: B.E Electrical and Electronics Engineering at Anna University, Chennai, Tamilnadu, India.

Experience:

1. Oct 2015 - present: Assistant Professor, Dept. of Electrical and Electronics Engineering, University of Petroleum and Energy Studies, Dehradun, Uttarakhand, India.
2. Jun 2014 - Oct - 2015 : Assistant Professor, Dept. of Electrical and Electronics Engineering, GMR Institute of Technology, Rajam, Andhra Pradesh, India.

Certification:

1. Virtual Teacher Specialization, issued by Coursera - University of California, Irvine. on June 2020.
2. Energy Production, Distribution & Safety Specialization, issued by Coursera - The State University of New York on April 2020.
3. Understanding Research Methods, issued by Coursera - University of London on April 2020.
4. Project: Clustering Geolocation Data Intelligently in Python, issued by Rhyme on April 2020.
5. Engineer - Power Distribution, issued by National Skill Development Corporation on August 2019.
6. Junior Engineer - Power Distribution, issued by National Skill Development Corporation on August 2019.

Publications:

Conference Papers:

1. Balaji Venkateswaran V, Devender Saini, "COVID19: Impact on environmental parameters during the lockdown period in India", National Conference on Sustainable Management of Environment & Natural Resource through Innovation in Science and Technology SMTST 2020.
2. Deepali Yadav, Balaji Venkateswaran V, "COVID-19 Fallout: India, Power Sector and Lockdown", National Conference on Sustainable Management of Environment & Natural Resource through Innovation in Science and Technology SMTST 2020.
3. Deepali Yadav, Balaji Venkateswaran V, "Assessing the Impact of Novel Coronavirus (COVID- 19) on Renewable Energy Sector of India during the lockdown", National Conference on Sustainable Management of Environment & Natural Resource through Innovation in Science and Technology SMTST 2020.
4. Atul Sharma, Balaji Venkateswaran V, Rashmi Singh, "Experimental Analysis of Electrical and Thermal Effects of Various Configurations of Partial Shading on Three Different Solar Module Technologies", IEEE Sponsored International Conference on Recent Trends in Electrical, Control and Communication (RTECC – 18) Organizing by Crescent University, Chennai, India and Universiti Teknologi Mara, Shah Alam , Malaysia. 2018.
5. Deepali Yadav, Neeraj Kumar Sharma, Devendra Rawat, Balaji Venkateswaran V, "A Novel Shunt Hybrid Active Filter To Eliminate Dominant Current Harmonics Under Realistic Utility Conditions", IEEE Sponsored International Conference on Recent Trends in Electrical, Control and Communication (RTECC – 18) Organizing by Crescent University, Chennai, India and Universiti Teknologi Mara, Shah Alam , Malaysia. 2018.
6. V. Balaji Venkateswaran, Manoj Vasuppali, "State Estimation of Power System Containing FACTS Controller and PMU", IEEE Sponsored 9th International Conference on Intelligent Systems and Control (ISCO – 2015), Karpagam College of Engineering, Coimbatore, January, 2015.
7. V. Balaji Venkateswaran, Subbu Chithira Kala "Observability Analysis and Optimal Placement of PMU using Differential Evolution Algorithm", IEEE Conference on Emerging Trends in Electrical Engineering and Energy Management (ICETEEEM – 2012), AVIT, Chennai, December, 2012.

Journal Publication

1. Devender K Saini, Ravikumaran Nair, Balaji Venkateswaran V, Monika Yadav, "Effect of Unaccounted Parameters on Reactive Power Compensation in Indian Electric Traction Line", IEEE Access, 2020.
2. Balaji Venkateswaran V, Deepali Yadav, Neeraj Kumar Sharma, "Experimental Verification of Reconfiguration Techniques Applied For Partial Shading on Solar PV", International Journal of Innovative Technology and Exploring Engineering (IJITEE). Vol-8 No.11, pp. 4196-4203, September-2019.
3. Balaji Venkateswaran V, Neeraj Kumar Sharma, Deepali Yadav, "State Estimation of Power System Embedded with FACTS devices and PMUs", International Journal of Engineering and Technology/UAE. 2018.
4. V Balaji Venkateswaran, "Observability Analysis and Optimal Placement of PMU using Krill Herd Algorithm", International Journal of Applied Engineering Research (IJAER), Research India Publication, Vol. 10 No.1, pp. 176-180, March-2015.

The following publications were written within the scope of this thesis:

1. V. Balaji Venkateswaran, Devender K Saini, Madhu Sharma, "Approaches for optimal planning of the energy storage units in distribution network and their impacts on system resiliency", Accepted for Publication in *CSEE Journal of Power and Energy Systems*, 2020. [Online]. Available: <https://ieeexplore.ieee.org/document/9098154>
2. V. Balaji Venkateswaran, Devender K Saini, Madhu Sharma, "Environmental Constrained Optimal Hybrid Energy Storage System Planning for an Indian Distribution Network", *IEEE Access*, vol.8, pp. 97793-97808, 2020. [Online]. Available: <https://ieeexplore.ieee.org/document/9099520>
3. V. Balaji Venkateswaran, Devender K Saini, Madhu Sharma, "Techno Economic Hardening Strategies to enhance Distribution System Resilience against Earthquake", Under review in first round by *Reliability Engineering and System Safety*, Elsevier, vol 213, pp.107682, 2021. [Online]. Available: <https://www.sciencedirect.com/science/article/abs/pii/S0951832021002209>

PLAGIARISM CERTIFICATE

1. We Dr. Madhu Sharma (Internal Guide), Dr. D.K. Saini Co Guide/
External Guide) certify that the Thesis titled
Optimal Configuration and Placement of Energy Storage Systems
to enhance the reliability of renewable energy integrated electric and
distribution system
submitted by Scholar Mr/ Ms Baby Venkateswar V having SAP ID
500049711 has been run through a Plagiarism Check Software and the Plagiarism
Percentage is reported to be 7 %.
2. Plagiarism Report generated by the Plagiarism Software is attached .

Madhu Sharma
Signature of the Internal Guide













D.K. Saini
Signature of External Guide/Co Guide

VK
Signature of the Scholar

Document Information

Analyzed document	Thesis_Doc.pdf (D91804771)
Submitted	1/12/2021 11:26:00 AM
Submitted by	Balaji Venkateswaran V
Submitter email	b.venkateswaran@ddn.upes.ac.in
Similarity	7%
Analysis address	b.venkateswaran.upes@analysis.orkund.com

Sources included in the report

SA	14022P0228.pdf Document 14022P0228.pdf (D84010698)		3
W	URL: https://scholarworks.utep.edu/cgi/viewcontent.cgi?article=3852&context=open_etd Fetched: 7/5/2020 8:30:20 AM		5
W	URL: https://ieeexplore.ieee.org/document/9098154 Fetched: 1/12/2021 11:27:00 AM		2
W	URL: https://ieeexplore.ieee.org/abstract/document/9099520/ Fetched: 1/12/2021 11:27:00 AM		2
W	URL: https://www.researchgate.net/publication/301717031_Optimal_Allocation_of_Battery_E... Fetched: 1/8/2020 8:32:59 AM		3
W	URL: https://www.researchgate.net/figure/Framework-of-optimal-planning-model_fig1_321930433 Fetched: 1/12/2021 11:27:00 AM		3
W	URL: https://core.ac.uk/download/pdf/144148652.pdf Fetched: 9/29/2019 10:09:08 PM		3
W	URL: https://tigerprints.clemson.edu/cgi/viewcontent.cgi?article=3300&context=all_disse... Fetched: 1/15/2020 2:22:25 PM		2
SA	1424489212-TS(BANUMALAR K).pdf Document 1424489212-TS(BANUMALAR K).pdf (D34908254)		4
W	URL: http://ieeexplore.ieee.org/document/7440864/ Fetched: 1/12/2021 11:27:00 AM		1
W	URL: https://www.tatapower.com/media/PressReleaseDetails/1617/tata-power-collaborates-w... Fetched: 1/12/2021 11:27:00 AM		2
W	URL: https://digitalcommons.du.edu/cgi/viewcontent.cgi?article=2416&context=etd Fetched: 11/3/2019 2:21:55 PM		6

URL: <https://digitalcommons.du.edu/cgi/viewcontent.cgi?article=2416&context=etd>